Preparation of Zeolite ZSM-5 Membranes

Thesis by

Yushan Yan

In Partial Fulfillment of the Requirements

for the Degree of

Doctor of Philosophy

California Institute of Technology

Pasadena, California

1997

(Submitted August 12, 1996)

To my mother and father

Acknowledgments

I would like to thank my advisors, Professor George R. Gavalas and Professor Mark E. Davis, for their support and encouragement throughout the course of this work. For their insightful comments and suggestions and the great degree of latitude they allowed me in conducting this research I am especially grateful.

I have benefited substantially from my interactions with many people at Caltech. In particular, I want to thank John Lewis, C. Y. Chen, Chris Dartt, and Neil Fernandes for their assistance at various stages of this research. I also want to thank Guy Duremberg of the Chemistry Machine Shop and Rick Gerhart of the Chemistry Glass Shop for their kind help on numerous occasions. I am thankful to Donna Johnson for typing part of this thesis. I am indebted to James Sun and Jeremy Martin for their great friendship and especially the camaraderie we shared during my first year in the basement.

Although my parents have passed away, I will forever be grateful to them for their unconditional love and support and for teaching me the value of learning. I am also grateful to my sisters and brother for their constant support and encouragement throughout my seemingly endless years at school. I would like to thank my parents-in-law for opening their home to me and for treating me as their own child.

Finally, I wish to acknowledge Shaocong Jiang, my wife, best friend, and colleague for the past eight years. She has been an unending source of support, motivation and inspiration. Together we have overcome many challenges, and her love and support has made the good times better and the bad times more bearable. I appreciate the sacrifices she has made and look forward to sharing whatever the future brings to us.

Abstract

Zeolite ZSM-5 membranes were prepared on porous α-Al_2O_3 disks by in-situ crystallization using a clear solution of optimized composition $100(TPA)_2O : 400Na_2O : Al_2O_3 : 1200SiO_2 : 114200H_2O$. During the synthesis, the disk was fixed horizontally at the air-liquid interface and a continuous polycrystalline zeolite film of about 10 μm thickness formed on the bottom surface of disk. Extensive experimentation was carried out to find the optimal composition. Pure gas permeation measurements of the most successful preparation yielded hydrogen:isobutane and n-butane:isobutane ratios of 151 and 18 at room temperature and 54 and 31 at 185 °C, respectively.

Electron probe microanalysis of the cross section of a membrane prepared on a bare alumina disk revealed a layer of crystalline or amorphous silica extending 80 μm inside the pores of the support. It is believed that this internal layer adds resistance to permeation and degrades selectivity. To limit the excessive penetration of siliceous species into the support pores, a diffusion barrier was introduced into the pores of the support prior to zeolite crystallization by impregnating the disk with a 1:1 molar mixture of furfuryl alcohol and tetraethylorthosilicate, polymerizing the mixture retained in the disk, and carbonizing the resulting polymer. Following carbonization, a partial carbon burnoff was carried out to generate a carbon-free region near the surface of the support. Membranes synthesized using barriers have n-butane flux and n-butane:isobutane selectivity $2.7x10^{-3}$ mol/m^2-s and 45 at 185 °C which are, respectively, about 1.6 and 4 times as large as those of membranes prepared without the use of barriers.

The n-butane:isobutane selectivity of ZSM-5 membranes was substantially improved (e.g. 322 vs. 45 at 185 °C) by a post-synthetic coking treatment which was accomplished by impregnating the membranes with liquid 1,3,5-triisopropylbenzene (TIPB) for 24 hours at room temperature and then calcining them in air at 500 °C for 2

hours. Calcination at 500 °C for up to 30 hours does not destroy the high n-butane:isobutane selectivity. Thermogravimetric analysis experiments suggest that micro-defects in the zeolite membranes were selectively eliminated by the TIPB coking treatment while the intracrystalline pore space of the ZSM-5 was not affected.

A model of surface-induced nucleation, crystal growth, and crystal adhesion was proposed for the aforementioned heterogeneous hydrothermal synthesis system. During the synthesis, aluminosilicates in the aged solution interact favorably with and travel toward the α-Al_2O_3 surface, resulting in concentration and nucleation in the vicinity of the surface. Some of the nuclei become attached to the surface and grow into a zeolite film while others settle and produce loose zeolite crystals at the bottom of the autoclave. The nutrients for crystal growth is supplied by active gel particles and the synthesis solution. Surface -OH groups on the substrate appear important for crystal adhesion via condensation. As for zeolite membrane formation on a surface of certain area, the location and orientation of the surface as well as the amount of synthesis liquid accessible to the surface are critical for the quality of the zeolite membrane.

Table of contents

List of Tables

List of Figures

Chapter 1

Introduction

1.1 Background

Membrane separation technology is becoming increasingly important in the chemical process industry. A variety of membrane separation processes have been commercialized including microfiltration, ultrafiltration, dialysis, reverse osmosis, pervaporation, and gas permeation (1). Categorical comparisons between a membrane process and other major separation processes such as distillation, extraction, and adsorption are difficult because each process has its own characteristics which can be advantageous or disadvantageous depending on the specific separation intended. But the benefits of using membranes often are low energy consumption and convenience (2). The advent of asymmetric polymeric membranes in flat sheet or hollow fiber form has been a key breakthrough in the development of membrane separation technology. As a result, current membrane processes are dominated by polymeric membranes (1). Polymeric membranes can be produced at high packing density and low cost but have certain disadvantages such as swelling in organic solvent, instability at high temperatures, and compressibility at high pressures. These limitations severely impede broader applications of membranes in the chemical process industry. It has been recognized that these limitations can be overcome by inorganic membranes. In fact, inorganic membranes for microfiltration and ulrtrafiltration have made a firm presence in many industries such as food and beverage, biotechnology, and pharmaceutical where alkaline cleaning and steam sterilization are essential (3). However, the development of inorganic membranes for the molecular sieving separations such as pervaporation and gas permeation has been limited due to the lack of membranes of adequate flux and selectivity.

A membrane must possess adequate flux and selectivity for the intended application in order to be considered attractive for industrial applications. Flux represents the rate at which a material passes through a membrane and higher flux translates into higher

productivity. Selectivity is the ability of a membrane to separate a component from a mixture. Higher selectivity means higher efficiency. A membrane can be generally classified as nonporous (dense) or porous according to its structure. Dense membranes are mainly used for gas separations. Such membranes include palladium and silica for hydrogen separation (4,5), and certain perovskite-type oxides for oxygen separation (6). These dense membranes usually have high selectivities, but low fluxes (7). Porous membranes usually offer high fluxes because of their relatively open structure. Currently the most studied microporous membranes are based on sol-gel derived oxides (8,9), carbon molecular sieves (10,11), and zeolites (12-23). Microporous silica and carbon molecular sieve membranes usually have high fluxes, but relatively low selectivities because of their wide pore size distribution.

Zeolites are crystalline, inorganic materials with channels and cages of precise dimension formed by TO_4 tetrahetra (T = tetrahedral atom, e. g., Si, Al) through sharing each apical oxygen. These materials are capable of separating molecules according to their size and shape with precision smaller than 1 Å (24). Many zeolite structures with pore size ranging from 4 Å to 14 Å are available for different separations. For example, shape selectivity has been achieved between normal butanol and isobutanol by zeolite CaA (4.2 Å pore diameter) (25) and between xylene isomers by ZSM-5 (5.5 Å pore diameter) (26). For the same zeolite structure, the pore size can be finely tuned by exchanging different cations into the channels. The precision and tunability of the pore size of each zeolite structure and the availability of many zeolite structures make zeolites uniquely suited for molecular sieving separations. The hydrophobicity of a zeolite can also be controlled by controlling its framework Si/Al ratio. Zeolites with a high Si/Al ratio are hydrophobic while those with a low Si/Al ratio are hydrophilic. The hydrophobicity is important for organic/water separation by pervaporation (21-23). It is clear from the aforementioned properties that zeolites are ideal membrane materials for pervaporation and gas permeation.

Zeolite membranes are also promising for catalytic membrane reactor processes where integration of separation with catalytic reaction can improve reaction conversion or selectivity.

In a standard hydrothermal synthesis, zeolites grow as loose crystals which settle by gravity to the bottom of the synthesis vessel. To prepare a zeolite membrane, however, the crystals must grow in an interlocking fashion to form a continuous layer free of nonzeolitic transmembrane pathways. This layer must be thin to provide good flux, and yet mechanically durable, hence, it must be grown on some porous support element. As recently as four years ago, the stringent requirements listed above made the synthesis of useful zeolite membranes a doubtful pursuit.

During the last three years, however, several research groups have reported the preparation of zeolite membranes with attractive selectivities for gas separation and pervaporation (12-23). All of these preparations involved the growth of a polycrystalline zeolite layer on a porous disk or tube that serves as a mechanical support. In most cases, the support was alpha alumina but gamma alumina and porous steel have also been used. The crystallization of the zeolite layer on the support was accomplished by a variety of procedures including in-situ hydrothermal crystallization and vapor phase transport on a support preloaded with the synthesis gel. Thus far, only ZSM-5 and silicalite membranes have been prepared with good selectivities for gas separations and pervaporation. Some of these membranes revealed n-butane:isobutane selectivities 1-90 at room temperature but only 1-10 at around 200 °C (12-19). Others were not tested for n-butane to isobutane separation but showed good pervaporation selectivities for organic/water mixture (21-23).

The flux ratio of n-butane to isobutane has commonly been used as a measure of membrane quality. For, with a kinetic diameter of 4.3 Å for n-butane and 5.0 Å for isobutane, and with the pore diameter of ZSM-5 5.5 Å, a high n-butane:isobutane flux ratio suggests the virtual absence of cracks or pores of diameter much above 5.5 Å.

1.2 Objectives

The objective of this research is to develop methods to prepare zeolite ZSM-5 membranes with high fluxes and selectivities. The thesis is organized as follows.

Chapter 2 describes the preparation of zeolite ZSM-5 membranes on porous α-Al_2O_3 disks by in-situ crystallization using a clear solution of optimized composition.

Chapter 3 presents the development of a temporary barrier pretreatment procedure to improve the membrane flux and selectivity by reducing the penetration of siliceous material into the pores of the support.

Chapter 4 contains the development of a post-synthetic coking treatment procedure to improve the membrane selectivity by eliminating the micro-defects in the membrane.

Chapter 5 proposes a model of surface induced nucleation, crystal growth, and crystal adhesion in the crystallization of ZSM-5 membranes on porous α-Al_2O_3.

Chaper 6 summarizes the findings of this dissertation.

References

[1] W. S. W. Ho and K. K. Sirkar, Membrane Handbook, Chapman & Hall, New York, 1992.

[2] J. L. Humphrey, Separation Processes: Playing a Critical Role, Chem. Eng. Pro., 10(1995)31.

[3] A. J. Burggaaf, K. Keiser, R. S. A. de Lange, Z. A. E. P. Vroon, and V. T. Zaspalis , Inorganic Membranes for Separations and Reactions, in "Proceedings of 9th International Zeolite Conference," R. von Ballmoos, J.B. Higgins and M.M.J. Treacy (Eds.), Butterworth-Heinemann, Boston, 1993.

[4] N. Itoh, A Membrane Reactor Using Palladium, AIChE J., 33(1987)1576.

[5] S. Jiang, Y. Yan, and G. R. Gavalas, Temporary Carbon Barriers in the Preparartion of H_2-Permselective Silica Membranes, J. Membr. Sci., 103(1995)211.

[6] U. Balachandran, J. T. Dusek, R. L. Mieville, R. B. Poeppel, M. S. Kleefisch, S. Pei, T. P. Kobylinski, C. A. Udovich, and A. C. Bose, Dense Ceramic Membranes for Partial Oxidation of Methane to Syngas, Appl. Catal., 133(1995)19.

[7] H. P. Hsieh, Imorganic Membranes, AIChE Symp. Seri., 84(1988)1.

[8] A. F. M. Leenaars, K. Keizer, and A. J. Burggraaf, Porous Alumina Membranes, CHEMTECH, 9(1986)560.

[9] A. F. M. Leenaars and A. J. Burggraaf, The Preparation and Characterization of Alumina Membranes with Ultrafine Pores. 2. The Formation of Supported Membranes, J. Colloi. Inter. Sci., 105(1985)27.

[10] J. E. Koresh and Soffer A, Molecular Sieve Carbon Permselective Membrane. Part I: Presentation of a New Device for Gas Mixture Separation, Sep. Sci. Tech., 18(1983)723.

[11] A. J. Bird and D. L. Trimm, Carbon Molecular Sieves Used in Gas Separation Membranes, Carbon, 21(1983).

[12] E. R. Geus, M. J. den Exter and H. van Bekkum, Synthesis and Characterization of Zeolite (FMI) Membranes on Porous Ceramic Supports. J. Chem. Soc. Farady Trans., 88(1992)3101.

[13] E. R. Geus, H. van Bekkum, W. J. W. Bakker, and J. A. Moulijn, High-Temperature Stainless Steel Supported Zeolite (FMI) Membranes: Module Construction and Permeation Experiments. *Microporous Mater., 1(1993)131.*

[14] W. J. W. Bakker, G. Zheng, F. Kapteijn, M. Makkee, J. A. Moulijn, E. R. Geus, and H. van Bekkum, Single and Multi-Component Transport through Metal Supported MFI Zeolite Membranes. In "Precision Process Technology"; M.P.C.

Weijnen, and A.A.H. Drinkenburg, Eds.; Kluwer Academic Publishers. The Netherlands, 1993.

[15] Z. A. E. P. Vroon, K. Keizer, M. J. Gilde, H. Verweij, A. J. Burggraaf, Transport-Properties of Alkanes through Ceramic Thin Zeolite FMI Membranes. J. Membr. Sci., 113(1996)293.

[16] M. D. Jia, K. V. Peinemann, and R. D. Behling, Ceramic Zeolite Composite Membranes: Preparation, Characterization and Gas Permeation, J. Memb. Sci., 82(1993)15.

[17] C. Bai, M. Meng, J. L. Falconer, and R. D. Noble, Preparation and Separation Properties of Silicalite Composite Membranes, J. Membr. Sci., 105(1995)79.

[18] M. D. Jia, B. Chen, R. D. Noble, and J. L. Falconer, Ceramic-Zeolite Composite Membranes and Their Application for Separation of Vapor/Gas Mixtures, J. Membr. Sci., 90(1994)1.

[19] Y. H. Ma, and S. Xiang, Formation of Zeolite Membranes from Sols. Patent PCT/US 9302384, 1993.

[20] N. Nishiyama, K. Ueyama, and M. Matsukata, A Defect-Free Mordenite Membrane Synthesized by Vapor-Phase Transport Method, J. Chem. Soc., Chem. Commun., (1995)1967.

[21] T. Sano, S. Ejiri, M. Hasegawa, Y. Kawakami, N. Enomoto, Y. Tamai, and H. Yanagishita, Silicalite Membranes for Separation of Acetic acid/Water Mixture, Chem. Lett., 2(1994)153.

[22] T. Sano, M. Hasegawa, Y. Kawakami, and H. Yanagishita, Separation of Methanol/Methyl-tert-butyl Ether Mixture by Pervaporation Using Silicalite Membrane, J. Memb. Sci. 107(1995)193.

[23] H. Kita, K. Horii, Y. Ohtoshi, K. Tanaka, and K. I. Okamoto, Synthesis of a Zeolite NaA Membrane for Pervaporation of Water/Organic Liquid Mixture, J. Mater. Sci. Lett., 14(1995)206.

[24] M. E. Davis and R. F. Lobo, Zeolite and Molecular Sieve Synthesis, Chem. Mater. 4(1992)756.

[25] P. B. Weisz, V. J. Frilette, R. W. Maatman, and E. B. Mower, Catalysis by Crystalline Aluminosilicates II. Molecular-Shape Selective Reactions. J. Catal., 1(1962)307.

[26] Y. G. Li, X. Chang, and Z. Zeng, Kinetics Study of the Isomerization of Xylene on HZSM-5 Zeolite. 1. Kinetic Model and Reaction Mechanism., Ind. Eng. Chem. Res., 31(1992)187.

Chapter 2

Preparation of Zeolite ZSM-5 Membranes by In-Situ Crystallization on Porous α-Al_2O_3

Reprinted with permission from the article

[Yushan Yan, Mark E. Davis, and George R. Gavalas, **Ind. Eng. Chem. Res.**, 34(1995)1652]

Preparation of Zeolite ZSM-5 Membranes by In-Situ Crystallization on Porous α-Al_2O_3

Yushan Yan, Mark E. Davis, and George R. Gavalas

Chemical Engineering, California Institute of Technology

Pasadena, CA 91125

Abstract

Zeolite ZSM-5 membranes were grown on porous α-Al_2O_3 disks by in-situ hydrothermal synthesis at 175 °C. The zeolite layers were formed on the bottom face of disks placed horizontally near the air-liquid interface of clear synthesis solutions. Extensive experimentation was carried out to find compositions that gave continuous polycrystalline films. The films grown with the optimized composition were about 10 μm thick and consisted of well intergrown crystals of about 2 μm size. Pure gas permeation measurements of the most successful preparation yielded hydrogen:isobutane and n-butane:isobutane ratios of 151 and 18 at room temperature and 54 and 31 at 185°C, respectively.

2.1 Introduction

Zeolites are used extensively in catalysis, and in gas separation and purification. Separations by zeolites are carried out by an unsteady process known as pressure swing adsorption (PSA) in which two or more columns packed with zeolite pellets (0.2-0.5 mm)

alternate between adsorption and desorption. If the zeolite could be employed in membrane form, gas separation could be accomplished by simpler and more economical steady flow. Zeolite membranes are also promising for membrane reactor processes where integration of separation with chemical reaction can improve reaction conversion or selectivity.

In standard hydrothermal synthesis, zeolites grow as loose crystals which settle by gravity to the bottom of the synthesis vessel. To prepare a zeolite membrane, however, the crystals must grow in an interlocking fashion to form a continuous layer free of nonzeolitic transmembrane pathways. This layer must be thin to provide good permeance, and yet mechanically durable, hence, it must be grown on some porous support element, e.g., flat plate or tube. As recently as three years ago, the stringent requirements listed above made the synthesis of useful zeolite membranes a doubtful pursuit. During the last two years, however, several groups have made significant progress in the preparation of supported ZSM-5 or silicalite membranes and have most recently demonstrated attractive separation selectivities and good thermomechanical stability. Parallel studies of zeolite growth on nonporous solids have provided useful mechanistic information.

The recent zeolite membrane preparations have all involved ZSM-5 or silicalite but have employed different supports and synthesis procedures. Jia et al. (1994) used as supports macroporous α–Al_2O_3 tubes coated on the inside by a mesoporous γ-Al_2O_3 layer (5 nm pore diameter). The tubes were filled with the synthesis gel and placed in an autoclave at 180 °C. After about 12 hours of heating, a zeolite layer was formed on the γ-Al_2O_3 surface. This crystal growth on the surface was attributed to local supersaturation caused by evaporation of water on the outside surface of the tube. After drying and calcination, permeation measurements were conducted for pure gases and mixtures. Pure gas permeances at 25 °C were 44 (H_2), 15.6 (N_2), 0.77 (n-butane) and 0.25 (isobutane),

all in 10^{-7} mol/m^2-s-Pa. Better selectivities were recently reported by the same group, (Bai et al., 1994); for example, the n-butane:isobutane ratio was over 20 at room temperature and about 10 at 180 °C.

A different preparation scheme was employed by Xiang and Ma (1993, 1994) to prepare silicalite/ZSM-5 membranes. This scheme involved preloading a porous α-Al_2O_3 tube or disk with the synthesis gel and bringing it in contact with water vapor (but not with liquid) at 130-200 °C under autogenous pressure. Repeated loading with the synthesis sol or repeated hydrothermal treatments were employed to improve membrane properties. The membranes prepared by this technique showed little selectivity between n-butane and isobutane (5:4) but very good selectivity relative to the components of a liquid 1-1-1 mixture of p-xylene, m-xylene and 1,3,5 triisopropylbenzene (94:6:0).

Researchers at Delft University have been conducting a broad experimental program on zeolite film growth and have advanced some interesting concepts to explain zeolite growth on solid surfaces. Geus et al. (1992, 1993a, 1993b) and Bakker el al. (1993) studied the growth of ZSM-5 membranes on various porous substrates including α-alumina, zirconia, and steel wool-sintered steel composites. One major finding (Geus et al., 1992) was that the substrate surface plays an important role in determining the type of zeolite film grown. For example analcime grew on α-Al_2O_3, ZSM-5 grew on clay, while a mixture of analcime and ZSM-5 grew on a ZrO_2-α-Al_2O_3 composite, all with the same synthesis composition and temperature. The ZSM-5 grown on clay was a continuous layer of randomly oriented intergrown crystals, but the crystals grown on the other supports formed clusters providing only partial coverage of the surface. It was suggested that insoluble solids like zirconia (or Teflon) support the growth of ZSM-5 (or silicalite) while α-Al_2O_3 leached by the strongly alkaline solution shifts the synthesis to analcime. Likewise, growth of ZSM-5 films on steel wool/sintered steel composites may

have been influenced by Fe^{3+} and Cr^{3+} ions leached from the support (Bakker et al, 1993). This structure-directing role of the solid surface is strongly coupled with the composition of the synthesis solution, for as was mentioned earlier, under somewhat different synthesis compositions, ZSM-5 rather than analcime grew on α-Al_2O_3 and γ-Al_2O_3 (Jia et al., 1994; Xiang and Ma, 1993, 1994).

The ZSM-5 films grown on clay were quite thick, 50-80 μm, and possessed very modest separation properties (Geus et al., 1992, 1993a). By contrast, ZSM-5 films grown on the steel wool-sintered steel composites using a different synthesis mixture showed excellent separation selectivities at room temperature (Geus et al, 1993b; Bakker et al, 1993). For example the pure gas permeation ratio of n-butane:isobutane was 64 at room temperature although it declined to 1–2 at 350 °C.

Delft University researchers (Jansen et al, 1993; Koegler et al., 1994) also studied the growth of ZSM-5 films on various solid supports without consideration of permeation properties but with a focus on the morphology of the zeolite layer. The most interesting results were obtained for film growth on smooth silicon surfaces. Using compositions without Al or Na, they observed that early during the synthesis the surface became covered with a 0.5 μm thick layer of silica gel within which crystallites emerged at a later time, apparently detached from the solid surface. These crystallites grew to a size of 1 μm and at the end of crystallization covered over 98% of the surface forming a layer which remained bonded to the support even after calcination at 400 °C. To explain these observations the authors proposed that zeolite nucleation occurs at the gel-solution interface forming loose crystallites which grow by drawing nutrients from the gel and later from the clear solution. As the crystallites grow in size, they contact and bond with the surface via condensation of silanol groups on the zeolite with those on the silicon (silanols on silicon were formed by oxidation in the strongly alkaline solution).

Vroon et al. (1994) recently reported in situ growth of ZSM films less than 5 μm thick on porous Al_2O_3 supports. These films had attractive selectivities, e.g., n-butane to isobutane pure gas permeation ratios of over 50 at room temperature and over 10 at 200°C.

Several other studies of zeolite growth on nonporous surfaces have been reported. Myatt et al. (1992) investigated the growth of zeolite NaA from initially clear synthesis solution (SiO_2-0.2Al_2O_3-10Na_2O-200H_2O). Zeolite NaA layers grew over the whole surface of polyethylene bottles. On the side walls the layer had uniform thickness (ca. 7 μm) and good crystallinity while the bottom layer was thicker and only partially crystalline. NaA films of good crystallinity also grew on glass and poly(tetrafluoroethylene). Examining various alternative mechanisms the authors suggested that crystal growth on the surface takes place by adsorption of homogeneously formed nuclei or amorphous particles followed by crystallization in the vicinity of the adsorbed particles. The role of the surface then is to adsorb precrystalline particles and thus form an environment highly favorable for crystallization. This suggestion is consistent with the model of Jansen et al. (1993) and Koegler et al. (1994) which identifies the gel layer, i.e., layer of loosely connected amorphous particles, as the site of crystallization.

Tsikoyannis and Haag (1992) studied the formation of ZSM-5 layers on a variety of flat, nonporous surfaces including Teflon, silver, steel and on porous Vycor disks. Using the synthesis composition SiO_2-0.022Na_2O-0.052TPABr-28.3H_2O they observed on all vertically placed surfaces as well as on the Teflon container uniform ZSM-5 films of intergrown crystals 10-100 μm in size coated with sub-micron sized particles of undetermined crystallinity. No homogeneously nucleated particles were observed to settle to the bottom of the container. Furthermore, the crystal layers formed on metals and Vycor were firmly bonded to the substrate but the layer formed on Teflon could be

easily peeled off. Permeability measurements carried out for one of the detached layers (ca. 250 μm thickness) yielded very modest permeance ratios (1-2) for O_2:N_2 and H_2:CO but a more substantial ratio (17) for n-hexane:dimethylbutane.

Sano et al. (1991) studied the growth of ZSM-5 films on the Teflon lining of their autoclaves. For the synthesis composition 0.1TPABr-0.05Na_2O-0.01Al_2O_3-SiO_2-xH_2O films grew only when x was above 70. The crystalline morphology and the Si:Al ratio varied between the face attached on the Teflon lining and the face at the solution side with the latter showing smaller crystals and having much higher SiO_2:Al_2O_3 ratio. In a later study, Sano et al. (1993) grew ZSM-5 and ZSM-11 films on filter paper immersed vertically in the hydrothermal synthesis solution. After 48 hours the filter paper was covered with a densely packed layer of zeolite crystals 5-30 μm in size. The layer had thickness 500 μm and retained its integrity after burning the paper off indicating that the zeolite crystals were strongly bonded to each other. The authors suggested that crystal growth may have initiated at -OH groups of the cellulose fibers.

The aforementioned studies document the large number of factors and degrees of freedom that are at work in zeolite membrane growth. The substrate surface is obviously an important factor. The chemical constitution of a nonporous substrate can influence crystal growth by releasing selected compounds into the solution, by adsorbing amorphous precursor particles or smaller nuclei, and by providing sites e.g., -OH groups, for crystal adhesion. With porous substrates pore size is the major property although the chemical constitution of the material remains important for the same reasons as for nonporous substrates.

As in conventional zeolite synthesis, the composition of the synthesis solution is of decisive importance. As amply documented in the above references, composition controls not only the type of zeolite crystallized but the quality of the zeolite layer as well; some compositions yield a continuous layer of intergrown and interlocking crystals,

other compositions yield layers that are macroscopically continuous but contain mesoporous transmembrane pathways, and still other compositions give isolated crystal patches with much of the surface remaining bare. Synthesis temperature is another important variable acting in conjunction with the synthesis composition.

In this paper we report the preparation of ZSM-5 membranes on porous α-Al_2O_3 disks. The preparation technique uses in-situ crystallization but starts with a clear synthesis solution rather than a gel as employed in previous studies and relies on a somewhat different orientation of the crystallization surface. As in previous studies, the choice of synthesis compositions is critical for preparing good quality membranes. After searching a wide range of compositions, we arrived at a composition producing membranes with good permeation selectivities up to the highest temperature tested (185°C).

2.2 Experimental

Supports

The nonporous supports were thin plates of square cross section (6.35 cm x 6.35 cm x 0.63 mm), 99.6% α-Al_2O_3 (Superstrate 996), obtained from Coors Ceramics Company. The porous supports were disks of 5 cm diameter, 6 mm thickness 99.8% α-Al_2O_3 and pore size about 0.5 μm also obtained from Coors Ceramics Company.

Synthesis Solution

The solution was prepared using the following components: tetraethylorthosilicate (TEOS, 98% liquid), aluminum foil (99.98%), NaOH (99% pellets), TPAOH (1M solution) all from Aldrich, and deionized water. A clear solution containing SiO_2, TPAOH and NaOH was prepared as follows. First, measured amounts of TPAOH and

NaOH were added to a measured amount of deionized water and the solution was stirred for a few minutes. A measured amount of TEOS was then added dropwise under stirring. After addition of TEOS the mixture usually appeared turbid, but after continuously stirring overnight, the solution became clear for certain compositions. To prepare Al-containing mixtures, a measured amount of aluminum foil was first dissolved into a 33.3 wt% aqueous solution of NaOH, and then the required amount of TPAOH and the balance of H_2O were added. After the solution was stirred for a few minutes, a measured amount of TEOS was added dropwise under stirring. Stirring of the solution was continued overnight.

Hydrothermal Synthesis

The nonporous support plates were fixed horizontally by a Teflon holder within the Teflon liner of a stainless steel autoclave and synthesis solution was added to a level approximately 4 mm above the plate. The porous disks were supported horizontally using a special holder as shown in Figure 2.1. Synthesis solution was added to a level about 1 mm below the top face of the disk. At the synthesis temperature of 175 °C the liquid level was estimated to rise slightly above the top face of the support disk.

After placing the alumina disk or plate and adding the solution, the autoclave was sealed and placed into a constant temperature oven preheated at the synthesis temperature. All syntheses were conducted without stirring. After the specified reaction time was completed, the autoclave was removed from the oven and quenched with tap water. In some cases, several autoclaves using the same synthesis solution and support were placed together in the oven and removed at different times to test the effect of reaction time. After cooling, the support disks or plates were washed thoroughly with water and dried in air at ambient temperature for 12 hours and then at 110 °C for 12 hours.

After hydrothermal synthesis and drying, the porous disks were calcined in stagnant air at 500 °C for 13 hours to free the zeolite from the trapped organic and its decomposition products. Heating to the calcination temperature was at a rate of 1 °C/min but cooling was carried out simply by turning off the power of the furnace.

Characterization

After drying, the bottom (downward facing) surface of the disks was examined by scanning electron microscopy (SEM) using a Camscan instrument operating at 15 kV. SEM was also conducted on the cross section of selected nonporous and porous disks. The cross section was examined by electron probe microanalysis (EPMA) using a JEOL 733 Superprobe.

X-ray diffraction analysis (XRD) was carried out on almost all nonporous disks after drying, and on one porous disk after drying and calcination. As with SEM, only the bottom side of the disks was examined. The instrument used for XRD was a Scintag XDS 2000 diffractometer using Cu-Kα radiation.

Permeation Measurements

Permeation measurements were conducted with H_2, He, N_2, CO_2, CH_4, n-butane and isobutane. The latter two gases have molecular diameters of 5.0 and 5.3 Å (from viscosity data, Hirschfelder et al., 1964) and are suitable for testing the permselectivity of the membrane given the pore dimensions of ZSM-5 which are 5.1 x 5.5 Å for the sinuisoidal channels and 5.4 x 5.6 Å for the straight channels (Szostak, 1989). In view of the small difference between the ZSM-5 pore diameters and the butane diameters it is expected that the 0.3 Å difference in the molecular size of isobutane and n-butane would cause a significant difference in the permeances. The different adsorption isotherms of the two hydrocarbons would also play a significant role on their permeances. A few measurements were also made with neopentane (molecular diameter from viscosity data 5.7 Å, Reed and Gubbins, 1973).

The setup for permeation measurements is shown in Figure 2.2. Each membrane disk after calcination was attached by epoxy cement to a Pyrex holder which was placed inside a larger Pyrex tube and connected to a sensitive pressure transducer and a vacuum line. In pure gas permeation measurements the feed gas was passed continuously at 1.27 atm pressure outside of the membrane holder while the inside of the holder was under vacuum. After allowing sufficient time to establish steady conditions, the inside of the holder was shut off from vacuum and the pressure buildup of the permeating gas was measured by the pressure transducer and stored in the computer. To complete a single measurement the pressure was allowed to reach a few Torr. To repeat a measurement the inside of the holder was once again evacuated and then isolated from vacuum in order to record the pressure rise.

Measurements began by obtaining the permeance of hydrogen. Subsequent contact of the membrane with some hydrocarbon gas resulted in a decline of hydrogen permeance, but after sufficient time under vacuum at 185 °C the permeance recovered to its original value signifying complete desorption of the hydrocarbon. The permeance of hydrogen was thus used to monitor the state of the membrane and ensure complete desorption before permeation measurements for any other gas were initiated. Permeation measurements were carried out at three temperatures 30 °C, 108 °C, and 185 °C. Measurements above 185 °C could not be safely performed because of possible decomposition of the epoxy cement. The molar flowrate through the membrane was calculated from the linear pressure rise $\dot{p}$,

$$\dot{n} = K(T)\ \dot{p}$$

where the coefficient K(T) was obtained for each measurement temperature by suitable calibrations with hydrogen permeation using a bubble flowmeter. This calibration was

possible because hydrogen adsorption was in the Henry's law regime at all temperatures and pressures used.

2.3 Results and Discussion for Zeolite Growth on Nonporous Alumina Plates

The purpose of these experiments was to identify solution compositions that produce zeolite films with complete surface coverage and free of cracks, at least as could be ascertained by SEM. The procedure followed for this purpose was to start from some basic composition and vary the amount of a single component until no further improvement could be obtained. Starting from the composition reached in this way the content of another component was varied until a new composition was reached, etc.

Effect of TEOS Content

In the first set of experiments the amount of TEOS in a three component mixture TEOS-TPAOH-H_2O was varied while keeping the amounts of the other two components constant. The reaction time was also varied as needed to allow sufficient crystal growth. As shown in Table 2.1 TEOS has a strong effect on crystal size and surface coverage. Composition YYA90 with the lowest content of TEOS produced no crystals after 21 hours of reaction. At the other extreme, composition YYS did not form a clear solution. Compositions between the two extremes provided full or partial surface coverage. Even for those compositions (YYA23 to YYA45) producing full coverage, however, the crystals were randomly stacked on each other and had poor intergrowth. Interestingly, crystal size did not change monotonically with the TEOS content but attained a minimum of 0.3 μm at the intermediate composition YYA23.

Effect of H_2O Content

The low dilution used in the previous set of experiments produced excessive crystallization (except for YYA90). To reduce the amounts of crystal mass another series of preparations using much larger dilution were carried out. The TEOS:TPAOH ratio for this series was chosen the same as for YYA22 (Table 2.1) which gave a crystal size of 1.3 μm suitable for membrane preparation on supports with 0.5 μm pore diameter. The results are shown in Figure 2.3 and Table 2.2. Both crystal size and surface coverage vary with the water content. The crystal size goes through a minimum of about 5 μm while the coverage is complete for the first three compositions and becomes incomplete for dilutions 1:6:765 and higher. Although compositions YYA48, YYA76 and YYA65 gave complete surface coverage, composition YYA76 gave somewhat better intergrowth and was retained as a basis for the next set of experiments.

Effect of NaOH

Without NaOH in the synthesis solution the crystals were always coffin-shaped for temperatures between 110 and 175 °C. Introducing NaOH as an additional component while maintaining the amounts of TEOS, TPAOH and H_2O equal to those of composition YYA76 (Table 2.2), we obtained the results shown in Table 2.3 and Figure 2.4. Increasing the NaOH content gradually changed the crystals from coffin-shaped to right parallelepipeds. The crystal size also gradually decreased but the surface coverage did not change monotonically. Compositions with high and low NaOH content failed to give good coverage, but the two intermediate compositions YYA107 and YYA108 produced full coverage and good intergrowth. Variation of the NaOH content in these experiments changes the pH as well as the Na^+ concentration. Increasing alkalinity is known to increase the nucleation rate and produce crystals of smaller size and smaller aspect ratio (Fegan and Lowe, 1986; Hayhurst et al., 1988). The results of Table 2.3 are consistent with this known trend. The presence of sodium ions has multifaceted effects

on crystal size and morphology (Mostowicz and Berak, 1985; Nastro et al., 1985; Gabelica et al., 1985). For syntheses utilizing TPA^+, the presence of Na^+ is known to decrease the nucleation and crystallization rates, but in the experiments listed in Table 2.3 the simultaneous change of Na^+ and alkalinity does not permit clear-cut comparisons with the known trends.

Effect of Al

In this last set of experiments Al was introduced as an additional component while maintaining all other components at the relative amounts specified by composition YYA108 of Table 2.3 which had produced useful crystal size, full coverage, and good intergrowth. The results are shown in Table 2.4. Only for very low Al content the solution remained clear upon mixing. The mixtures which became cloudy were allowed to settle and the clear supernatant part was used for the hydrothermal synthesis (YYA139 and YYA129). The three compositions of Table 2.4 gave films of comparable crystal size and coverage. As shown in Figure 2.5, the shape of the crystals was similar to that without Al consistent with a previous observation by Mostowicz and Berak (1985) that Al did not affect the shape or size of ZSM-5 crystals formed from TPA^+-containing mixtures. To examine further the role of Al, the course of crystallization for YYA129 was followed by SEM. As shown in Figure 2.6, an amorphous blanket was initially formed uniformly on the substrate, then crystal features appeared that resulted finally in a well-intergrown polycrystalline zeolite film. By contrast, in the absence of Al, the course of crystallization was different. After two hours of reaction many small particles were observed on the substrate (top of Figure 2.7) and shown by XRD to be ZSM-5 crystals. At longer times these crystals increased in size and additional crystals appeared and finally formed a well-intergrown film. Comparison of the SEM pictures of Figures 2.6 and 2.7 suggest somewhat better intergrowth for the materials shown in Figure 2.6,

consequently, the Al-containing compositions were chosen for membrane preparations on porous supports.

As mentioned earlier an initially clear solution was employed before each hydrothermal synthesis. Although perhaps not essential, the clear solution facilitates uniformity of composition across the surface of the support and is more conducive to experimental reproducibility.

2.4 Results and Discussion for Zeolite Membranes Grown on Porous Disks

Three membranes were prepared, M1, M2 and M3 with a clear synthesis solution of composition TPAOH–6SiO_2–571H_2O–4NaOH–0.005 Al_2O_3 (very close to YYA128). Of those M1 and M2 were prepared as discussed in Experimental Section. Before heating, the synthesis solution was about 1 mm below the top of the disk and probably expanded to just cover the disk at the synthesis temperature. Membrane M3 was prepared by a somewhat different procedure. When the autoclave was opened after the 16-hour hydrothermal reaction, the support disk was found flat at the bottom of the autoclave rather than on the holder. Evidently the disk was not firmly attached on the holder and fell to the bottom of the autoclave during heating to the synthesis temperature. The bottom side of the disk was then polished, placed once more in a fresh solution and hydrothermal reaction was repeated for another 16 hours. After drying and calcination, the top side of the disk was polished to remove material accumulated during the first synthesis exposure and the disk was ready for permeation measurements. Polishing the bottom side after the first synthesis and the top side after the second synthesis were carried out manually using a 600 grit SiC sandpaper. No polishing was employed for membranes M1 and M2.

X-ray diffraction analysis was conducted on all membranes and on the untreated support disks. The XRD patterns of all membranes showed ZSM-5 as the only crystalline phase.

Figure 2.8 shows SEM micrographs of membrane M1 before synthesis (A) and after synthesis (B,C) at two magnifications. Micrographs B and C show a layer of well intergrown crystals of rectangular parallelepiped shape with 4-7 μm sides along the base and 1-3 μm thickness. There is considerable spread in crystal size. Micrograph 2.8D shows the cross section of the membrane (the light side) where the irregular vertical line at the left is the boundary between zeolite layer and epoxy. The boundary between the zeolite layer and the α-Al_2O_3 support suggests that the crystals follow the contour of the support and probably penetrate into the pore mouths of the support forming a transition layer of interspersed ZSM-5 and α-Al_2O_3. This transition layer may be responsible for the good stability of the membrane during the slow heating to the calcination temperature of 500 °C and the subsequent fast cooling to room temperature.

Figure 2.9 shows an EPMA trace of the membrane cross section. The Si:Al ratio provides an approximate measure of the zeolite layer thickness and of the depth of penetration into the porous support. The Si:Al ratio starts at about 300 at the top of the crystal layer and declines to about10 within 10 μm distance from the top. This part of the layer clearly lies outside of the pores and the Al content is due to zeolitic Al. The approximately 10 μm thickness of the layer lying outside of the support is consistent with the SEM micrograph in Figure 2.8D. In the succeeding region the Si:Al ratio declines from 10 to 0.1–0.15 within 3 μm. At least part of this transition region must lie inside the pores of the support. Beyond that point, the Si:Al ratio fluctuates between 0.1–0.15 for the remaining 20 μm of the cross section examined, with the variation probably due to the porous nature of the substrate.

Taking into account the void fraction of the substrate (0.20) and the densities of Al_2O_3 (3.96 g/cm^3) and ZSM-5 (about 1.8 g/cm^3), we estimate that a Si:Al ratio of 0.1-0.15 could be as much as 80% of the pore volume if occupied by ZSM-5. The internal silica-containing material could, of course, be amorphous or mixed amorphous-crystalline. The content of Si within the 20 μm depth from the surface is far higher than the Si content of the initial solution imbibed into the pores (the latter would give a Si:Al ratio of 0.0046). Clearly then siliceous clusters or particles must be adsorbed from the bulk solution onto the pore surface. In another EPMA measurement, significant Si signal was observed as far as 80 μm from the substrate surface. The core of the substrate, however, was essentially free of Si indicating significant diffusional hindrance to the penetration of silica containing species. Amorphous particles similar to those identified by Jansen et al. (1993) and Koegler et al. (1994) or other siliceous material adsorbed on the pore surface near the external surface of the substrate could have hindered deeper penetration into the interior.

Permeation Measurements for Membrane M1 and M2

Permeation measurements for membrane M1 were conducted only at the two higher temperatures 108 and 185°C with the results shown in Table 2.5. As discussed under Experimental Section, the permeance of H_2 was used to monitor the desorption of any previously adsorbed hydrocarbon gas before a new gas was admitted in the system. At 108°C it took about one hour for the H_2 permeance to recover to its original value after n-butane measurements and more than 3 hours after the isobutane measurements. More interestingly, after neopentane was admitted into the feed side at 458K for about 40 minutes the hydrogen permeance did not fully recover and after 8 hours it was only about 70% of its original value. The strong adsorption of neopentane also explains the subsequent low permeances for N_2 and O_2 at 185 °C (Table 2.5).

A few permeation measurements were carried out with membrane M2 to check the reproducibility of membrane properties. The measured permeances are indeed approximately equal to those of membrane M1 (Table 2.6). At the conclusion of these permeation measurements the top face of disk M2 was polished and the hydrogen permeance measured once more at 303 K. The permeance was the same as before polishing showing that any amorphous or crystalline material accumulated on the top face had negligible effect on the membrane properties. For membranes M1 and M2 the synthesis liquid was at most 1 mm above the disk, limiting the amount of accumulation of amorphous or crystalline material on the top surface of the disk.

Permeation Measurements for Membrane M3

Measurements were carried out at 30, 108 and 185 °C with the results listed in Table 2.7. The permeances are much higher than those measured with membrane M1. For example, the hydrogen and the n-butane permeances are about 5-6 and 3 times higher, respectively. Furthermore, the n-butane:isobutane ratio is also much higher than before, about 30 versus 6-9. At this time we do not have sufficient information to determine whether the higher permeance of membrane M3 is due to a thinner external ZSM-5 layer or to a lesser accumulation of material in the pores. Likewise, the higher selectivity of M3 could be attributed to structural differences in the external layer or in the material accumulated inside the pores. These issues will be addressed in our continuing investigations.

At room temperature the permeance of membrane M3 was five to ten times lower and the n-butane:isobutane ratio approximately three times lower than those of selected membranes prepared by other groups. However, instead of decreasing with temperature as with the other membranes the n-butane:isobutane ratio increased with temperature and at 185 °C it reached a value of 31 three times that of the other membranes.

2.5 Conclusions

Supported ZSM-5 membranes were prepared on macroporous α-Al_2O_3 disks by in-situ crystallization from an initially clear solution. The membranes consisted of a 10 μm thick polycrystalline film on top of the substrate, but unidentified material occupied a sizable fraction of the pore volume at a depth of several tens of micrometers below the substrate surface. The n-butane permeance and n-butane:isobutane ratio of these membranes at room temperature was lower than those of selected membranes prepared by other groups. However, the temperature dependence was different with the n-butane to isobutane ratio increasing with temperature. Certain changes in the preparation procedure produced large and as yet unexplained changes in membrane permeance and selectivity.

Acknowledgment

This work was funded by NSF Grant No. CTS-9114829.

References

Bai, C.; Jia, M. ; Falconer, J. L. and Noble, R. D., Preparation and Separation Properties of Silicalite Composite Membranes, Abstract in Third International Conference on Inorganic Membranes, Worcester, Massachusetts, July 10-14, 1994.

Bakker, W. J. W.; Zheng, G.; Kapteijn, F.; Makkee, M. and Moulijn, J. A., Single and Multi-Component Transport through Metal-Supported MFI Zeolite Membranes, in

Precision Process Technology, M. P. C. Weijnen and A. A. H. Drinkenburg (Eds.), Kluwer Academic Publishers, The Netherlands, 1993.

Fegan, S. G. and Lowe, B. M., Effect of Alkalinity on the Crystallization of Silicalite-1 Precursors, Chem. Soc., Faraday Trans. 1986, 82, 785.

Gabelica, Z., Cavez-Bierwan, M., Bodart, P., Gourgue, A. and Nagy, J. B., Nature and Structure of High Silica Zeolites Synthesized in Presence of (Poly) Alkyl Mono- and Diamines, in Zeolites, Studies in Surface Science and Catalysis 1985, No. 24, 55.

Geus, E. R.; Bakker, W. J. W.; Verheijen, P. J. T.; den Exter, M. J.; Moulijn, J. A. and van Bekkum, H., Permeation Measurements on In Situ Grown Ceramic MFI Type Films, in Proceedings from the Ninth International Zeolite Conference, R. von Ballmoos, J. B. Higgins and M. M. J. Treacy (Eds.), Butterworth-Heinemann, Boston, 1993a.

Geus, E. R.; den Exter, M. J. and van Bekkum, H., Synthesis and Characterization of Zeolite (MFI) Membranes on Porous Ceramic Supports, J. Chem. Soc. Faraday Trans. 1992, 88, 3101.

Geus, E. R.; van Bekkum, H.; Bakker, W. J. W. and Moulijn, J. A., High-Temperature Stainless Steel Supported Zeolite (MFI) Membranes: Module Construction, and Permeation Experiments, Microporous Materials, 1993b, 1, 131.

Hayhurst, D. T., Nastro, A., Aiello, R., Crea, F. and Giordano, G., Effect of Hydroxide on Growth Rate and Morphology in Silicalite Synthesis, Zeolites 1988, 8, 416.

Hirschfelder, J. O.; Curtiss, C. F. and Bird, R. B., Molecular Theory of Gases and Liquids, Wiley, New York, 1964.

Jansen, J. C.; Nugroho, W. and van Bekkum, H., Controlled Growth of Thin Films of Molecular Sieves on Various Supports, in Proceedings from the Ninth International Zeolite Conference, R. von Ballmoos, J. B. Higgins and M. M. J. Treacy (Eds.), Butterworth-Heinemann, Boston, 1993.

Jia, M.; Chen, B.; Noble, R. D. and Falconer, J., Ceramic-Zelite Composite Membranes and their Application for Separation of Vapor/Gas Mixtures, J. Membr. Sci., 1994, 90, 1.

Kärger, J. and Ruthven, D. M., Diffusion in Zeolites, Wiley-Interscience, New York, 1992.

Koegler, J. H.; Zandbergen, H. W.; Harteveld, J. L. N.; Nieuwenhuizen, M. S.; Jansen, J. C. and van Bekkum, H., Oriented Coatings of Silicalite-1 for Gas Sensor Applications, Studies in Surface Science and Catalysis, Vol. 84, 1994.

Ma, Y. H. and Xiang, S., Formation of Zeolite Membranes from Sols, Patent PCT/US 9302384.

Mostowicz, R. and Berak, J. M., Factors Influencing the Crystal Morphology of ZSM-5 Type Zeolites, in Zeolites, Studies in Surface Science and Catalysis 1985, No. 24, 65.

Myatt, G. J.; Budd, P. M.; Price, C. and Carr, S. W., Synthesis of a Zeolite NaA Membrane, J. Mater. Chem., 1992, 2, 1103.

Nastro, A., Collella, C. and Aiello, R., Synthesis of ZSM-5-Type Zeolites in the System $(Na,K)_2O$-Al_2O_3-SiO_2-H_2O without and with TPBr, in Zeolites, Studies in Surface Science and Catalysis 1985, No. 24, 39.

Reed, T. M. and Gubbins, K. E., Applied Statistical Mechanics, McGraw-Hill, New York, 1973.

Sano, T., Kiyozumi, Y.; Maeda, K.; Toba, M.; Niwa, S. and Mizukami, F., in Proceedings of Ninth International Zeolite Conference, R. von Ballmoos, J. B. Higgins and M. M. J. Treacy (Eds.), Butterworth-Heinemann, Boston, 1993.

Sano, T.; Kiyozumi, Y.; Kawamura, M.; Mizukami, F.; Takaya, H.; Mouri, T.; Inaoka, W.; Toida, Y.; Watanabe, M. and Toyoda, K., Preparation and Characterization of ZSM-5 Zeolite Film, Zeolites, 1991, 11, 842.

Szostak, R., Molecular Sieves, Van Nostrand, New York, 1989.

Tsikoyiannis, J. G. and Haag, W. O., Synthesis and Characterization of a Pure Zeolitic Membrane, Zeolites, 1992, 12, 126.

Vroon, Z.A.E.P.; Keizer, K.; Verweij, H. and Burggraaf, A. J., Transport Properties of a Ceramic Thin Zeolite MFI Membrnae, preprint presented in Third International Conference on Inorganic Membranes, Worcester, Massachusetts, July 10-14, 1994.

Xiang, S. and Ma, Y. H., Formation and Characterization of Zeolite Membranes from Sols, Abstract in Third International Conference on Inorganic Membranes, Worcester, Massachusetts, July 10-14, 1994.

Table 2.1. Effect of TEOS content on zeolite crystal layer formed on a nonporous alumina plate at 175 °C.

Sample no.	Solution composition[a]	Crystallization time (h)	Crystals on plate			
			Shape	Size[b] (μm)	Coverage	Intergrowth[c]
YYA90	1.0 : 0.5 : 96.4	21.0	no crystals formed			
YYA24	1.0 : 1.0 : 96.4	6.0	prismatic	4.0	partial	poor
YYA23	1.0 : 3.0 : 96.4	5.0	prismatic	0.3	full	poor
YYA22	1.0 : 6.0 : 96.4	5.0	prismatic	1.3	full	poor
YYA41	1.0 : 7.5 : 96.4	4.0	prismatic	6.0	full	poor
YYA45	1.0 : 8.5 : 96.4	4.0	prismatic	5.0	full	poor
YYS	1.0 : 9.5 : 96.4		no clear solution formed			

[a] molar ratio TPAOH : TEOS : H_2O

[b] dimension estimated along c axis

[c] judged from the morphology of the top layer

Table 2.2. Effects of H_2O content on morphology of the zeolite layer formed on nonporous alumina plates at 175 °C.

Sample no.	Solution composition[a]	Crystallization time (h)	Crystals on plate			
			Shape	Size[b](μm)	Coverage	Intergrowth[c]
YYA48	1 : 6 : 525	14.0	prismatic	11.3	full	ok
YYA76[d]	1 : 6 : 565	23.0	prismatic	5	full	good
YYA65	1 : 6 : 712	10.0	prismatic	11.3	full	ok
YYA64	1 : 6 : 765	22.0	prismatic	13.6	partial	bad
YYA61	1 : 6 : 885	21.0	prismatic	15.9	partial	bad
YYA46	1 : 6 : 1005	14.0	prismatic	18.6	partial	bad

[a] molar ratio TPAOH : TEOS : H_2O

[b] dimension estimated along c axis

[c] judged from the morphology of the top layer

[d] crystallization at 150°C

Table 2.3. Effect of NaOH on crystallization of silicalite on nonporous alumina plate (crystallization temperature 175 °C) with amount of TPAOH and TEOS fixed and amount of water approximately constant.

Sample no.	Solution composition[a]	Crystallization time (h)	Crystals on plate			
			Shape	Size[b] (μm)	Coverage	Intergrowth
YYA76[c]	1: 6 : 565 : 0	23.0	prismatic	5	full	good
YYA107	1: 6 : 578 : 3	18.0	cubes	2.8	full	good
YYA108	1: 6 : 583 : 4	9.0	cubes	1.2	full	good
YYA91	1: 6 : 591 : 6	16.5	no crystals formed			

[a] molar ratio TPAOH : TEOS : H_2O : NaOH

[b] dimension estimated along a or b axis

[c] crystallization at 150 °C

Table 2.4. Effect of Al on crystallization of ZSM-5 on nonporous alumina plate (crystallization temperature 175°C) with amounts of TPAOH, TEOS, H_2O and NaOH fixed.

Sample no.	Solution composition[a]	Crystallization time (h)	Crystals on plate			
			Shape	Size[b] (μm)	Coverage	Intergrowth
YYA128	1: 6 : 583 : 4 : 0.01	9.5	cubes	4.2	full	excellent
YYA139[c]	1: 6 : 583 : 4 : 0.04	9.5	cubes	4.2	full	excellent
YYA129[c]	1: 6 : 583 : 4 : 0.06	24.0	cubes	4.2	full	excellent

[a] molar ratio TPAOH : TEOS : H_2O : NaOH : Al

[b] dimension estimated along a or b axis

[c] clear solution was used after sedimentation

Table 2.5. Pure gas permeation measurements for membrane M1

T(K)	Permeances (10^{-8} mol/m^2-s-Pa)							Permeance Ratios		
	H_2	n-C_4H_{10}	i-C_4H_{10}	neo-C_5H_{12}	N_2	O_2	CO_2	n-C_4H_{10}/i-C_4H_{10}	CO_2/N_2	O_2/N_2
381	1.86	1.11	0.178	---	1.09	0.972	2.55	6.2	2.3	0.89
458	1.81	1.73	0.184	0.169	0.516*	0.595*	1.94*	9.4	3.7	1.15

* Permeances measured after the neo-pentane measurement

Table 2.6. Pure gas permeation measurements for membrane M2

T(K)	Permeance (10^{-8}mol/m^2-s-Pa)			Permeance Ratios
	H_2	n-C_4H_{10}	i-C_4H_{10}	n-C_4H_{10}/i-C_4H_{10}
303	1.00			
381	1.83			
458	2.09	1.45	0.133	10.9

Table 2.7. Pure gas permeation measurements for membrane M3

T(K)	Permeance (10^{-8} mol/m^2-s-Pa)								Permeance Ratios			
	H_2	n-C_4H_{10}	i-C_4H_{10}	N_2	O_2	CO_2	CH_4	He	n-C_4H_{10}/i-C_4H_{10}	H_2/i-C_4H_{10}	CO_2/N_2	O_2/N_2
303	6.19	0.75	0.041	3.16	3.68	8.77	3.73	3.00	18.4	151	2.8	1.16
381	9.01	3.40	0.120	4.79	4.51	9.43	7.96	4.33	28.3	75.2	2.0	0.94
458	10.1	5.85	0.188	4.02	4.10	7.39	7.34	4.97	31.1	53.9	1.8	1.02

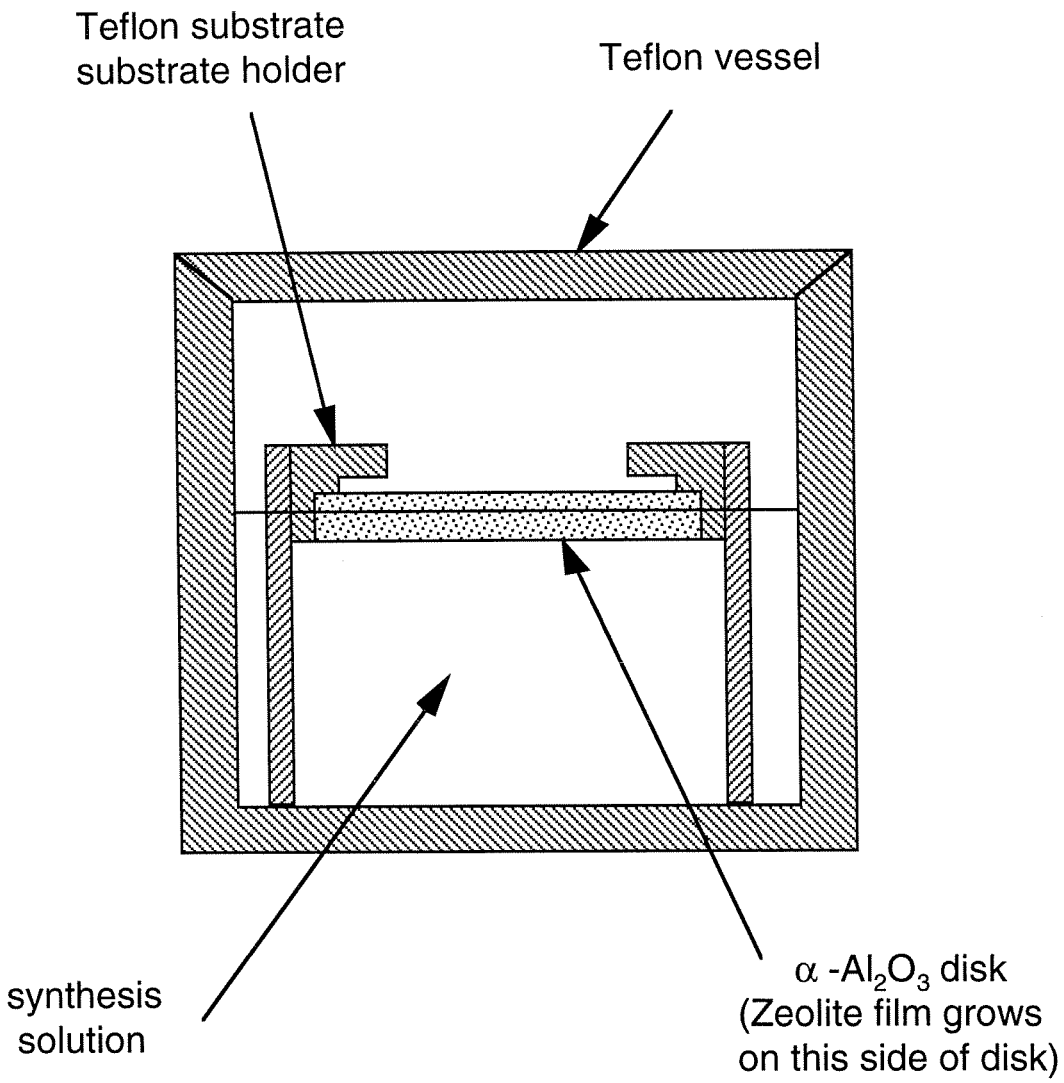

Figure 2.1 Cross-sectional view of synthesis autoclave showing placement of porous support disk.

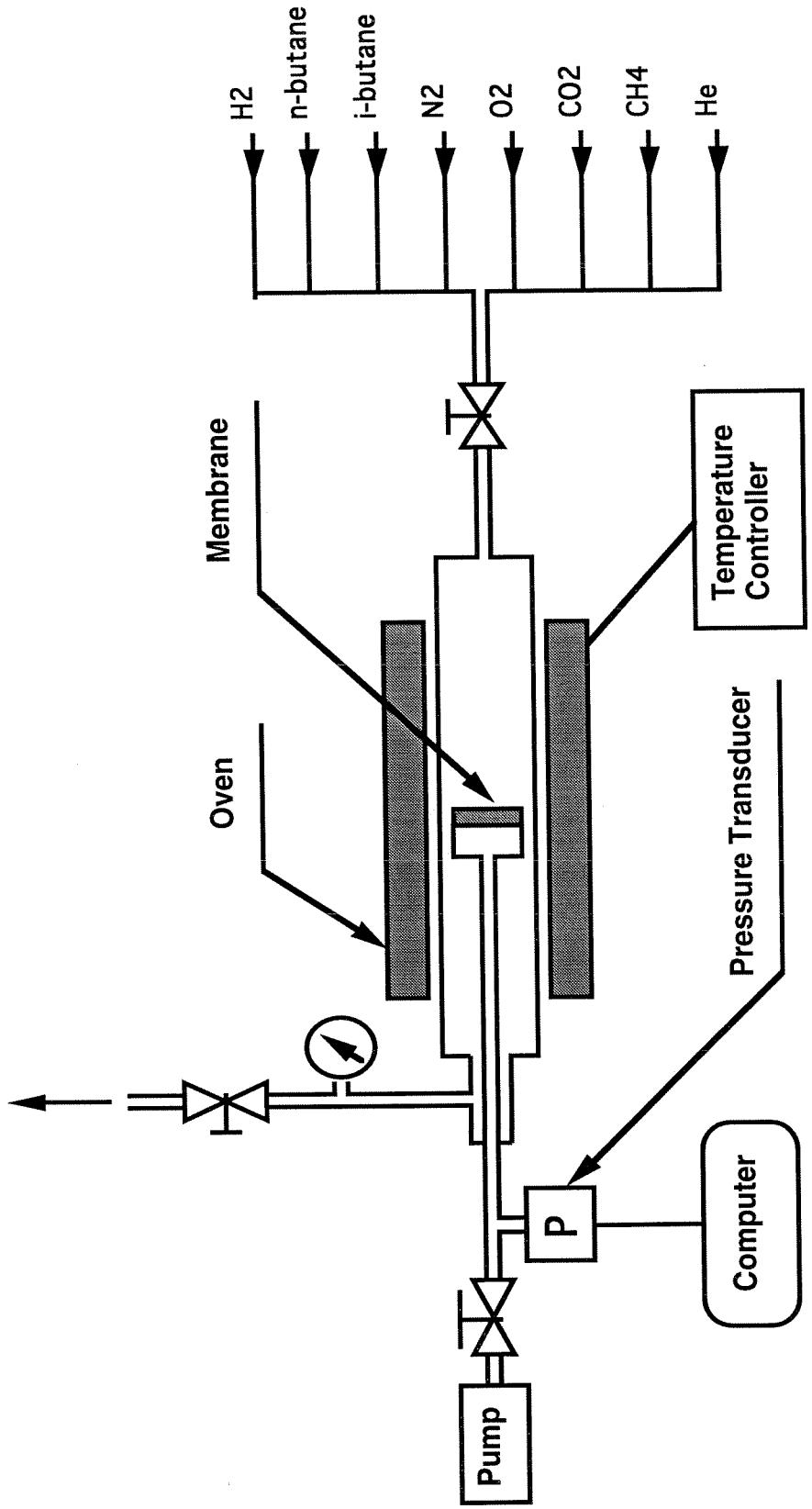

Figure 2.2 Apparatus for gas permeation measurements.

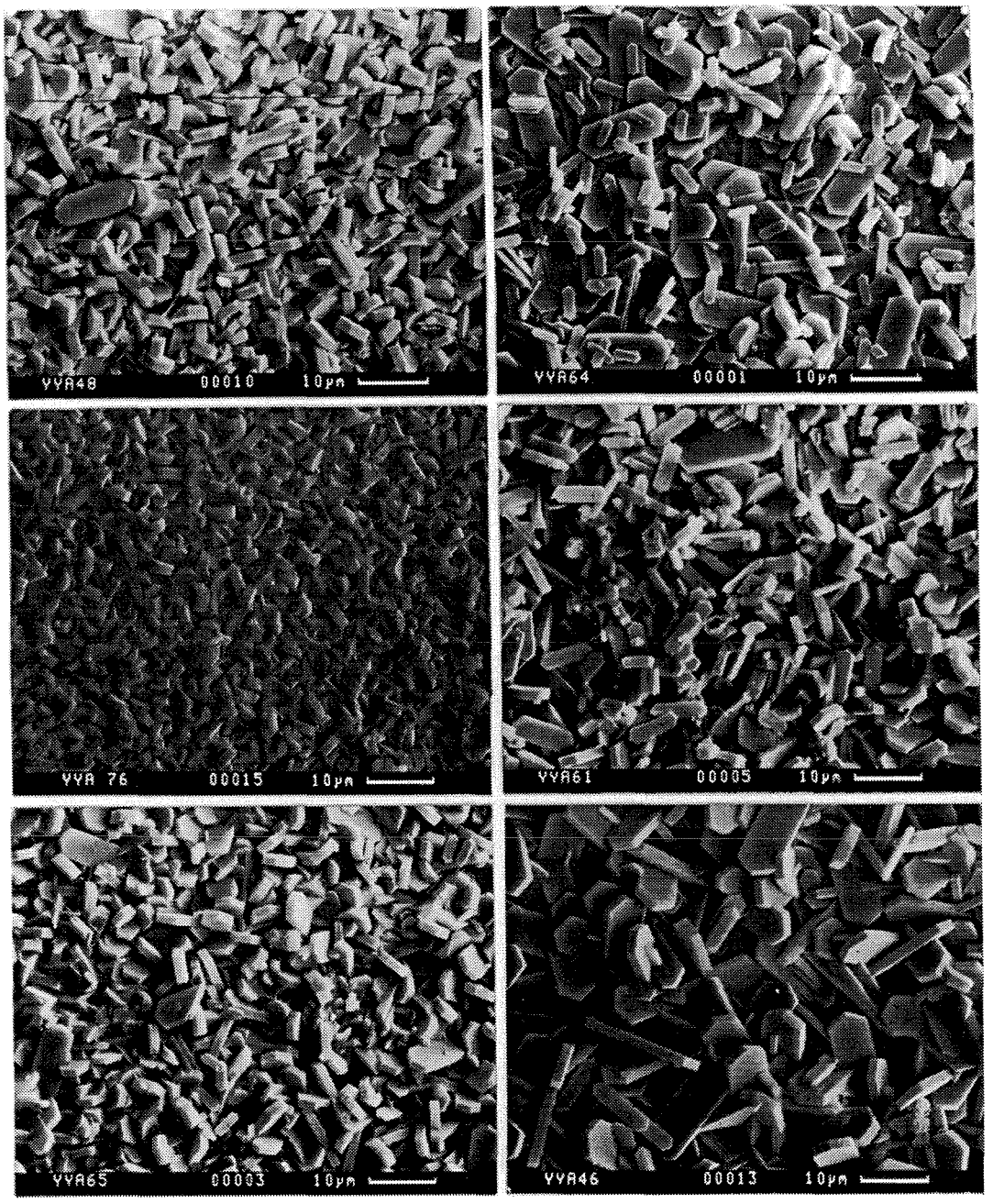

Figure 2.3 SEM micrographs of films prepared using solutions of different H_2O content. Codes defined in Table 2.2.

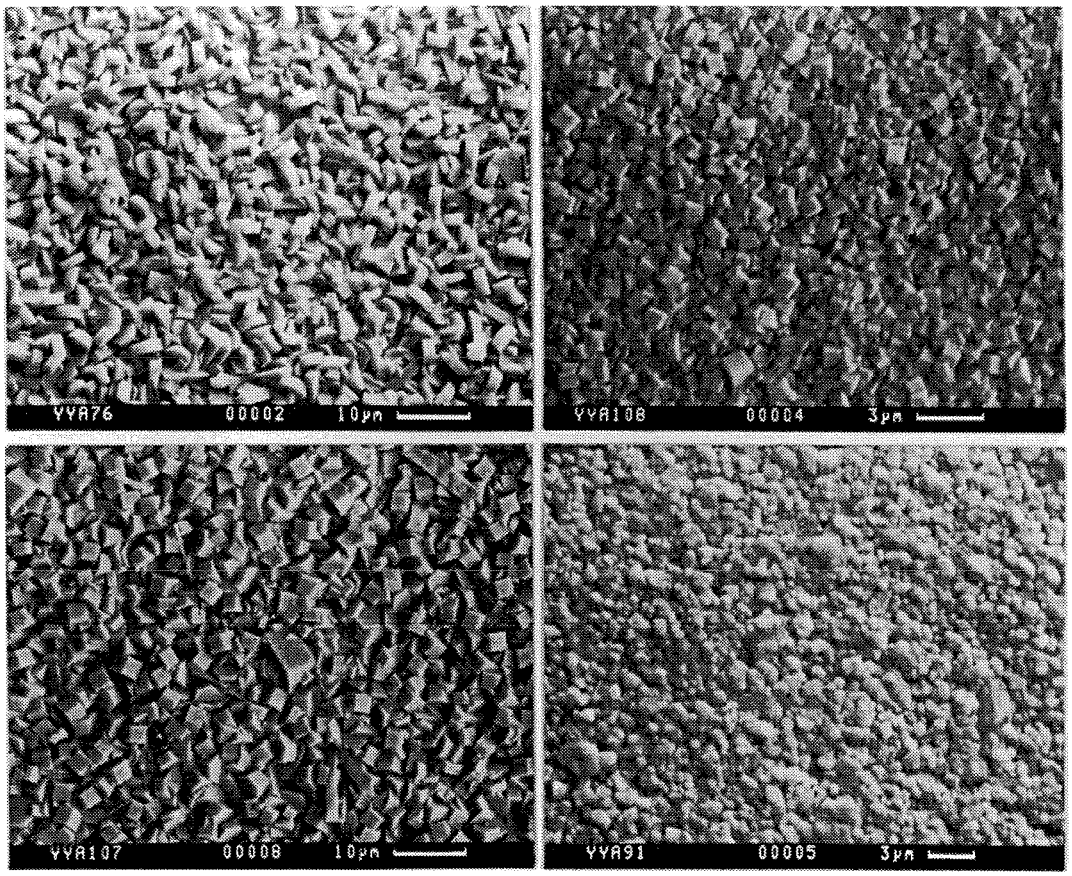

Figure 2.4 SEM micrographs of films prepared using solutions of different NaOH content. Codes defined in Table 2.3.

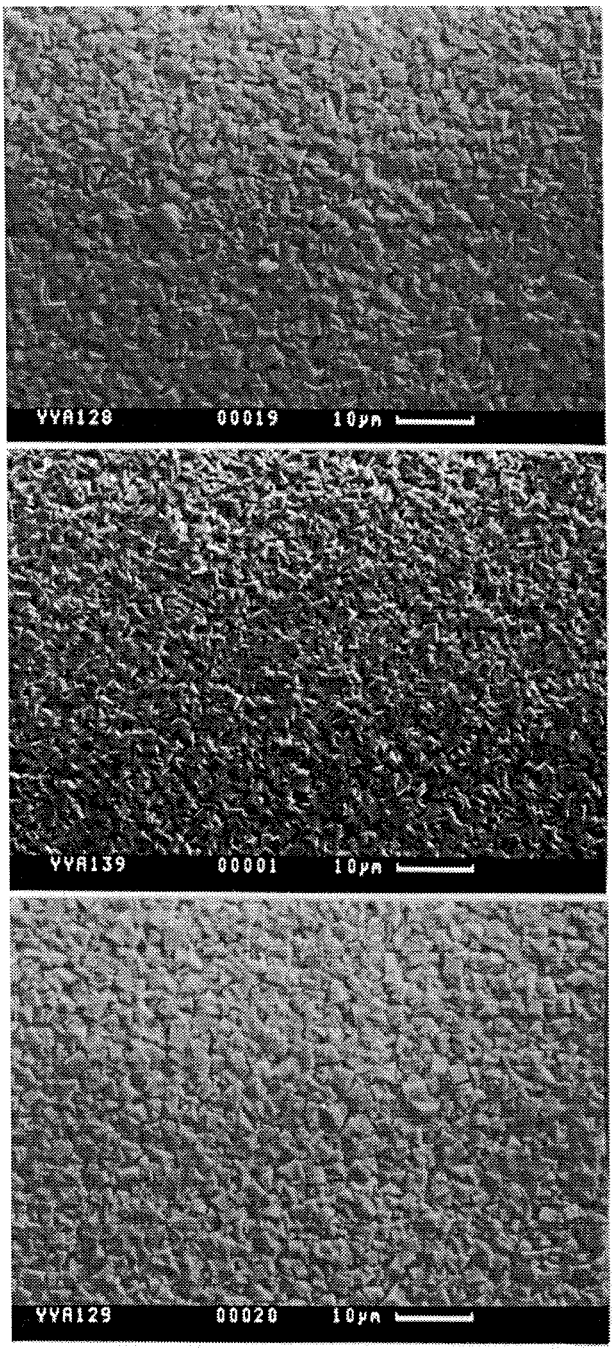

Figure 2.5 SEM micrographs of films prepared using solutions of different Al content. Codes defined in Table 2.4.

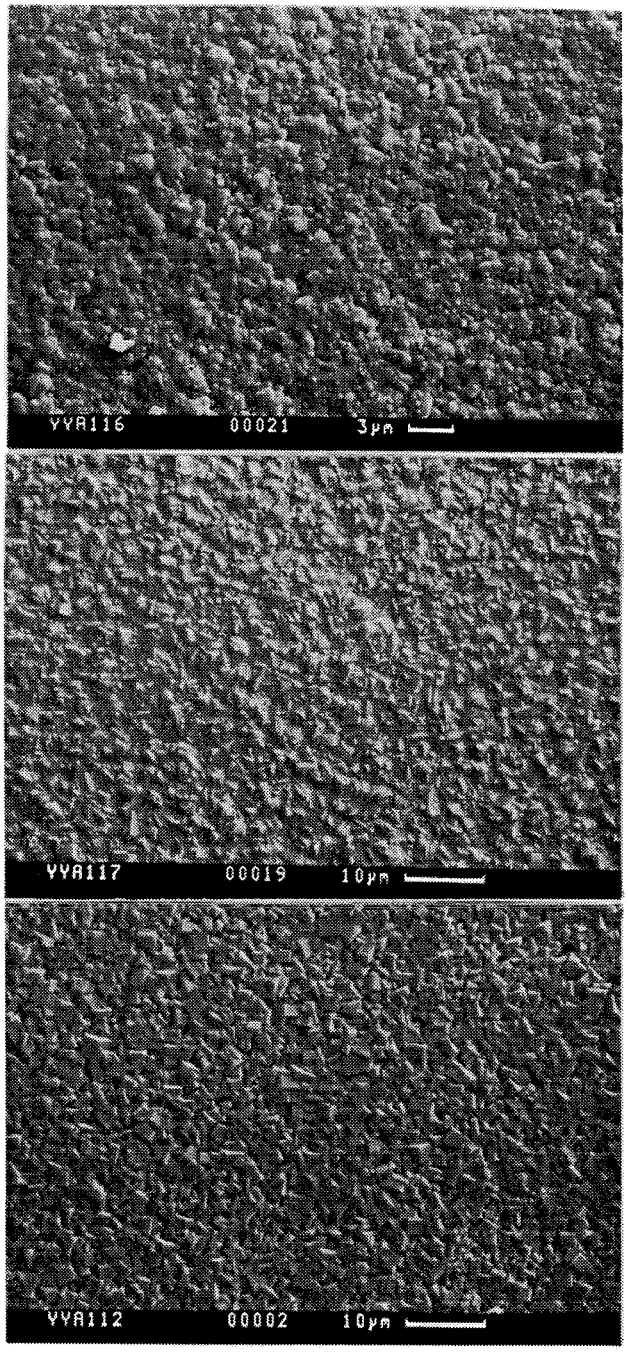

Figure 2.6 SEM micrographs showing the evolution of a film prepared in the presence of Al. YYA116, 3h; YYA117, 4.5h; YYA112, 25h.

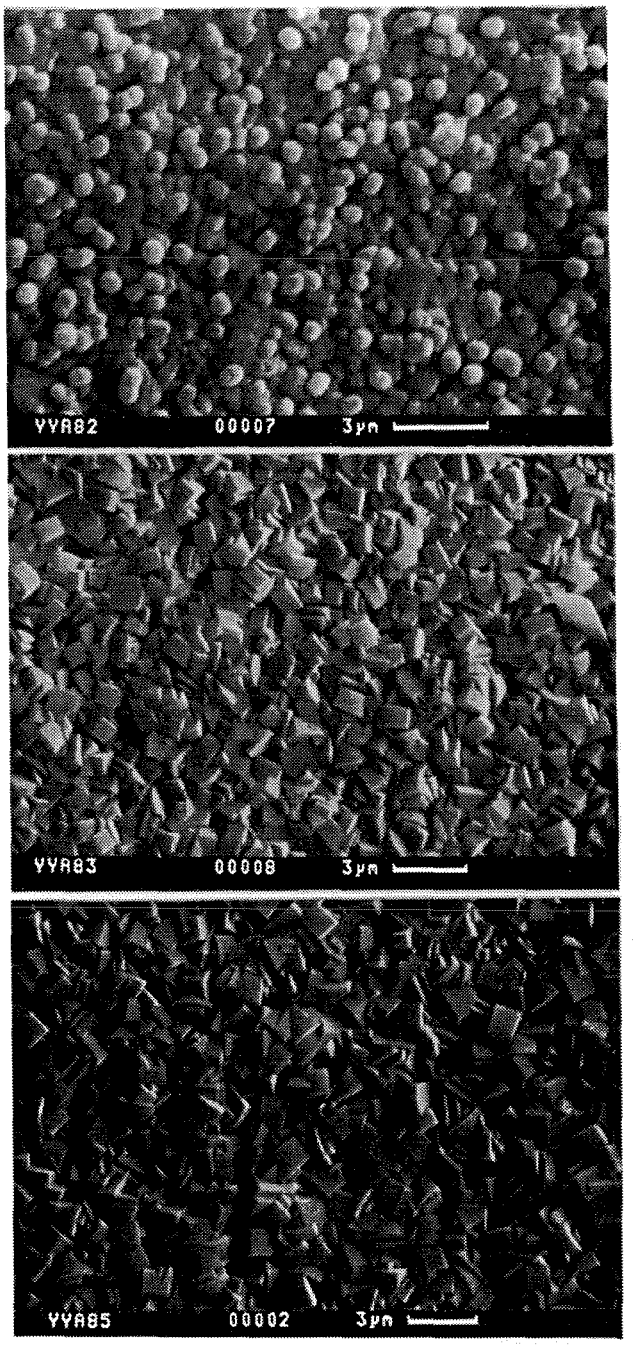

Figure 2.7 SEM micrographs showing the evolution of a film prepared in the absence of Al. YYA82, 2h; YYA83, 3h; YYA85, 12.5h.

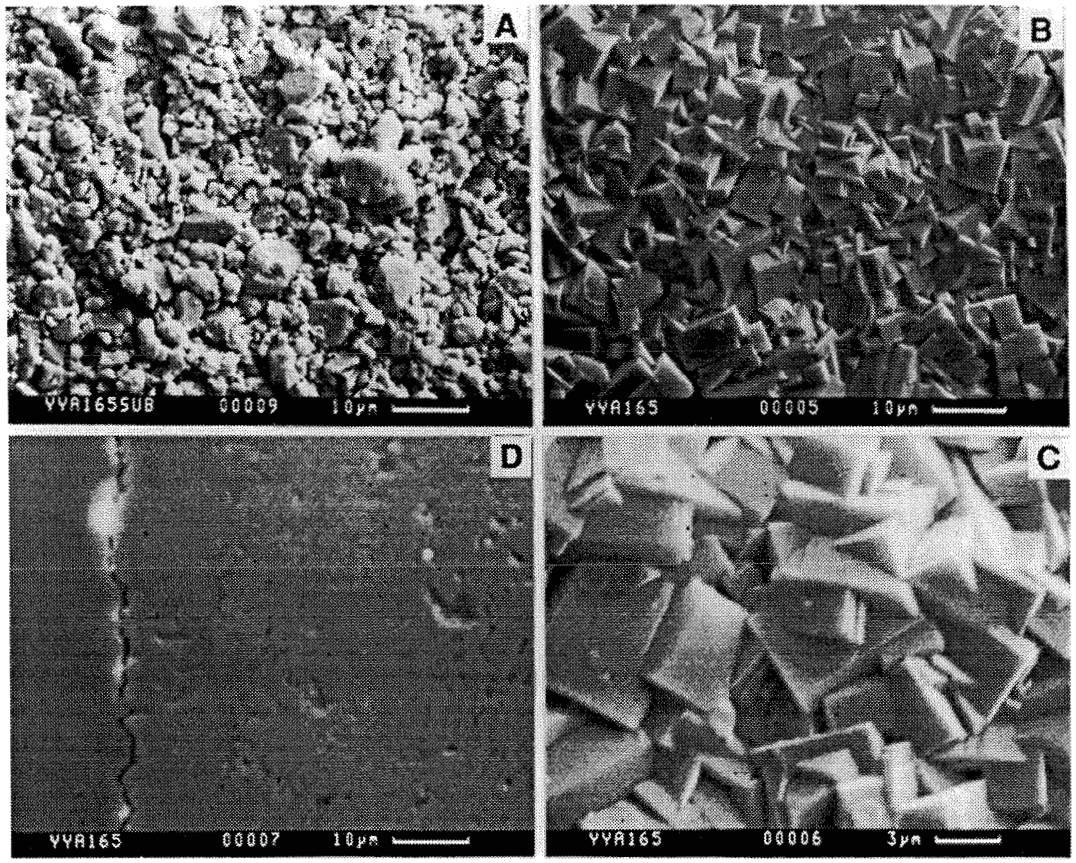

Figure 2.8 SEM micrographs of membrane M1 before synthesis (A) and after synthesis (B,C) at two different magnifications. Micrograph D shows the cross section of the membrane.

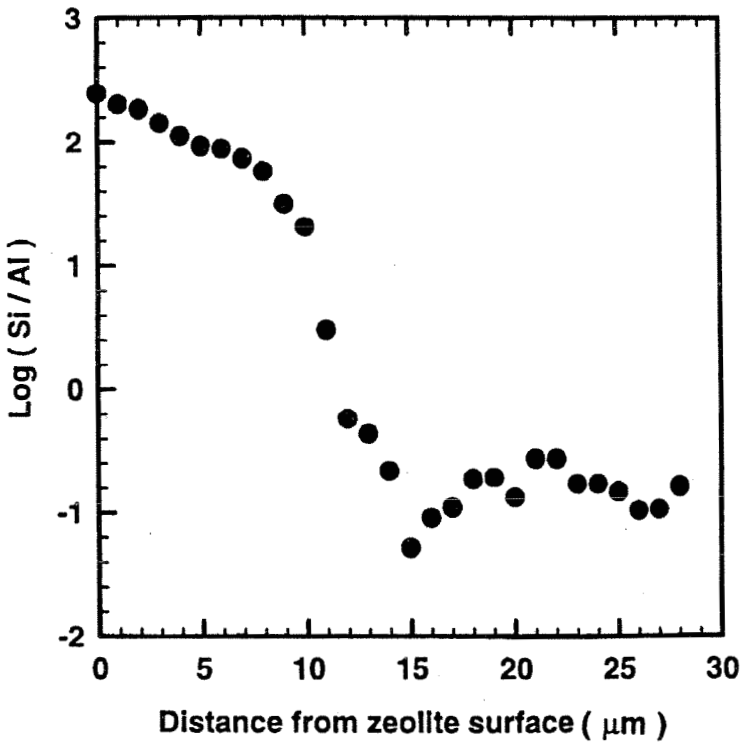

Figure 2.9 EPMA trace of the Si:Al ratio over the cross section of membrane M1

Chapter 3

Use of Diffusion Barriers in the Preparation of Supported Zeolite ZSM-5 Membranes

Reprinted with permission from the article

[Yushan Yan, Mark E. Davis, and George R. Gavalas, **Journal of Membrane Science**, in press]

Use of Diffusion Barriers in the Preparation of Supported Zeolite ZSM-5 Membranes

Yushan Yan, Mark E. Davis, and George R. Gavalas

Chemical Engineering, California Institute of Technology

Pasadena, CA91125

Abstract

Zeolite ZSM-5 membranes were prepared by in situ crystallization on porous α-Al_2O_3 disks that contained a diffusion barrier to limit excessive penetration of siliceous species into the alumina pores. The barrier was introduced into the alumina pores by impregnating the porous disk with a 1:1 molar mixture of furfuryl alcohol (FA) and tetraethylorthosilicate (TEOS), polymerizing the mixture retained in the disk, and carbonizing the resulting polymer at 600 °C in N_2. Following carbonization, a partial carbon burnoff was carried out by catalyzed oxidation in 2% O_2-N_2 at 600 °C to generate a carbon-free region near the surface of the support. After zeolite crystallization the remaining carbon and the organic structure directing agent were removed by calcination in air at 500 °C. It was found that pure carbon does not support zeolite growth while the solid obtained from a mixture of FA and TEOS does due to the presence of dispersed silica. Membranes synthesized using barriers have n-butane flux and n-butane/isobutane selectivity 2.7×10^{-3} mol/m^2-s and 45 at 185 °C which are, respectively, about 1.6 and 4 times as large as those of membranes prepared without the use of barriers. Electron probe microanalysis (EPMA) and X-ray diffraction (XRD) revealed that the internal layer of the

barrier-pretreated membrane has smaller thickness and higher crystallinity accounting for the increased flux and selectivity.

3.1 Introduction

Several groups have recently prepared supported ZSM-5 or silicalite membranes having attractive permeation properties (1-8). For example, n-butane/isobutane selectivities as high as 90 at room temperature and 10 at 200 °C were achieved with corresponding n-butane fluxes of 2-4 MFU (1 MFU=10^{-3} mol/m^2-s) at room temperature and 12 MFU at 350 °C (1-5). In each case the transmembrane pressure difference was in the range 50-100 kPa. The flux ratio of n-butane to isobutane has been used in several of these studies as a measure of membrane quality. For, with a kinetic diameter of 0.43 nm for n-butane and 0.50 nm for isobutane, and with the pore diameter of ZSM-5 0.55 nm, a high n-butane/isobutane flux ratio suggests the virtual absence of cracks or pores of diameter much above 0.55 nm.

To achieve the aforementioned fluxes and selectivities in the aforementioned studies it was usually necessary to prepare the membranes using two or more repeated crystallizations. Our group has prepared ZSM-5 membranes using single crystallization and double crystallization (9). The membrane prepared with a single crystallization had relatively low n-butane flux and n-butane/isobutane selectivity, 2.7 MFU and 9 at 185 °C and 100 kPa Δp. The double crystallization involved first removing part of the membrane layer by polishing and then carrying out a second crystallization (9). This procedure yielded a membrane with n-butane flux 5.85 MFU and n-butane/isobutane selectivity 31 at 185 °C and 100 kPa Δp. Electron probe microanalysis (EPMA) of the cross section of a single-crystallization membrane on an α-alumina disk of 0.5 μm mean pore diameter revealed a 10 μm fully crystalline layer on top of the support and additional crystalline or

amorphous silica extending 30 μm or deeper inside the pores of the support. Although the effect of the internal siliceous layer on the permeances and selectivities of the membrane was not quantified, it is quite reasonable to expect that it adds significant resistance to permeation and degrades the separation selectivity. In fact, the aforementioned improvement of flux as well as selectivity by polishing followed by a second crystallization could be largely due to a thinner and/or more crystalline internal layer.

The thickness of the internal layer can probably be reduced by using supports of smaller pore diameter. However membranes prepared in our laboratory using α-Al_2O_3 supports of 0.1 μm pore size were defective having no n-butane/isobutane selectivity. Another means to limit the thickness of the internal layer is by using some temporary diffusion barrier that is introduced into the pores before zeolite crystallization and removed from the pores after the crystallization is completed.

Temporary carbon barriers have been used previously by our group to prepare hydrogen permselective membranes by chemical vapor deposition of silica on mesoporous Vycor supports (10). The carbon barrier was introduced into the pores of Vycor by vapor deposition polymerization of furfuryl alcohol followed by curing and carbonization of the resulting poly(furfuryl alcohol). Furfuryl alcohol was chosen as the carbon precursor because of its simple polymerization and the relatively high carbon yield obtained upon carbonization of the poly(furfuryl alcohol) polymer. In this paper we report the use of temporary barriers in preparing ZSM-5 membranes. There are significant differences between the two applications, however. One major difference is that for zeolite synthesis, the barrier must not occupy the complete pore space; a thin carbon-depleted region must be available for bonding of zeolite on the support. The surface properties of the carbonaceous barrier also seem to be important for a crack-free membrane. This paper will consequently focus on the procedure for introducing the barrier and the effect of the barrier on the properties of the resulting membranes.

3.2 Experimental

Support

The supports were porous α-Al_2O_3 (99.8%) disks of 5 cm diameter, 6 mm thickness, and about 0.5 μm mean pore diameter obtained from Coors Ceramic Company. Before zeolite synthesis, all supports were pretreated according to the following procedures:

Polishing and ultrasonication. One face of the porous disk was polished with 600 grit sand paper from Buehler after which the disk was cleaned in water in a Branson 1200 ultrasonic cleaner for about 5-10 minutes to remove loose particles created during polishing. The disk was then dried at 110 °C for about 24 hours.

Polymerization and carbonization. The polished and dried disk was immersed in neat FA or in a 1:1 molar mixture of FA and TEOS for 12 hours at room temperature. After the disk was removed from the liquid it was placed horizontally with the polished face up on a paper towel at room temperature until the polished surface appeared dry. To start polymerization, the disk was transferred into a 2 M p-toluenesulfonic acid solution preheated to 90 °C in a sealed container. The disk was suspended in the acid solution horizontally with the polished surface facing the bottom of the container. After allowing 1 hour for polymerization, the disk was removed from the acid solution and placed in flowing N_2 first at 90 °C for 12 hours and then at 200 °C for 3 hours to cure the polymer. The disk was then cooled to room temperature, dipped in a 0.5 M calcium acetate solution for 10 seconds, and dried at 110 °C for about 12 hours. Finally, the disk was heated in flowing N_2 at 600 °C for 2 hours to carbonize the polymer. The curing step (3 hours at 200 °C) was performed to increase polymer crosslinking which is necessary to

obtain high carbon yield (11). Curing also decreases penetration of the calcium used as catalyst for selective carbon burnoff.

Selective carbon burnoff Immediately following carbonization, the sample was exposed to a flow of 2% O_2-N_2 at 600 °C for specified lengths of time to selectively burn off the carbon on the external surface of the support and within a certain depth inside the pores. The depth of burnoff is determined by the length of the oxidation period and by the distribution of calcium which is a catalyst for carbon oxidation (12). The purpose of the carbon burnoff is to create a carbon free region near the surface of the support and to expose silica inclusions formed from the FA-TEOS precursor. After the selective burnoff, the support was cooled down to room temperature and soaked in warm water for several hours to leach any free Ca^{2+} which might interfere with the subsequent zeolite synthesis. The support was finally dried at 110 °C for 24 hours.

Hydrothermal Synthesis

The details of the hydrothermal synthesis have been described previously (9). Briefly, the support disk was placed in a Teflon-lined stainless steel autoclave containing a clear solution of composition $100(TPA)_2O : 400Na_2O : Al_2O_3 : 1200SiO_2 : 114200H_2O$. The support was fixed in a horizontal orientation with the polished side of the disk facing the bottom of the autoclave and the gas-liquid interface at approximately the midpoint of the disk. In this geometry the crystal layer grew on the bottom face of the disk. Synthesis was carried out at 175 °C for 16 hours under autogenous pressure without stirring. At the end of the synthesis the disk was removed from the autoclave, dried at 110 °C for 12 hours and calcined at 500 °C in stagnant air for 15 hours. Finally, the top face of the calcined disk was polished to remove any zeolite grown on that face before permeation measurements were carried out.

Permeation Measurements

Details of the apparatus and procedures for the permeation measurements were given elsewhere (9). Permeation measurements were conducted only for n-butane, isobutane and H_2, in most cases at temperatures of 185 °C. Lower temperatures were not used to avoid the need for lengthy desorption periods. Caution has been exercised to desorb hydrocarbons completely after each measurement with desorption considered complete when the permeance of hydrogen recovered to its original value.

Characterization

The bottom surface of substrates after zeolite synthesis was examined by scanning electron microscopy (SEM) using a CamScan instrument operating at 15 kV. Electron probe microanalysis (EPMA) using a JEOL 733 Superprobe was performed on the cross sections of one membrane prepared without using barriers and one membrane prepared using barriers. These two membranes were also analyzed by X-ray diffraction (XRD) using a Scintag XDS 2000 diffractometer with Cu-Ka radiation. The membrane disks were placed into the sample holder with zeolite films facing the incident X-ray beam.

3.3 Results and Discussion

Formation and Properties of Barriers

As mentioned in the introduction, and as will be discussed in more detail in a later section, the product of hydrothermal synthesis penetrates a depth of several tens of microns into the porous support resulting in decreased membrane permeance and selectivity. One way to limit the pore penetration of siliceous material is to use a diffusion barrier consisting of a material which is stable to highly alkaline solutions at 175 °C and yet readily removable

after zeolite synthesis. Carbon has the properties well suited for these purposes and can be readily introduced by carbonization of a suitable polymer.

Carbonization temperature It is known that poly(furfuryl alcohol) (PFA) can be converted into pure carbon at temperatures of 800 °C or higher in an inert atmosphere (11). However, to serve as a barrier PFA need not be carbonized to such a high temperature. Therefore, to limit the shrinkage accompanying carbonization, the first few preparations were carried out using carbonization temperatures between 350 °C and 500 °C. After exposure to hydrothermal synthesis, it was observed that the synthesis solution turned light brown, evidently due to leaching of non-carbonized or partially carbonized polymeric material by the highly alkaline solution. After the usual calcination in stagnant air to 500 °C, these membranes showed very high fluxes for both n-butane and isobutane but little selectivity between them suggesting extensive cracks or pinholes in the zeolite film. To prevent leaching of organic material into the synthesis mixture, the carbonization temperature of all subsequent preparations was raised to 600 °C. The carbon thus obtained did not show any visible leaching under zeolite synthesis conditions.

Zeolite growth on FA carbon and FA-TEOS carbon Incorporation of carbon into the substrate raises the question whether ZSM-5 can grow on the surface of the carbon inclusions inside the pores. Previous work has examined zeolite growth on a variety of substrates such as alumina, clay, stainless steel, silicon, and glass, but carbon was not included [1-9, 13-16]. Therefore a few experiments were conducted to examine the growth of ZSM-5 on carbon produced from pure FA (FA carbon) and carbon produced from a FA-TEOS mixture (FA-TEOS carbon). The hydrothermal synthesis conditions and the geometric arrangement of the substrate with respect of the autoclave and the solution were the same as those specified for membrane preparations. However, the carbon used in these experiments was prepared by a slightly different procedure from that used for preparing the carbon barrier. More specifically, curing, carbonization, and carbon burnoff

(if performed) were the same but some changes were made in the polymerization step. The substrate was first impregnated with a 2 M p-toluenesulfonic acid solution and after drying at 110 °C and cooling, it was transferred into a sealed container and heated to 90 °C. Pure FA or a FA-TEOS mixture was then added to the container to cover the top surface of the substrate and polymerization was allowed to proceed for 1 hour.

With this modified procedure, a thick carbon layer was formed shielding the alumina substrate from the synthesis solution. Fig. 3.1a shows the micrograph of a FA-carbon supported on porous alumina after zeolite synthesis. The carbon layer has broken into flakes due to the shrinkage accompanying carbonization and some of these flakes have fallen off the support. The weak bonding between carbon and alumina was even more pronounced in an experiment using a non-porous alumina support where the carbon layer did not break into small flakes but rather shrank and was detached from the support in one piece. Fig. 3.1b is a close-up of the surface of a selected FA-carbon flake (area 1) while Fig.3.1c shows an area where a carbon flake had fallen off before zeolite synthesis (area 2). No zeolite crystals were observed on the carbon surface (Fig. 3.1b) suggesting that the FA-carbon does not support zeolite growth. However, zeolite crystals did grow (Fig. 3.1c) where the FA-carbon flakes had fallen off, presumably because the alumina surface was exposed in that area. Fig. 3.2a,b are SEM micrographs at different magnifications of a FA-TEOS carbon before zeolite synthesis. Similar to those of the FA-carbon, these micrographs also reveal a network of crack lines generated by the carbon shrinkage. However, the domains are much smaller in size than those observed on the FA carbon possibly due to the presence of silica particles of 1-2 μm size distributed uniformly inside the carbon. It is believed that these particles are silica formed from TEOS during polymerization, curing, and carbonization of the mixture. Hydrolysis by the water from FA polymerization or transesterification by exchange of ethanol with FA can trap TEOS in the condensed phase either as pure-silicate oligomers or as mixed FA-silicate oligomers.

During carbonization these silicate species will be freed and condensed to silica particles. Part of the TEOS may be lost to the gas phase. Fig. 3.2c is the SEM micrograph of a FA-TEOS carbon after hydrothermal treatment. Apparently no zeolite has been formed on this FA-TEOS carbon surface. Fig. 3.3a shows the SEM micrograph of the surface of a FA-TEOS carbon after oxidation in 2% O_2-N_2 at 600 °C for 21 minutes. The silica particles are clearly more exposed due to the burnoff of the top layer of carbon. Zeolite synthesis was carried out on a sample of FA-TEOS carbon after the partial carbon burnoff and Fig. 3.3b,c show the corresponding SEM micrographs at different magnifications. Zeolite crystals are clearly shown on the FA-TEOS carbon. It is believed that the silica particles exposed after the partial carbon burnoff provide sites for zeolite crystallization. Based on these observations, all membrane preparations were carried out with FA-TEOS carbon as the barrier and with selective carbon burnoff after carbonization.

Permeation Measurements

Table 3.1 shows pure gas permeation data for a membrane prepared using a FA-TEOS composite barrier with carbon burnoff time of 10.5 minutes. For comparison purposes permeation data at 458 K are also provided for a membrane prepared under identical synthesis conditions but without using a barrier and the permeation data reported recently by Vroon et al. (4) for a silicalite membrane prepared by double crystallization using an α-Al_2O_3 support with approximately 0.15 μm pore diameter and 0.46 porosity. The membrane prepared with the barrier-pretreatment has n-butane permeance 1.6 times as large as that of the membrane prepared without the barrier indicating that the pore penetration of siliceous material is reduced by the temporary barrier. It is also interesting to notice that the barrier-pretreated membrane has a n-butane/isobutane selectivity 4 times as large as that of the unpretreated membrane. The membrane prepared by Vroon et al. (4) has higher flux and selectivity at room temperature but lower selectivity at 200 °C. While

several factors including the thickness of the external crystal layer, the structure and thickness of the internal layer and the different porosity (0.46 vs. 0.2) may be responsible for the flux difference, no explanation is available for the different temperature dependence of selectivity.

Effects of Burnoff Time

Membranes prepared with different burnoff times have been tested and the permeation results at 458 K are presented in Fig. 3.4. The burn-off time of about 250 minutes is an extrapolation from 5 minutes oxidation in pure O_2 assuming a first order reaction. Notwithstanding the uncertainty due to this extrapolation the data support the expected trend. For an oxidation time of about 250 minutes the carbon removal is excessive and the membrane has permeation properties similar to that prepared without the barrier. The membrane obtained with burnoff time 10.5 minutes shows enhanced properties and is the one reported in Table 3.1. As the burnoff time decreases below 10.5 minutes, the permeances of n-butane and H_2 increase but the selectivity declines indicating the increasing presence of defects in the zeolite layer. The low selectivity membranes have n-butane to isobutane and hydrogen to n-butane permeance ratios of 1 and 6 suggesting the prevalence of mesoporous defects such that Knudsen diffusion is operative.

To understand better the poor selectivity of membranes prepared without adequate carbon burnoff, SEM was performed on the surface of a membrane prepared with a 2 minutes burnoff time. The zeolite film was found to contain a number of pinholes as the one shown in Fig. 3.5a and small line cracks as the one indicated by an arrow in Fig. 3.5b. It appears that the large pinholes are voids left over by carbon particles that were incorporated into the zeolite layer during zeolite synthesis and burned off later during calcination. The cause of the line cracks is more difficult to establish although they also seem to be generated by the removal of carbon during calcination.

To confirm that pinholes and cracks are created mainly during calcination, permeation measurements were conducted on a membrane (FA-TEOS carbon barrier; 8 minutes burnoff time) as synthesized and after calcination. The as-synthesized membrane was impermeable to n-butane, isobutane and H_2 but after calcination, large and approximately equal permeances were obtained for n-butane and isobutane revealing the formation of cracks or pinholes.

The extent of burnoff needed to generate a carbon-free layer clearly depends on the location of the bounding carbon surface relative to the external surface of the support. The location of the bounding carbon surface in turn depends on the exact procedure of introducing the TEOS-FA precursor, the mixing taking place during polymerization, and the shrinkage during carbonization. Some of these factors are difficult to control precisely causing considerable irreproducibility in the final membrane properties. Improved procedures are, therefore, desirable for generating the composite barrier and adjusting the carbon-free layer to an optimal thickness (10 μm).

Penetration of the Hydrothermal Reaction Products in the Support

To verify that pore penetration was reduced by the composite barrier, electron probe microanalysis (EPMA) was performed on the cross sections of membranes prepared without (Fig. 3.6a) and with (Fig. 3.6b) a composite barrier. For both membranes the wt% of Si in the first 10 μm is close to 46% which is the weight percentage of Si in pure SiO_2. At around 10 μm, the wt % of Si declines sharply while the wt% of Al jumps sharply signaling the boundary between the external zeolite layer and the alumina support in good agreement with our previous SEM and EPMA results (9). For the membrane prepared without using the barrier (Fig. 3.6a) penetration of siliceous matter continues to about 80 μm depth into the support while for the membrane pretreated with the barrier penetration extends to approximately 55 μm depth into the support (Fig. 3.6b). In both

traces the concentrations of Si and Al fluctuate probably because of the porous nature of the support disk. In trace (a) beyond 80 μm from the boundary the wt% of Al is very close to that of pure Al_2O_3 (53 wt%) and more importantly the Si/Al ratio is about 0.005 which is the value corresponding to the composition of the solution initially imbibed into the pores. In trace (b) the wt% Si and Al are somewhat lower possibly due to the adoption of calibration parameters from the previous EPMA run. The wt% Si in trace b includes the silicon contained in the barrier as well as the silicon in the product of hydrothermal synthesis.

X-ray diffraction (XRD) analysis was performed to examine the differences between the two membranes. Calcined membrane disks with surface areas larger than the beam size were placed in the XRD sample holder with the zeolite film facing the incident X-ray beam. Fig. 3.7 shows the recorded XRD patterns of the two membrane disks (A, unpretreated; B, barrier-pretreated). The peaks from α-Al_2O_3 support are labeled by solid circles. Clearly, the barrier-pretreated membrane has higher ZSM-5 and lower α-Al_2O_3 diffraction peaks than the unpretreated membrane. Several other barrier-pretreated and untreated membranes were similarly examined by XRD and the increased ZSM-5 intensity was consistently observed for barrier-pretreated membranes indicating that the observed intensity change is characteristic of the barrier-pretreated membrane. EPMA and SEM show that both these membranes have external ZSM-5 layers of approximately the same thickness (10 μm). Therefore, based on the XRD data the internal layer of the barrier-pretreated membrane has a higher fraction of crystalline material. The reason for the increased crystallinity is not apparent although it is probably related to the silica particles contained in the carbon-free region.

The structural changes observed by XRD and EPMA explain qualitatively the improved permeation properties of the barrier-pretreated membrane. In particular, the much higher n-butane/isobutane selectivity (45 vs. 9 at 185 °C) can be explained by the

combination of a thicker crystalline layer and a thinner amorphous layer while the moderate increase of n-butane flux can be attributed to the thinner overall layer of the barrier-pretreated membrane.

3.4 Conclusions

Zeolite ZSM-5 membranes with improved n-butane flux and n-butane/isobutane selectivity (2.7 vs. 1.7 MFU; 45 vs. 9 at 458 K) were prepared by in situ crystallization on porous α-Al_2O_3 supports containing a carbon-silica diffusion barrier. The barrier should allow a carbon-free region near the support surface, otherwise pinholes and cracks are generated in the zeolite film during calcination. Improved procedures are needed to obtain a reproducible carbon-free layer with optimal thickness. The moderately higher n-butane flux and considrably higher n-butane/isobutane selectivity of the membrane prepared using the barrier can be attributed to the smaller thickness and higher crystallinity of the internal siliceous layer.

Acknowledgment

This research was supported by NSF grant CTS-9114829 and by the donors of The Petroleum Research Fund administered by the ACS.

References

[1] E. R. Geus, H. van Bekkum, W. J. W. Bakker, J. A. Moulijn, High-temperature stainless steel supported zeolite (FMI) membranes: Module construction, and permeation experiments. Microporous Mater., 1(1993)131.

[2] W. J. W. Baker, G. Zheng, F. Kapteijn, M. Makkee, J. A. Moulijn, E. R. Geus, H. van Bekkum, Single and multi-component transport through metal supported MFI zeolite membranes. In "Precision Process Technology", M.P.C.Weijnen, and A.A.H. Drinkenburg, Eds., Kluwer Academic Publishers. The Netherlands, 1993

[3] E. R. Geus, M. J. den Exter and H. van Bekkum, Synthesis and characterization of zeolite (FMI) membranes on porous ceramic supports. J. Chem. Soc. Farady Trans., 88(1992)3101.

[4] Z. A. E. P. Vroon, K. Keizer, M. J. Gilde, H. Verweij, A. J. Burggraaf, Transport-properties of alkanes through ceramic thin zeolite FMI membranes. J. Membr. Sci., 113(1996)293.

[5] H. W. Deckman, A. J. Jacobson, J. A. McHenry, K. Keizer, A. J. Burggraff, Z. A. E. P. Vroon, L. R. Czarnetzki, F. Lai, A. J. Bons, W. J. Mortier, J.P. Verduun, and E. W. Corcoran, Jr. Molecular sieve layers and processes for their manufacture, Patent PCT/EP 9401301,1994.

[6] C. Bai, M. Meng, J. L. Falconer, R. D. Noble, Preparation and separation properties of silicalite composite membranes. Abstract, the third international conference on inorganic membranes, Worcester, MA, July 10-14, 1994.

[7] M. D. Jia, B. Chen, R. D. Noble, and J. L. Falconer, Ceramic-zeolite composite membranes and their application for separation of vapor / gas mixtures, J. Membr. Sci., 90(1994)1.

[8] Y. H. Ma, S. Xiang, Formation of zeolite membranes from sols. Patent PCT/US 9302384, 1993.

[9] Y. Yan, M. E. Davis, and G.R. Gavalas, Preparation of zeolite ZSM-5 membranes by in-situ crystallization on porous a-Al_2O_3, Ind. Eng. Chem. Res., 34(1995)1652.

[10] J. Jiang, Y. Yan, and G. R. Gavalas, Temporary carbon barriers in the preparation of H_2 permselective silica membrane, J. Membr. Sci.,103(1995)211.

[11] E. Pitzer and W. Schafer, The effect of crosslinking on the formation of glasslike carbon from thermosetting resins, Carbon, 8(1970)353.

[12] D.W. McKee, The catalyzed gasification reactions of carbon, Chem. Phys. Carbon, 16(1981)1.

[13] T. Sano, Y. Kiyozumi, K. Maeda, M. Toba, S. Niwa, and F. Muzukami, Preparation of zeolite film using cellulose moulding, In Proc. of 9th Inter. Zeolite

Conf., R. Ballmoos, J.B.Higgins, and M.M.J. Treacy Eds., Butterworth-Heinemann, Boston,1993.

[14] J. G. Tsikoyiannis, W. O. Haag, Synthesis and characterization of a pure zeolitic membrane. Zeolite, 12(1992)126.

[15] G. J. Myatt, P. M. Budd, C. Price, S. W. Carr, Synthesis of a zeolite NaA membrane, J. Mater. Chem.,2(1992)1103.

[16] J. H. Koegler, H. W. Zandbergen, J. L. N. Harteveld, M. S. Nieuwenhuizen, J. C. Jansen, and van Bekkem, Oriented coatings of silicalite-1 for gas sensor applications. Stud. Surf. Sci. Catal., 84(1994)307.

Table 3.1. Pure gas permeation measurements on a membrane prepared with the assistance of FA-TEOS carbon barriers; burn-off time 10.5 minutes.

	Flux at 100 kPa Δp (MFU)			Flux ratios
Measurement temperature, K	H_2	n-butane	iso-butane	n-butane/iso-butane
303	3.6	0.52	0.015	32
381	3.5	1.8	0.045	39
458	3.6	3.5	0.077	45
458*	2.3	2.2	0.24	9.4
298**		1.8	0.02	90
473**		3	0.27	11

* Membrane prepared without the assistance of carbon barriers.

** Membrane prepared by Vroon et al. (4) using double crystallization; transmembrane Δp is 50 kPa.

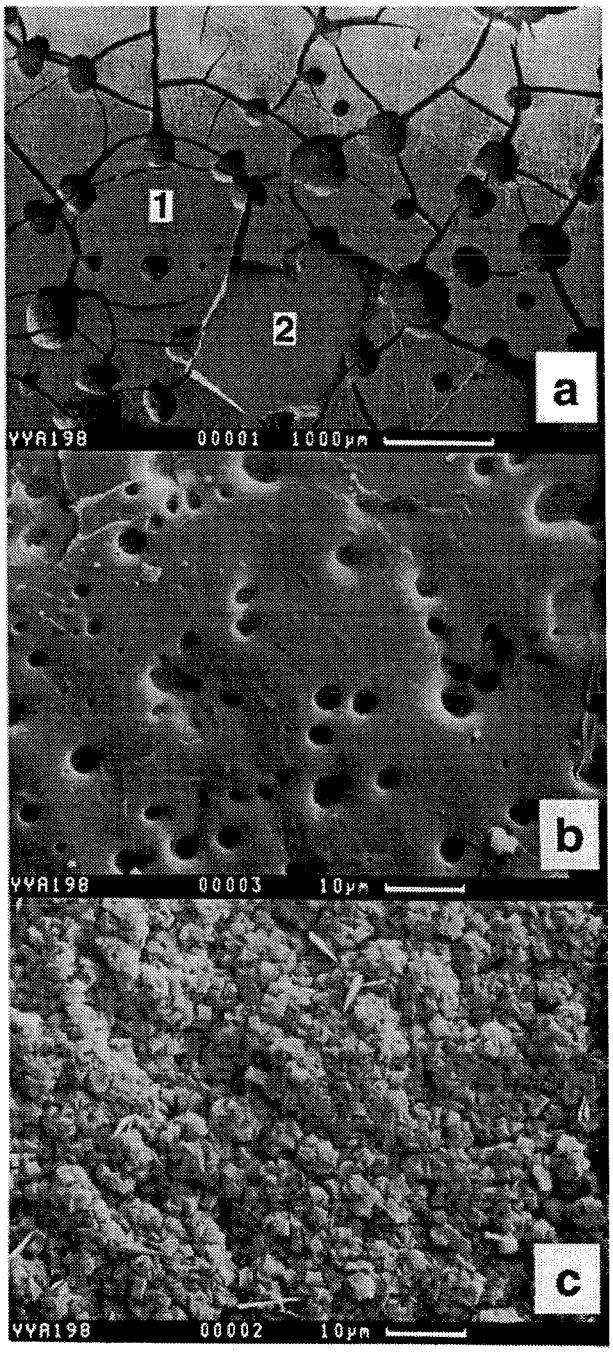

Figure 3.1 SEM micrographs of a FA carbon supported on porous α-Al_2O_3 after zeolite synthesis: (a) an overlook of the carbon surface, (b) a close-up of area 1 as indicated in (a), (c) a close-up of area 2 as indicated in (a).

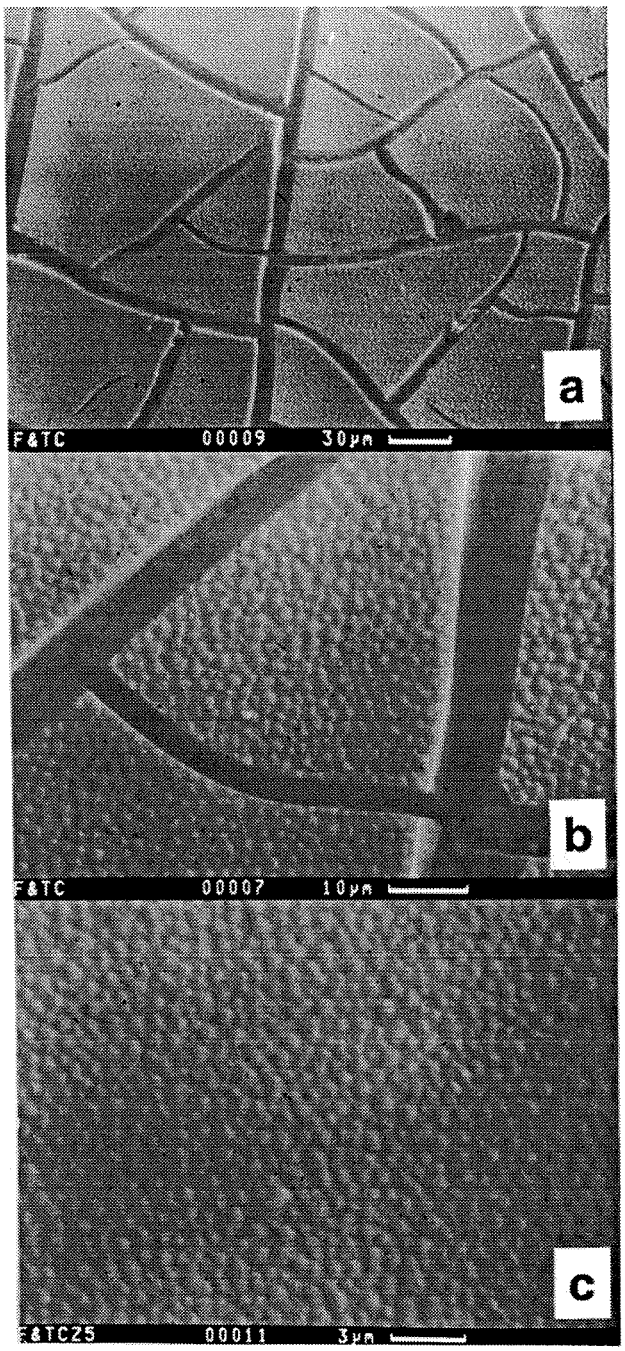

Figure 3.2 SEM micrographs of a FA-TEOS carbon supported on porous α-Al_2O_3: (a) before zeolite synthesis, (b) before zeolite synthesis at a higher magnification, (c) after zeolite synthesis.

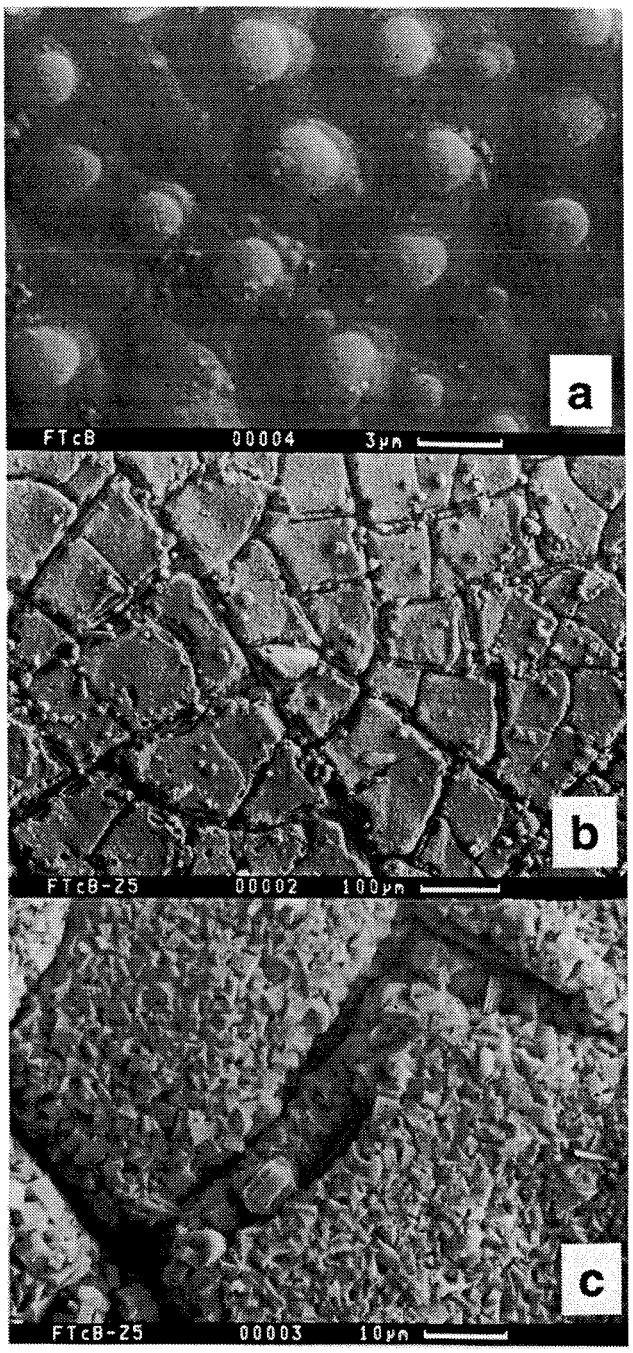

Figure 3.3 SEM micrographs of a FA-TEOS carbon supported on porous α-Al_2O_3: (a) after partial oxidation, (b) after partial oxidation and zeolite synthesis, (c) after partial oxidation and zeolite synthesis at a higher magnification.

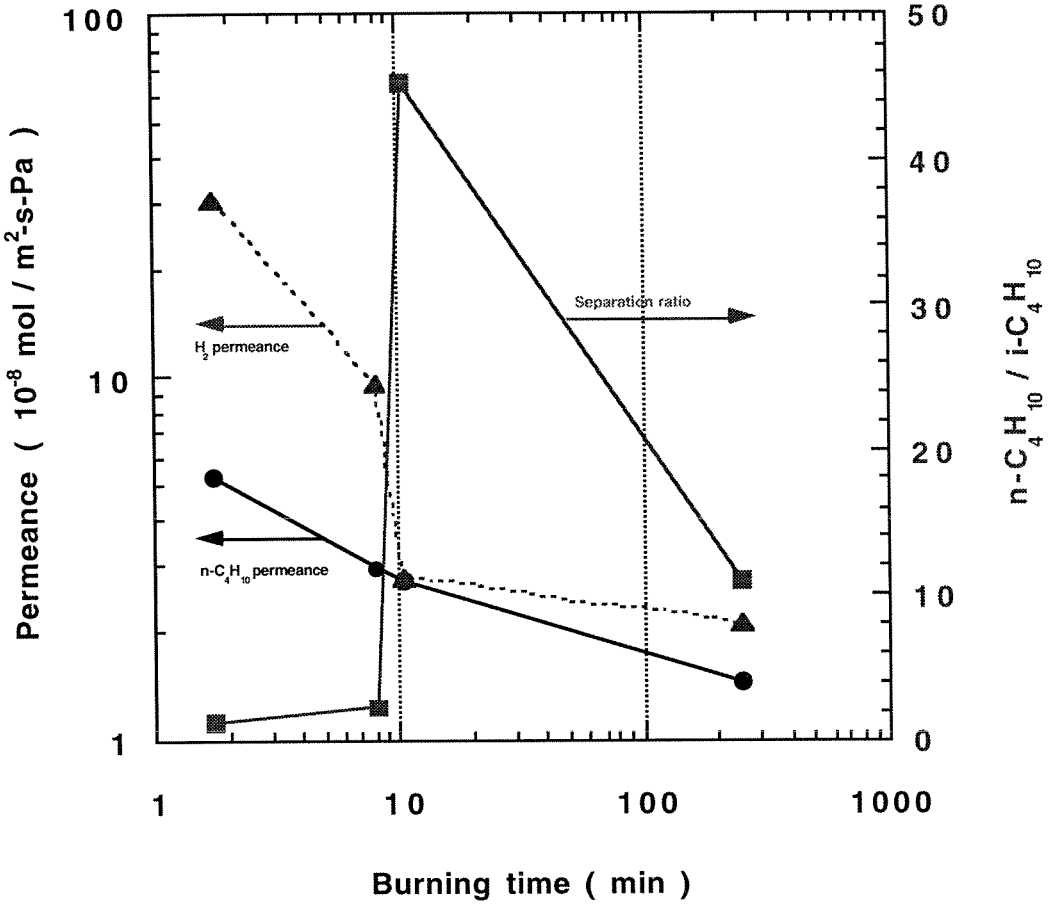

Figure 3.4 Permeances of hydrogen and n-butane and n-butane/isobutane ratio versus oxidation time in 2% O_2-N_2 at 600 °C.

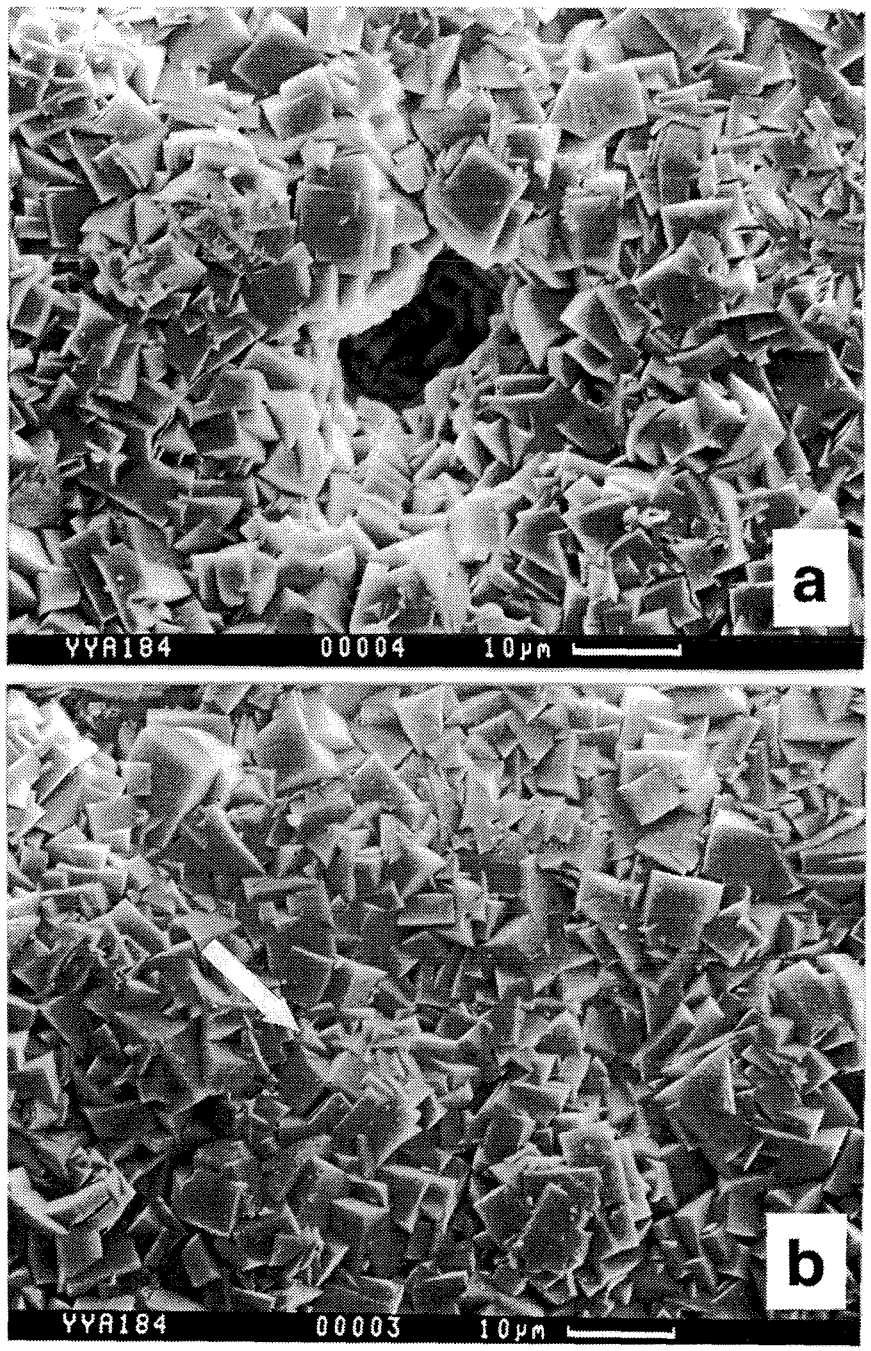

Figure 3.5 SEM micrographs of the surface of a membrane prepared using FA-TEOS carbon barrier with a burnoff time 2 min.

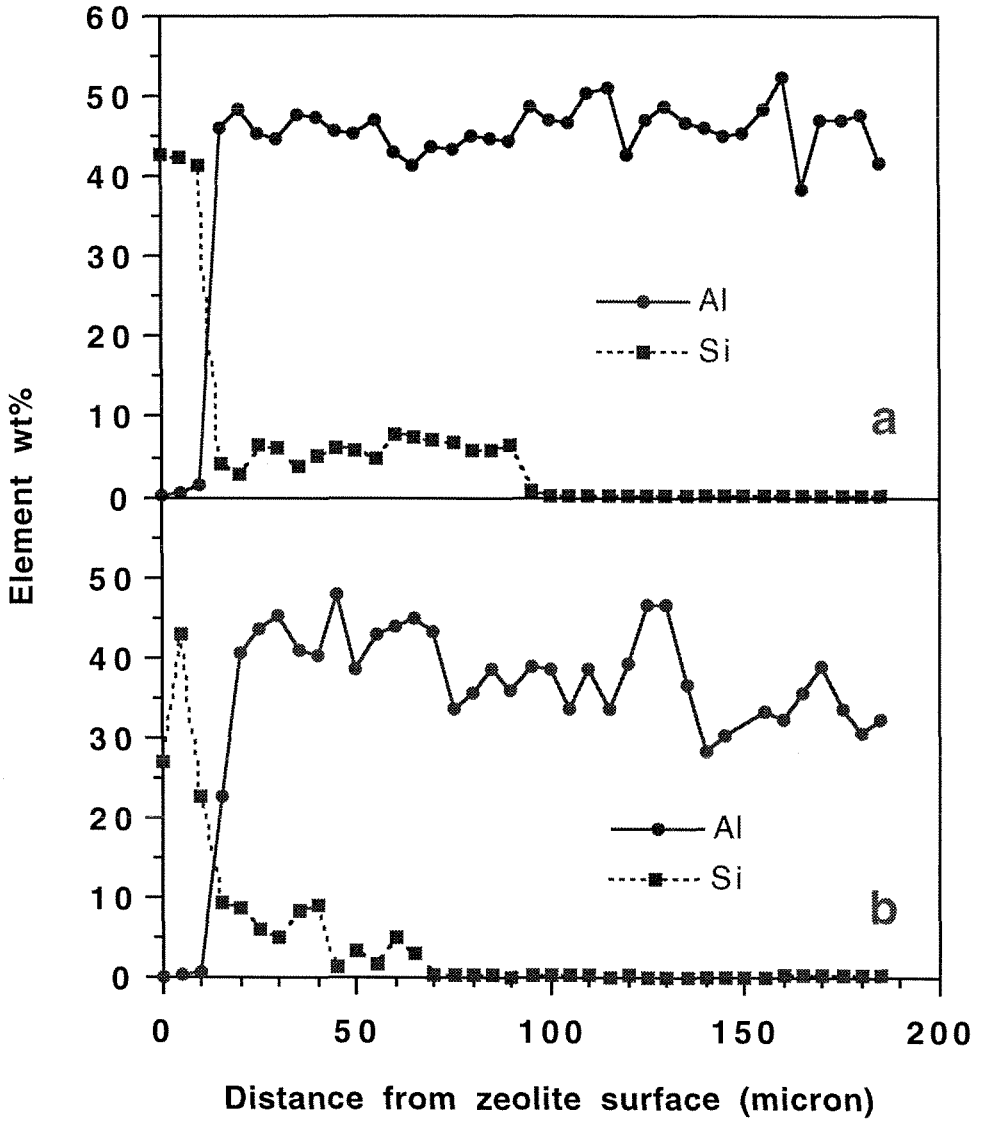

Figure 3.6 EPMA traces of Si and Al on the cross section of membranes prepared on α-Al_2O_3 disks: (a) without barrier-pretreatment, (b) with barrier-pretreatment.

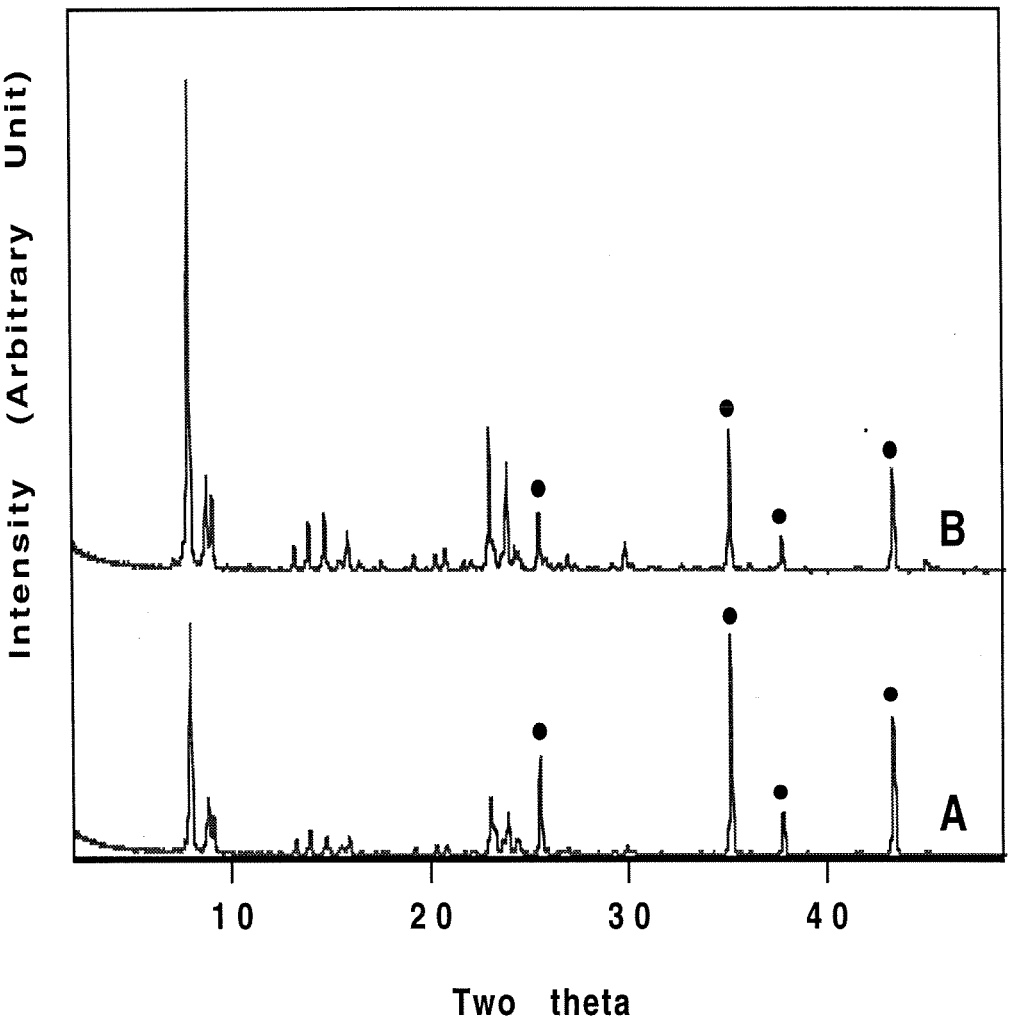

Figure 3.7 XRD patterns recorded on zeolite membranes prepared without (A) and with (B) the help of diffusion barriers. The full circles label α-Al_2O_3 peaks.

Chapter 4

Preparation of Highly Selective Zeolite ZSM-5 Membranes by a Post-Synthetic Coking Treatment

Reprinted with permission from the article

[Yushan Yan, Mark E. Davis, and George R. Gavalas, **Journal of Membrane Science**, in press]

Preparation of Highly Selective Zeolite ZSM-5 Membranes by a Post-Synthetic Coking Treatment

Yushan Yan, Mark E. Davis, and George R. Gavalas

Chemical Engineering, California Institute of Technology

Pasadena, CA 91125

Abstract

Zeolite ZSM-5 membranes with high n-butane:isobutane selectivities, e.g. 322 at 185 °C, are obtained by a selective deposition of coke into non-zeolitic pores. The zeolite membranes are prepared by in situ crystallization on either bare porous α-Al_2O_3 support disks or disks that are pretreated to include a diffusion barrier. The post-synthetic coking treatment is accomplished by impregnating these membranes with liquid 1,3,5-triisopropylbenzene (TIPB) for 24 hours at room temperature and then calcining them in air at 500 °C for 2 hours. Calcination at 500 °C for up to 30 hours does not destroy the high n-butane:isobutane selectivity. Thermogravimetric analysis (TGA) experiments on two model pore systems ZSM-5 (5.5 Å) and Vycor glass (40-50 Å) suggest that micro-defects are selectively eliminated by the TIPB coking treatment while the intracrystalline pore space of the ZSM-5 is not affected. The elimination of non-zeolitic pores results in a large increase of n-butane:isobutane pure gas flux ratio (45 vs 320 at 185 °C) accompanied by a fourfold reduction of the n-butane flux. The permeation experiments reveal that the n-butane flux increases non-linearly with the partial pressure in the feed while the n-butane:isobutane pure gas flux ratio remains relatively unchanged.

4.1 Introduction

During the last three years, several research groups have reported the preparation of zeolite membranes with useful selectivities for gas separation and pervaporation (1-17). All of these preparations involved the growth of a polycrystalline zeolite layer on a porous disk or tube that serves as a mechanical support. In most cases, the support was alpha alumina but gamma alumina and porous steel have also been used. The crystallization of the zeolite layer on the support was accomplished by a variety of procedures including in-situ hydrothermal crystallization and vapor phase transport on a support preloaded with the synthesis gel.

Similar to other types of membranes, zeolite membranes must possess adequate productivity or flux, selectivity, and stability. Thus far, only silicalite and ZSM-5 membranes have been prepared with good selectivities for gas separations. Several of these membranes revealed n-butane:isobutane selectivities as high as 90 at room temperature and about 10 at around 200 °C (14,15). Other membranes showed the opposite temperature dependence, e. g. n-butane:isobutane selectivity of 18 at room temperature and 31 at 185 °C (16,17). The large variation of selectivity among membranes obtained by different preparation protocols is most likely due to differences in the number and size of defects present in these membranes. The term defects here denotes transmembrane pathways larger than the intracrystalline zeolite pores. In this respect, it might be expected that permeation measurements with single crystal membranes would give higher selectivity than polycrystalline films. However, measurements with a single crystal silicalite membrane (18) yielded n-butane:isobutane selectivities well below the values quoted above for polycrystalline membranes. This surprising result may be due to the presence of some strong surface barrier associated with the single crystal.

Defects in polycrystalline zeolite membranes can be classified according to their sizes into macro-defects, meso-defects, and micro-defects following the IUPAC definitions (macro >500 Å; 500 Å > meso > 20 Å; and micro < 20 Å). Macro-defects are usually pinholes or cracks while meso-defects and micro-defects are primarily formed by non-perfect intergrowth between zeolite crystals during hydrothermal synthesis. The larger sized of the defects can be eliminated by repeated crystallization as employed in several of the aforementioned studies (6,7,15). Repeated crystallization involves some loss of permeance without necessarily eliminating the smaller sized defects.

Elimination of small defects may be possible by chemical vapor deposition of silica via reaction with a silicon alkoxide or other silylation agents. This type of treatment has been studied as a means of improving the adsorption selectivity of loose zeolite crystals. For example, silica deposition by reaction with $Si(OCH_3)_4$ has been used to improve the selectivity of zeolite A for O_2-N_2 separation and for light olefin separation (19,20). The same reaction was also used to improve the selectivity of ZSM-5 for separation of para from ortho and meta xylenes (21). All these treatments involved reduction of the pore openings on the external surface of the crystals by silica deposition. Very recently, silane coupling reagents were used to improve the ethanol/water pervaporation selectivity of a silicalite membrane by enhancing its surface hydrophobicity (22).

In this paper we report improvement of ZSM-5 membrane selectivity by a post-synthetic treatment designed to provide selective coking. Coking has been used previously to modify pore openings of granular carbon molecular sieves used in air separation by pressure swing adsorption (23,24). Usually a light hydrocarbon such as propylene is used for this purpose. By controlling the coking conditions such as time and temperature, controlled reduction of the micropore openings is achieved. Our selective coking method is fundamentally different from the previous use of coking in two respects. First, by using a large aromatic hydrocarbon, TIPB, which has a kinetic diameter 8.4 Å and does not enter

the ZSM-5 channels of 5.5 Å (25), the treatment plugs the defects while leaving the intracystalline zeolite channels intact. Second, coking is conducted not by exposure to vapors of the hydrocarbon but by impregnation with the liquid hydrocarbon followed by heat treatment in air at high temperatures. It is known that coking with light hydrocarbon vapor leaves carbon residue inside ZSM-5 channels (26) which would obviously be undesirable for our purposes. Using the selective coking of TIPB it has been possible to obtain n-butane to isobutane selectivity as high as 320. Unfortunately, the increased selectivity is achieved at the cost of a serious flux decrease. The balance of selectivity gain versus flux loss is expected to depend on the morphology of the membrane and deserves further investigation.

4.2 Experimental

Support

The supports were porous α-Al_2O_3 (99.8%) disks of 5 cm diameter, 6 mm thickness with about 0.5 μm mean pore diameter and were obtained from Coors Ceramic Company.

Membrane Preparation

Membranes were prepared by in-situ hydrothermal crystallization as described previously (17). In the preparation of one membrane (M2), a diffusion barrier was introduced into the support pores to limit the membrane thickness prior to crystallization. The details of the barrier technique will be presented elsewhere. Briefly, the support was impregnated with a 1:1 molar mixture of tetraethylorthosilicate (TEOS) and furfuryl alcohol (FA). The mixture retained in the support pores was then polymerized and carbonized to produce a silica-carbon composite barrier inside the pores of the support. After 10-minute oxidation in 2% O_2-N_2 at 600 °C to create a carbon-free superficial layer, zeolite

crystallization was carried out according to the same protocol (17). After zeolite crystallization the membrane was calcined in air to remove the carbon barrier and the structure directing tetrapropylammonium ions occluded in the zeolite crystals.

Gas Permeation Measurements

The apparatus for permeation measurements is shown in Figure 4.1. The calcined membrane disk was attached to the membrane holder by epoxy cement and then the holder with the attached membrane was placed into a stainless steel permeation cell through a flange connection. The feed gas---either pure hydrocarbon or hydrocarbon in nitrogen---was passed continuously outside of the membrane holder while the inside of the holder was continuously swept by nitrogen. Both the feed and the sweep gas are at atmospheric pressure and a flowrate 60 ml/min. The volume fraction of the hydrocarbon in the sweep gas was analyzed by a HP5890 Series II gas chromatograph equipped with a flame ionization detector (FID) and an Alltech 1/8" packed column (0.19 Picric acid/Graphpac). The feed gas was switched to H_2 and the temperature was raised to 185 °C after each hydrocarbon measurement to remove adsorbed hydrocarbons. This desorption was continued for 24 hours or longer until no hydrocarbon could be detected in the sweep gas at the highest sensitivity of the gas chromatograph (10^{-7} mol/m^2-s). N-butane (>99.5%, isobutane<0.15%) and isobutane (>99.5%, n-butane<0.40%) were purchased from Matheson Gases.

Post-Synthetic Treatment by TIPB Coking

After completing the permeation measurements, the membrane holder carrying the membrane disk was removed from the permeation cell and positioned vertically. A quantity of TIPB liquid in excess of the pore volume of the membrane disk was transferred into the holder and covered the (nonzeolitic) face of the membrane disk. The liquid level quickly receded indicating imbibition into the pores but 24 hours were allowed at ambient temperature to ensure complete impregnation. Subsequently the membrane holder was

placed in the center of a tubular furnace (8 cm bore diameter and 70 cm length) that was open at both ends to atmospheric air. The furnace temperature was ramped to 500 °C at 1 C°/min and held at 500 °C for 2 hours (or 30 hours) before it was cooled to ambient temperature at 1 C°/minute. The epoxy cement was decomposed into a gray powder during the calcination. The membrane disk was cleaned and then reattached to the holder with fresh epoxy cement before performing a new series of permeation measurements.

Thermogravimetric Analysis (TGA)

Measurements of weight loss were performed in a thermogravimetric analysis system (Cahn D-200 microbalance with 10^{-4} mg sensitivity) on two porous materials with well defined pore sizes, namely, ZSM-5 (5.5 Å) and Vycor glass (40 Å). It is known that TIPB can be adsorbed into Vycor glass (16) but not into ZSM-5 crystals. The temperature schedule used in the TGA experiment was identical to the one used in the TIPB coking treatments. A blank calcination run was first carried out on the sample before TIPB impregnation and the weight change was recorded. Then, after the sample was cooled to room temperature, an ample amount of TIPB liquid was added in situ to the sample in the TGA sample basket. The mixture was allowed to stand for 24 hours at room temperature before another TGA run was carried out.

The ZSM-5 crystals used in the TGA measurements were excess product collected from the bottom of the autoclave after membrane preparation. These crystals are 5-10 mm in size and have similar morphology as those in the membrane films. Vycor tubes with 40-50 Å diameter pores were provided by Corning Inc. A few small pieces of crushed tubes were used in the TGA experiments.

In an additional test, 200 mg ZSM-5 powder contained in a vial was soaked with TIPB liquid, placed in the membrane holder and subjected to an identical thermal treatment as that used for the TIPB-impregnated membrane (previous section). The sample weight were recorded before impregnation and after the thermal treatment.

Optical and UV Diffuse Reflectance Spectroscopy

After the TIPB treatment the membrane surface was examined with an optical microscope (Model Z45L, Cambridge Instruments) for large scale coke accumulation. To determine coke formation inside the membrane, UV diffuse reflectance spectra were obtained on a Shimadzu UV-2101 PC spectrometer equipped with a diffuse reflectance accessory. Barium sulfate powder was used as the reference material. The composite membrane disks recovered from the permeation measurements were dried at 150 °C for 24 hours before they were loaded into the diffuse reflectance accessory with the zeolite film toward the incoming UV beam.

4.3 Results

Permeation Results for Membrane M1

Membrane M1 was prepared by in situ crystallization on a bare porous α-Al_2O_3 disk. Table 4.1 shows the fluxes of pure n-butane and isobutane through M1 before and after TIPB coking at 500 °C for 2 hours. The n-butane/isobutane selectivity increased from 9 to 107 while the n-butane flux decreased from 1.7 MFU to 0.3 MFU as a result of the coking treatment (1 MFU=10^{-3}mol/m^2-s).

Permeation Results for Membrane M2

Membrane M2 was prepared by in situ crystallization on a porous α-Al_2O_3 disk containing a diffusion barrier. After TIPB coking, gas permeation measurements were performed at three temperatures. For the measurements at the two elevated temperatures (108 °C and 185 °C), the feed gas was either n-butane in N_2 or isobutane in N_2 at 1 atm total pressure at a flowrate 60 ml/min. In each case, the steady-state composition of the sweep gas was measured for a series of hydrocarbon partial pressures in the feed. When the permeation measurements were conducted at the lower temperature of 30 °C, the feed

was pure n-butane or isobutane at atmospheric pressure and a flowrate of 60 ml/min. The n-butane fluxes and n-butane:isobutane selectivities for membrane M2 are shown in Figure 4.2 as a function of partial pressure in the feed. The n-butane flux increases with the n-butane partial pressure while the n-butane:isobutane flux ratio remains approximately constant. As expected, the hydrocarbon flux does not increase linearly with the feed partial pressure even at the higher temperature of 185 °C. Because of this nonlinear dependence, the membrane productivity is reported in flux units (mol/m^2-s) rather than in permeance units (mol/m^2-s-Pa). The n-butane:isobutane pure gas selectivity is about 65 at 30 °C, 100 at 108 °C and 210 at 185 °C and the corresponding n-butane flux is about 0.1 MFU, 0.6 MFU, and 0.7 MFU, respectively. Before the TIPB coking treatment, the n-butane:isobutane selectivity is 45 and n-butane flux is 2.7 MFU at 185 °C. An approximate 10% loss of n-butane flux is observed after 9 permeation measurements despite prolonged flushing with H_2 at 185 °C between measurements. This loss of flux is more pronounced after ambient temperature measurements due to the much longer time required to reach steady-state permeation. The loss of n-butane flux is probably caused by adsorption of higher hydrocarbons contained at impurity levels in the feed.

After the aforementioned permeation measurements, membrane M2 was calcined again at 500 °C for 30 hours. Table 4.2 shows the pure gas permeation data after this prolonged calcination. Gas permeation data are also provided for the membrane before the coking treatment and for membranes prepared by the Delft group (3) for comparison purposes. To our surprise, the prolonged calcination did not reduce but rather increased further the selectivity (210 to 322). Comparison between Figure 4.2 and Table 4.2 shows that the prolonged calcination did not affect the n-butane flux but reduced the isobutane flux. Compared with the membranes prepared by the Delft group (1-3) the membranes reported here have much lower flux but much higher selectivity, especially at elevated

temperatures. N-butane:isobutane selectivities reported by other groups were always below 10 at temperatures about 200 °C.

TGA on ZSM-5 powder and Vycor glass

TGA measurements were carried out on two well defined pore systems to obtain information about the size of defects in the zeolite membrane that are affected by coking of TIPB. The two materials, ZSM-5 and Vycor glass, have pore diameter 5.5 Å and 40 Å, respectively. The TGA profiles for ZSM-5 powder during the initial calcination and the calcination following impregnation with TIPB are shown in Figure 4.3. The solid line represents the weight loss during calcination of the as-synthesized ZSM-5 powder consisting of 5-10 mm crystals. The weight loss at about 350 °C is due to the removal of occluded TPA (tetrapropylammonium cation) used in the synthesis as the structure-directing agent. The purpose of this calcination was to free the ZSM-5 channels for adsorption and establish the base dry weight of the sample at 500 °C. The dashed line represents the weight change during calcination of the TIPB-impregnated sample. The large weight loss at about 100 °C is due to evaporation of TIPB liquid coating the ZSM-5 crystals. The fact that the sample weight reaches its dry weight value at only 100 °C suggests that TIPB does not enter the ZSM-5 channels consistent with the large kinetic diameter of this molecule. Similarly to the test in the TGA system, the coking test for the ZSM-5 powder placed in the membrane holder showed no weight gain within the error of the analytical balance ($\pm$ 0.1 mg).

Vycor glass has pores of mean diameter of about 40-50 Å that can obviously be penetrated by TIPB. The solid line in Figure 4.4 is the profile recorded during heating of the bare Vycor glass in air. The first weight decline completed at about 100 °C is due to the desorption of physically adsorbed water while the second weight decline extending to 500 °C is due to removal of surface silanol groups via condensation. The dashed line shows the weight profile of the Vycor sample that had been impregnated with TIPB. This data show

weight loss beginning at 50 °C and being complete at 150 °C. Compared with the TIPB pyrolysis profile of ZSM-5, the weight loss occurred at a higher temperature (150 °C versus 100 °C) and at a slower rate suggesting that TIPB had adsorbed into the pores of Vycor glass. The sample weight after heating beyond 150 °C was identical to that before impregnation with TIPB indicating complete removal of TIPB by evaporation.

Optical and UV Diffuse Reflectance Spectroscopy

Optical microscopy showed no coke accumulation on the membrane surface. UV diffuse reflectance spectroscopy was used to confirm the existence of coke inside the zeolite layer. Two zeolite membranes one treated by the post-synthetic coking and the other untreated were examined and the difference spectrum is reported in Figure 4.5. UV spectroscopy has been used previously by Karge to monitor the coke evolution in ZSM-5 crystals using methanol as the coking agent (27). According to their assignments, the pair bands at about 320 and 420 nm indicate the existence of bulky polyaromatics and the bands at 220 nm and 265 nm are due to dienes and benzene, respectively.

4.4 Discussion and Conclusions

The combined results from the permeation and thermogravimetric measurements provide a qualitative understanding of the changes in the porous structure of the membrane resulting from the coking treatment. First, the TGA experiment on ZSM-5 powder verifies that TIPB treatment does not leave coke inside the zeolitic channels. The question remains, however, whether coking may reduce the pore openings on the external surface of the crystals. If that was the case the flux of n-butane would be affected more than the flux of hydrogen. However, the reduction of the two fluxes by approximately the same factor shown in Table 4.1 strongly suggests that the modification of the pore openings is not a key factor in the observed selectivity change. The absence of residual coke on Vycor

further suggests that the membrane defects removed by the coking treatment must be smaller than 40 Å. This argument is not conclusive, however, because coking may require strong acid sites possessed by ZSM-5 but not by Vycor. It nevertheless appears likely that the size of the defects eliminated by coking is much closer to the size of TIPB molecules (8.4 Å), otherwise rapid desorption and diffusion out of the membrane would not have allowed sufficient time for coking. Moreover, inspection of the surface of both M1 and M2 membranes showed no residual carbon present on the surface that could have caused the large (85% & 73%, resp.) reductions in the n-butane flux after TIPB treatment.

Another important observation to explain is the large decrease of flux upon treatment with TIPB. If the defects (non-zeolitic transmembrane pathways) are strictly in parallel with the zeolitic pathways, their contribution to the n-butane flux would be small given the large initial n-butane:isobutane selectivity (9.5 for M1 and 45 for M2)). In this case, coking would only cause a minor decrease of n-butane flux. The observed major decrease of flux suggests that the defects are in series as well as in parallel with the zeolitic pathways. Blocking of defects in a series-parallel combination could cause a strong reduction of n-butane flux as experimentally observed. Figure 6 shows schematically the effect of coking in such a series-parallel structure of the membrane.

As discussed in a previous paper (17), silica-containing products formed during membrane preparation by hydrothermal synthesis extend into the pores of the alumina support to a depth 80-100 mm. In much of this internal layer, permeation takes place predominantly through non-zeolitic pathways. When these pathways are blocked by coking, the resistance to permeation obviously increases causing a large reduction of permeance. Application of the TIPB coking treatment to a membrane having a thinner internal product layer would cause a proportionally smaller reduction in permeance while providing comparable selectivity improvement. We thus expect that the coking treatment would be particularly beneficial to membranes prepared using supports of smaller pore size

that may contain thinner internal layers. We also believe that coking treatment with a hydrocarbon of suitable molecular size is promising for use with microporous silica and carbon membranes as well as with other types of zeolite membranes.

Acknowledgment

The authors would like to thank Christopher B. Dartt for his help with the UV diffuse reflectance measurements and Neil E Fernandes, John E. Lewis and Dr. Masahito Yoshikawa for their assistance with the TGA experiments. This research was funded by National Science Foundation Grant No. CTS-9504901.

References

[1] E. R. Geus, M. J. den Exter and H. van Bekkum, Synthesis and characterization of zeolite (FMI) membranes on porous ceramic supports. J. Chem. Soc. Farady Trans., 88(1992)3101.

[2] E. R. Geus, H. van Bekkum, W. J. W. Bakker, and J. A. Moulijn, High-temperature stainless steel supported zeolite (FMI) membranes: Module construction and permeation experiments. Microporous Mater., 1(1993)131.

[3] W. J. W. Bakker, G. Zheng, F. Kapteijn, M. Makkee, J. A. Moulijn, E. R. Geus, and H. van Bekkum, Single and multi-component transport through metal supported MFI zeolite membranes. In "Precision Process Technology", M.P.C.Weijnen, and A.A.H. Drinkenburg, Eds., Kluwer Academic Publishers. The Netherlands, 1993

[4] M. D. Jia, K. V. Peinemann, and R. D. Behling, Ceramic zeolite composite membranes. Preparation, characterization and gas permeation, J. Memb. Sci., 82(1993)15.

[5] C. Bai, M. Meng, J. L. Falconer, and R. D. Noble, Preparation and separation properties of silicalite composite membranes. Abstract, the third international conference on inorganic membranes, Worcester, MA, July 10-14, 1994.

[6] M. D. Jia, B. Chen, R. D. Noble, and J. L. Falconer, Ceramic-zeolite composite membranes and their application for separation of vapor / gas mixtures, J. Membr. Sci., 90(1994)1.

[7] Y. H. Ma, and S. Xiang, Formation of zeolite membranes from sols. Patent PCT/US 9302384, 1993.

[8] T. Sano, M. Hasegawa, Y. Kawakami, Y. Kiyozumi, H. Yanagishita, D. Kitamoto, D Kitamoto and F. Mizukami, Stud. Sur. Sci. Catal., 84(1994)1175.

[9] T. Sano, S. Ejiri, M. Hasegawa, Y. Kawakami, N. Enomoto, Y. Tamai, and H. Yanagishita, Silicalite membranes for separation of acetic acid/water mixture, Chem. Lett., 2(1994)153.

[10] T. Sano, M. Hasegawa, Y. Kawakami, and H. Yanagishita, Separation of methanol/methyl-tert-butyl ether mixture by pervaporation using silicalite membrane, J. Memb. Sci. 107(1995)193.

[11] M. Matsukata, N. Nishiyama, and K. Ueyama, Preparation of a thin zeolitic membrane, Stud. Surf. Sci. Catal., 84(1994)1183.

[12] N. Nishiyama, K. Ueyama, and M. Matsukata, A defect-free mordenite membrane synthesized by vapor-phase transport method, J. Chem. Soc., Chem. Commun., (1995)1967.

[13] H. Kita, K. Horii, Y. Ohtoshi, K. Tanaka, and K. I. Okamoto, Synthesis of a zeolite NaA membrane for pervaporation of water/organic liquid mixture, J. Mater. Sci. Lett., 14(1995)206.

[14] Z. A. E. P. Vroon, K. Keizer, H. Verweij, and A. J. Burggraaf, Transport properties of a ceramic thin zeolite FMI membrane. Presented at the third international conference on inorganic membranes, Worcester, MA, July, 10-14, 1994.

[15] H. W. Deckman, A. J. Jacobson, J. A. McHenry, K. Keizer, A. J. Burggraff, Z. A. E. P. Vroon, L. R. Czarnetzki, F. Lai, A. J. Bons, W. J. Mortier, J.P. Verduun, and E. W. Corcoran, Jr., Molecular sieve layers and processes for their manufacture, Patent PCT/EP 9401301,1994.

[16] Yushan Yan, Michael Tsapatsis, George R. Gavalas, and Mark E. Davis, Zeolite ZSM-5 membranes grown on porous α-Al_2O_3, J. Chem. Soc., Chem. Commun., 2(1995)227.

[17] Y. Yan, M. E. Davis, and G.R. Gavalas, Preparation of zeolite ZSM-5 membranes by in-situ crystallization on porous α-Al_2O_3, Ind. Eng. Chem. Res., 34(1995)1652.

[18] A. Paravar and D. T. Hayhurst, Direct measurement of diffusivity for butane across a single large silicalite crystal, in the Proceedings of the 6th international zeolite conference, D. Olson and A. Bisio Ed., Butterworths, 1984.

[19] Miki Niwa, Kiyoshi Yamazaki, and Yuichi Murakami, Separation of oxygen and nitrogen due to the controlled pore-opening size of chemical vapor deposited zeolite A, Ind. Eng. Chem. Res., 30(1991)38.

[20] M. Niwa, K. Yamazaki, and Y. Murakami, Separation of lower olefins by chemical vapor deposited zeolite A, Ind. Eng. Chem. Res., 33(1994)371.

[21] Miki Niwa, Masaaki Kato, Tadashi Hattori, and Yuichi Murakami, Fine control of the pore opening size of zeolite ZSM-5 by chemical vapor deposition of silicon methoxide, J. Phys. Chem., 90(1986)6233.

[22] T. Sano, M. Hasegawa, S. Ejiri, Y. Kawakami, and H. Yanagishita, Improvement of the pervaporation performance of silicalite membranes by modification with a silane coupling reagent, Microporous Mater., 5(1995)179.

[23] S. K. Verma and P. L. Walker, Jr., Preparation of carbon molecular sieves by propylene pyrolysis over microporous carbons, Carbon, 30(1992)829.

[24] T. A. Braymer, C. G. Coe, T. S. Farris, T. R. Gaffney, J. M. Schork, and J. N. Armor, Granular carbon molecular sieves, Carbon, 32(1994)445.

[25] D. W. Breck, Zeolite Molecular Sieves, Wiley, New York, 1974.

[26] J. Karger, H. Pfeifer, J. Caro, M. Bulow, H. Schlodder, R. Mostowicz, and J. Volter, Controlled coke deposition on zeolite ZSM-5 and its influence on molecular transport, Appl. Catal., 29(1987)21.

[27] H. G. Karge, Coke formation on zeolites, Stud. in Surf. Catal. 58(1991)531.

Table 4.1. Pure gas permeation fluxes at 185 °C on membrane M1 before and after post-synthetic 1,3,5-triisopropylbenzene (TIPB) coking treatment at 500 °C for 2 hours

	Flux (MFU, 10^{-3} mol/m^2-s)			Flux ratios
	H_2	n-butane	isobutane	n-butane/isobutane
Before coking treatment	1.8	1.7	0.18	9.4
After coking treatment	0.27	0.27	0.0025	107

Table 4.2. Pure gas permeation fluxes on membrane M2 after post-synthetic coking treatment followed by prolonged calcination at 500 °C for 30 hours.

	Flux (MFU, 10^{-3} mol/m^2-s)		Flux ratio
Measurement temperature, °C	n-butane	isobutane	n-butane/isobutane
108	0.25	0.00077	325
185	0.74	0.0023	322
185*	2.7	0.060	45
27**	4	0.06	67
350**	12	7	1.7

* Membrane M2 before triisopropylbenzene pyrolytic post-treatment.

** Results of Bakker et al. (3)

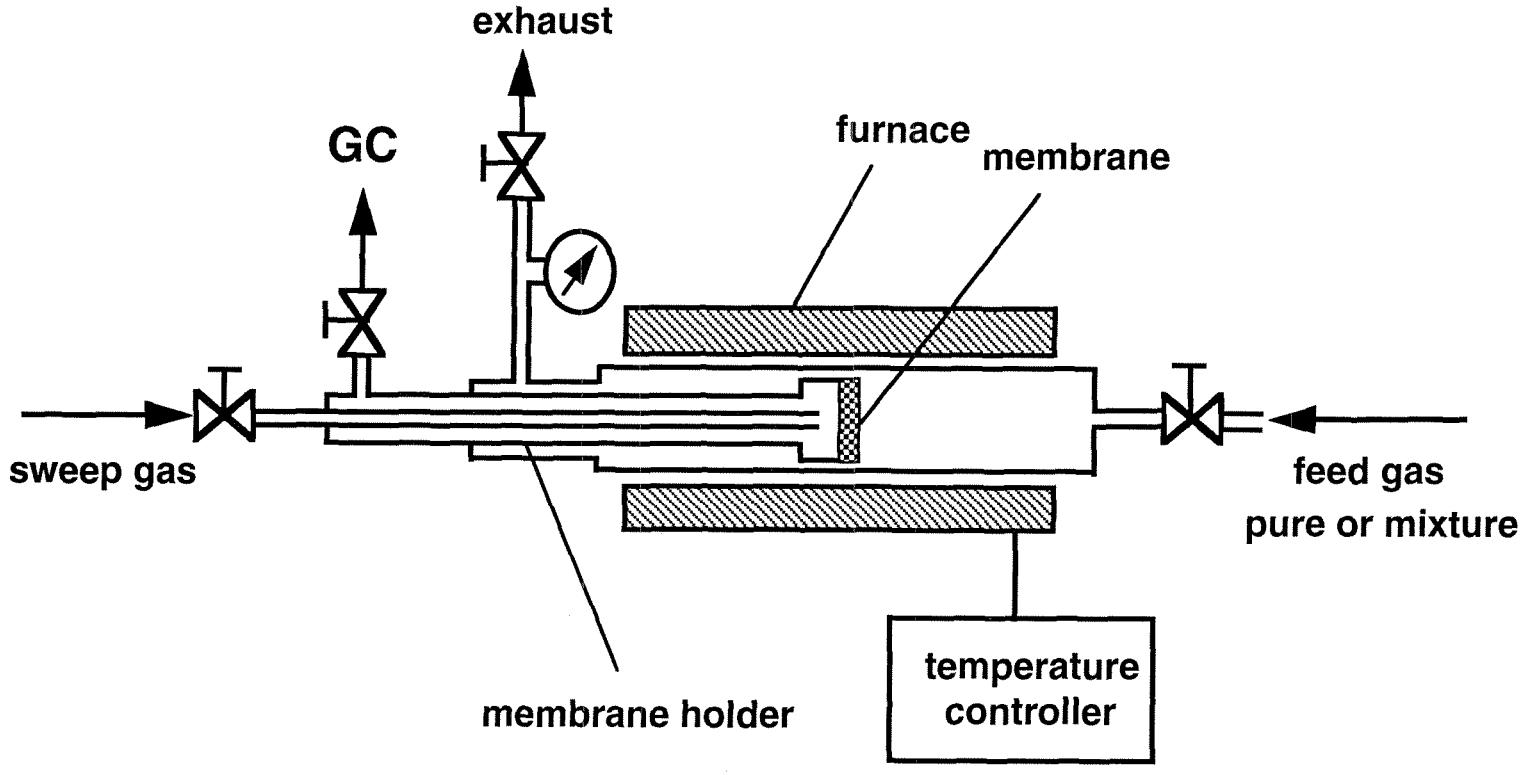

Figure 4.1 Apparatus for gas permeation measurements

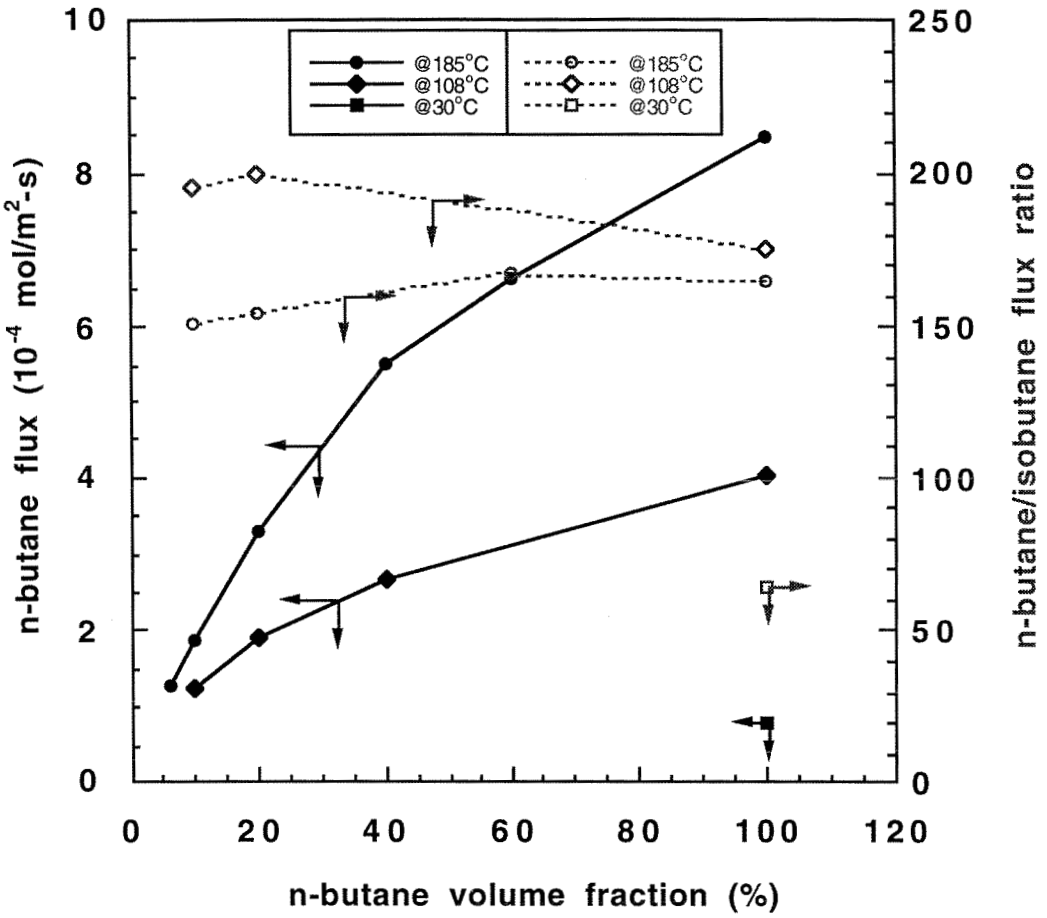

Figure 4.2 N-butane flux and n-butane:isobutane selectivity versus butane partial pressure for membrane M2 after TIPB coking at 500 °C for 2 hours. The feed was n-butane-N_2 or isobutane-N_2 and both feed and sweep streams were at atmospheric pressure and 60 ml/min.

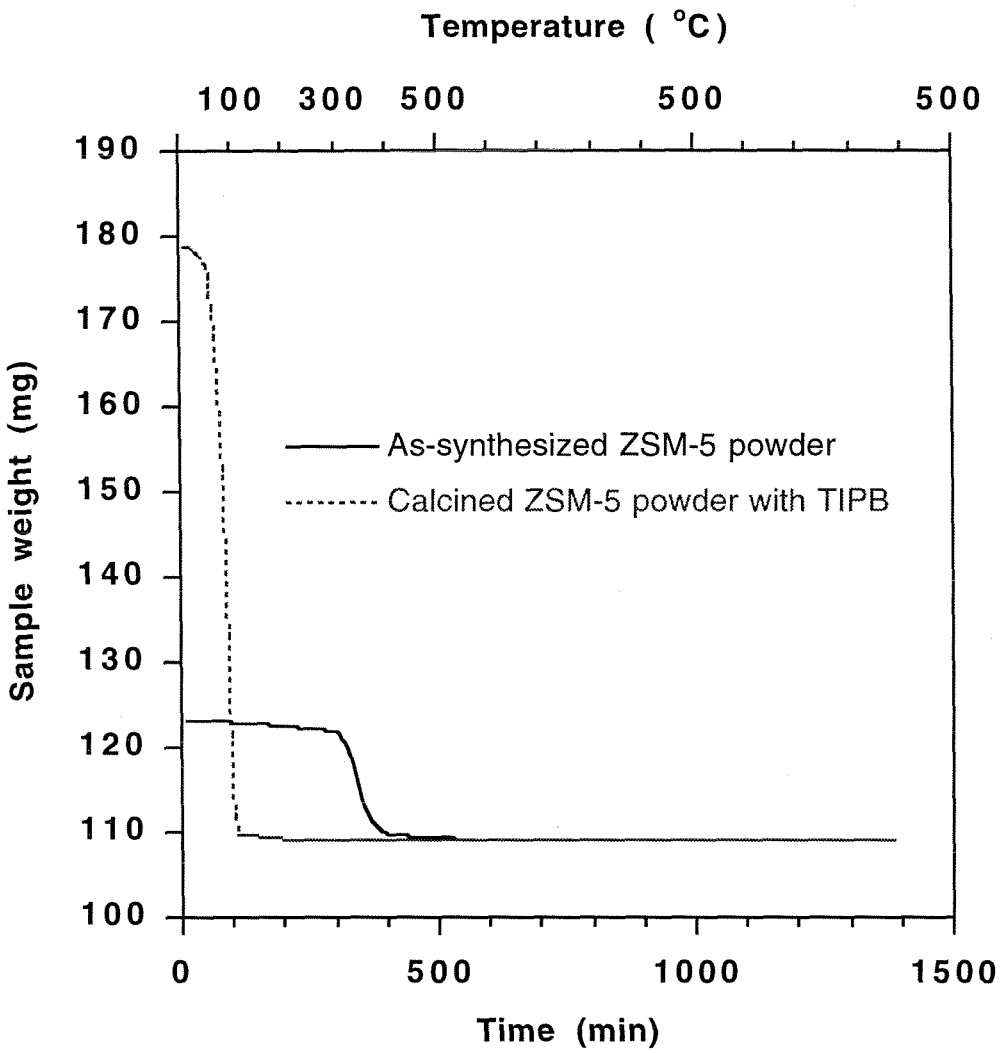

Figure 4.3 TGA of ZSM-5 powder. Temperature profile: from RT to 500 °C at 1 °C/min and at 500 °C for 15 hours.

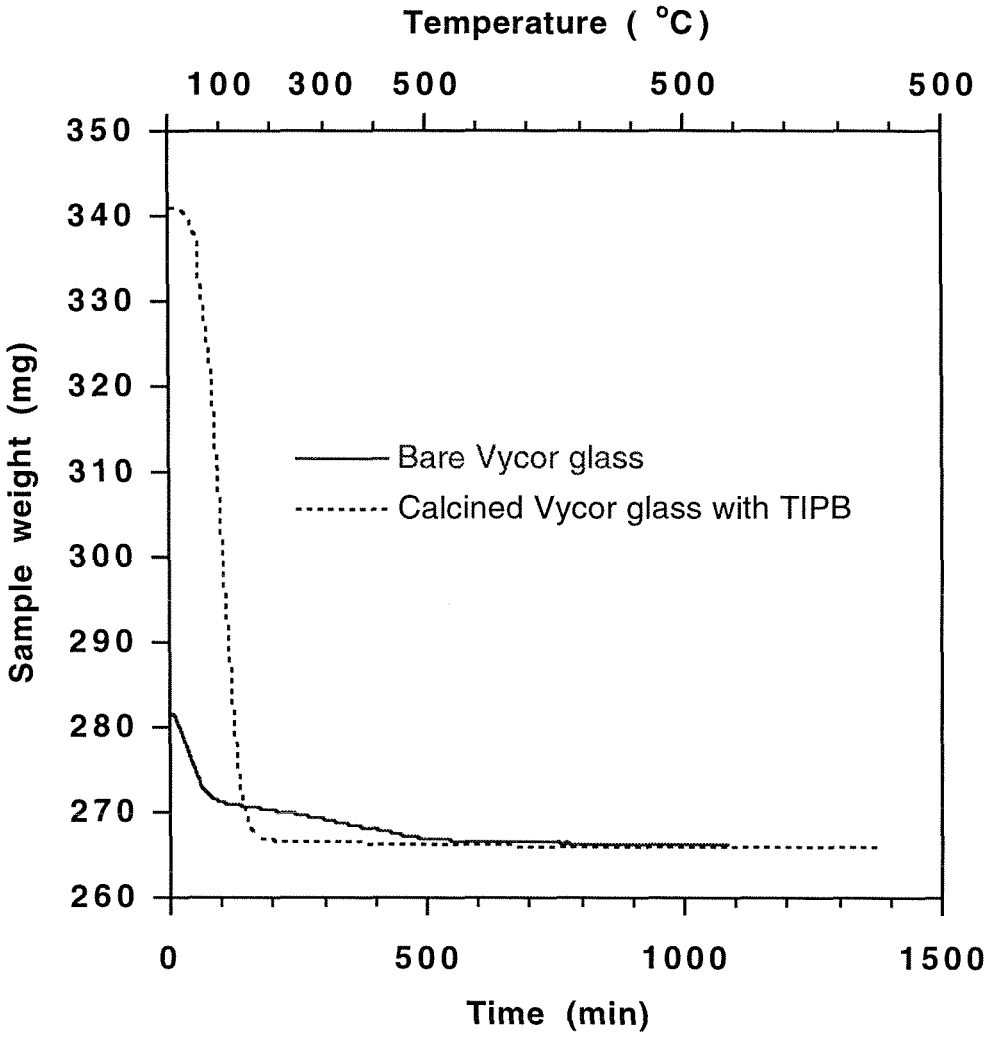

Figure 4.4 TGA of Vycor glass. Temperature profile: from RT to 500 °C at 1 °C/min and at 500 ° C for 15 hours.

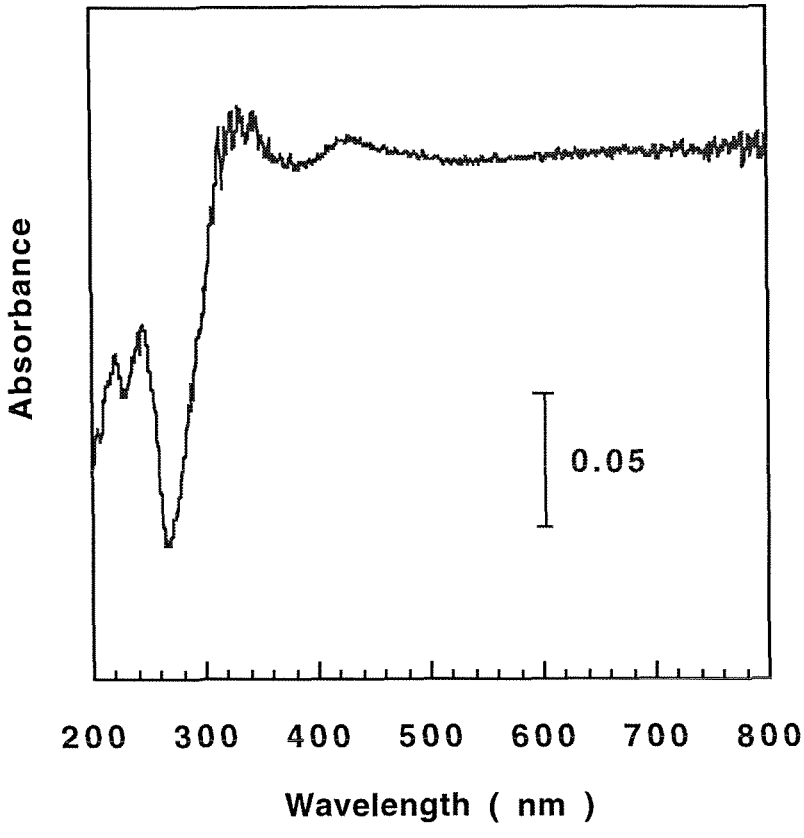

Figure 4.5 UV-diffuse reflectance spectrum of a zeolite membrane treated by coking of TIPB.

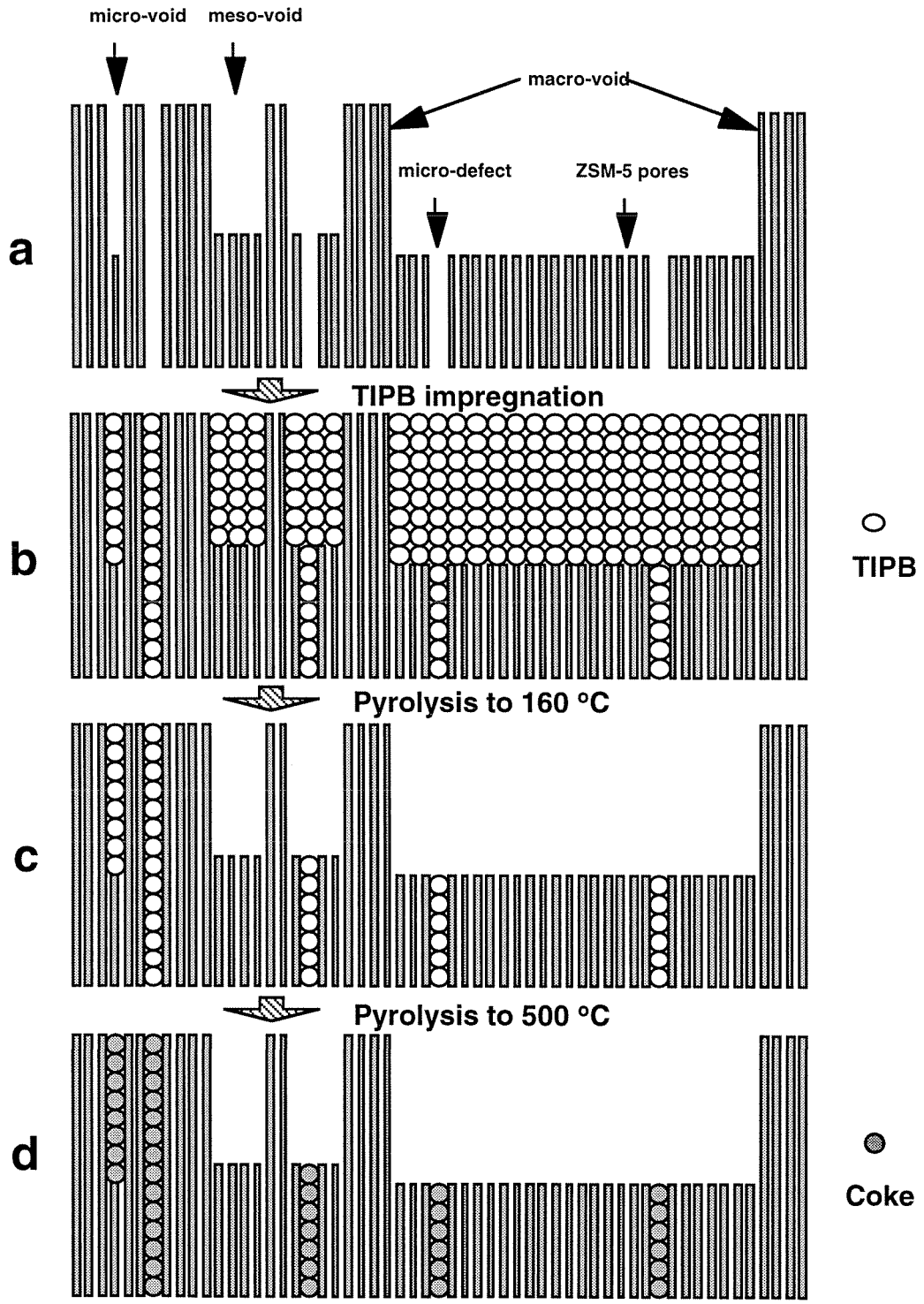

Figure 4.6 Schematic of post-synthetic TIPB coking process.

Chapter 5

Nucleation, Crystal Growth, and Crystal Adhesion in the Preparation of ZSM-5 Films on α-Al_2O_3 Substrates

Nucleation, Crystal Growth, and Crystal Adhesion in the Preparation of ZSM-5 Films on α-Al_2O_3 Substrates

Abstract

A model of surface-induced nucleation, crystal growth, and crystal adhesion was proposed for a heterogeneous hydrothermal synthesis system involving a α-Al_2O_3 substrate in a clear synthesis solution of composition $100(TPA)_2O : 400Na_2O : Al_2O_3 : 1200SiO_2 : 114200H_2O$. During the synthesis, aluminosilicates (and/or silicates and aluminates) in the aged solution, interact favorably with and travel toward the α-Al_2O_3 surface, resulting in concentration and nucleation in the vicinity of the surface. Some of the nuclei become attached to the surface and grow into a polycrystalline zeolite film on the substrate while others settle and produce loose zeolite crystals at the bottom of the autoclave. The nutrients for crystal growth are supplied by active gel particles and the synthesis solution. Crystal growth continues until the synthesis solution is depleted to a certain extent. Surface -OH groups on the substrate appear important for crystal adhesion via condensation. For zeolite film formation on a surface of certain area, the location and orientation of the surface as well as the amount of synthesis liquid accessible to the surface are critical for the quality of the zeolite film. Important remaining issues are discussed and further experimentation is suggested to substantiate the proposed model.

5.1 Introduction

Nucleation, crystal growth, and crystal adhesion are the three key steps in the preparation of supported zeolite membranes and their importance has been recognized.

Geus et al. (1) studied the growth of zeolite membranes on various porous supports including clay, ZrO_2 and α-Al_2O_3 immersed horizontally at the bottom of the synthesis solution and found that silicalite grew on clay and ZrO_2 while analcime grew on α-Al_2O_3. It was suggested that insoluble solids like zirconia support the growth of silicalite while α-Al_2O_3 strongly leached by the alkaline solution shifts the synthesis to analcime. In another similar study, Geus et al. (2) investigated the growth of silicalite membranes on porous stainless steel supports and suggested that surface trivalent ions such as Fe^{+3} and Cr^{+3} favor heterogeneous nucleation of the synthesis solution which otherwise nucleates homogeneously. Sano et al. (3) studied the growth of ZSM-5 films on filter paper immersed vertically in the synthesis solution and suggested that crystal growth may have initiated at -OH groups of the cellulose fibers. Koegler et al. (4) studied the growth of silicalite films on vertically positioned smooth silicon surfaces and observed that early during the synthesis the surface became covered with a 0.5 μm thick layer of silica gel within which crystallites emerged at a later time. These crystallites eventually grew into a zeolite film which remained bonded to the support even after calcination at 400 °C. To explain these observations the authors proposed that zeolite nucleation occurs at the gel-solution interface forming loose crystallites which grow by drawing nutrients from the gel and later from the clear solution. As the crystallites grow in size, they contact and bond with the surface via condensation of silanol groups on the zeolite with those on the silicon (silanols on silicon were formed by oxidation in the strongly alkaline solution). Tsikoyannis and Haag (5) studied formation of ZSM-5 films on Teflon, silver, steel and Vycor glass all vertically immersed in the synthesis solution. They found that ZSM-5 films on steel and Vycor were firmly bonded to the substrate while the films formed on Teflon and silver could be easily detached. Myatt et al. (6) investigated formation of zeolite NaA films on Teflon from an initially clear synthesis solution. After examining various alternative mechanisms, the authors suggested that favorable conditions for nucleation and

crystal growth are achieved by diffusion of colloidal and amorphous aluminosilicates to, and concentration at the substrate. The aforementioned studies show clearly that the nature of substrate surface is an important factor in the growth of supported zeolite membranes. For an example, the chemical constitution of a nonporous substrate can influence crystal growth by releasing selected elements into the solution, by adsorbing amorphous precursor particles or smaller nuclei, and by providing sites e.g., -OH groups, for crystal adhesion.

We have synthesized zeolite ZSM-5 membranes by in-situ crystallization on porous α-Al_2O_3 disks using a clear synthesis solution of optimized composition (7-10). With the disk fixed horizontally at the gas-liquid interface during the hydrothermal synthesis, a polycrystalline ZSM-5 film of about 10 μm thickness forms on the bottom surface of the disk. The ZSM-5 membranes so obtained show attractive permeation properties and are stable even after repeated calcination at 500 °C. However the mechanism of their formation remains unclear in terms of nucleation, crystal growth and crystal adhesion.

It is believed that a better understanding of nucleation, crystal growth, and crystal adhesion would provide insight into this complex crystallization process and consequently suggest improved preparation protocols. A qualitative model is described in this chapter for nucleation, crystal growth, and crystal adhesion under the conditions studied. However, the purpose of this chapter is not to offer a conclusive mechanistic picture of nucleation, crystal growth, and crystal adhesion, but rather to stimulate discussion and further experimentation, with the hope that a complete understanding will eventually be attained.

5.2 Experimental

Synthesis Solution

A clear solution of composition $100(TPA)_2O : 400Na_2O : Al_2O_3 : 1200SiO_2 : 114200H_2O$ was used for the hydrothermal synthesis unless otherwise specified. Detailed procedures for the preparation of this synthesis solution were described previously (8).

Hydrothermal Conditions

A measured amount (c.a. 150 g) of synthesis solution was loaded and sealed in a cylindrical Teflon-lined stainless steel autoclave of 7.8 cm inside diameter. The hydrothermal synthesis was carried out under autogenous pressure without stirring in a convection oven at 175 °C for 16 hours. After each synthesis, the Teflon liner and the Teflon substrate holder were soaked in a 48 wt% HF solution for 24 hours at room temperature, neutralized with 0.5M KOH solution, and rinsed with plenty of tap water followed by distilled water. For some experiments, new Teflon liners were used to avoid contamination. The nature and location of the substrates used will be specified in the next section.

Substrates

The substrates in most cases were non-porous α-Al_2O_3 plates of 99.6% purity (Superstrate996) obtained from the Coors Ceramic Company. Their locations in the autoclave relative to the synthesis solution are defined as follows.

Substrate@top: Rectangular shaped substrates of dimensions 5.5 x a cm (a depends on the surface area) were fixed horizontally using a Teflon substrate holder in the solution. The top surface of the substrate was about 4 mm below the liquid surface.

Substrate@bottom. Square shaped substrates of a certain surface area were placed at the bottom of the autoclave. The substrate rests naturally on the bottom surface. The

gap between the substrate and the bottom surface of the Teflon liner is estimated to be smaller than 0.5 mm.

Sample Collection and Characterization

The synthesis solution, dried substrate, and dried Teflon substrate holder were all accurately weighed before they were placed in the autoclave. After the synthesis, the autoclave was quenched with tap water. The substrate and the substrate holder were washed with warm water and then dried at room temperature. The solid powder at the bottom of the autoclave was collected, washed and dried at room temperature. The dried substrate, Teflon substrate holder, and solid powder collected at the bottom were all weighed to calculate the zeolite deposited.

Both the top and bottom surfaces of the substrate were examined by scanning electron microscopy (SEM) using a Camscan instrument operating at 15 kV. SEM was also performed on the cross section of some of the substrates. X-ray diffraction analysis (XRD) was performed on a Scintag 2000 diffractometer using Cu Ka radiation

5.3 Results

Hydrothermal Synthesis in the Absence of Substrate

To test the intrinsic nucleation and crystal growth behavior of the standard synthesis solution, a blank (no substrate is used) experiment was carried out under the standard hydrothermal conditions (16 hours at 175 °C). Using 150 g synthesis solution, a very small amount of solid (0.06 g) was collected at the bottom of the autoclave. This experiment was repeated two times and similar results were obtained. New Teflon liners were used in these three experiments. Contrary to the above observation, much more solid (0.4 g) was produced at the bottom of the autoclave when a nonporous α-Al_2O_3 substrate

of 3.3 cm^2 surface area was used in the synthesis solution (substrate@top). Both solids were examined by SEM and the corresponding micrographs are shown in Fig. 5.1. The solid particles collected in the blank experiment (Fig. 5.1a) appear amorphous while those collected when α-Al_2O_3 substrate was used (Fig. 5.1b) are highly crystalline. XRD analysis verified that the particles shown in Fig. 5.1a are amorphous and those shown in Fig. 5.1b are ZSM-5.

Substrate@top

Baseline Experiment. With an α-Al_2O_3 substrate of 3.3 cm^2 surface area immersed in the synthesis solution (substrate@top), zeolite films formed on both surfaces of the substrate. All surface areas specified in this study are the projected surface areas of the substrates. At the same time about 0.4 g of ZSM-5 crystals were obtained at the bottom of the autoclave. Fig. 5.2a,b,c are SEM micrographs of the bottom film (the zeolite film on the bottom surface of the substrate). More specifically, Fig. 5.2a,b are the top view at different magnifications and Fig. 5.2c is the cross-sectional view. Similarly Fig. 5.2d,e,f are the SEM micrographs of the top film (the zeolite film on the top surface of the substrate). It is clear from Fig. 5.2a,d that the bottom film is more flat than the top film although locally these two films appear similarly flat (Fig. 5.2b,e). The SEM pictures also show that the bottom film is thicker (10.4 vs. 6.8 μm; Fig. 5.2c,f) and has smaller crystal size (Fig. 5.2b,e).

Effect of Surface Area. To study the effect of surface area, syntheses were carried out with three substrates of different surface areas. These three substrates are designated as S1, S2, and S3 and their corresponding surface areas along with the data obtained from the weight measurements are presented in Table 5.1. These three syntheses produced approximately the same total amount of zeolite crystals in spite of the different

surface areas used. Fig. 5.3 shows the SEM micrographs of the top and bottom surfaces of S1, S2, and S3 after hydrothermal synthesis (a,b,c for top films and d,e,f for bottom films, all in the order S1, S2, and S3). With relatively large surface area, S3 and S2 are covered by pure ZSM-5 films on both surfaces (Fig. 5.3e,f,b,c). As the surface area decreases, however, patches of amorphous gel appear on the surfaces of S1 (Fig. 5.3a,d)

Effect of Different Surfaces. As mentioned in the introduction, the nature of the surface plays an important role in nucleation, crystal growth and crystal adhesion. Three nonporous substrates were examined, polystyrene, Nafion, and stainless steel. After hydrothermal synthesis, ZSM-5 powder was observed at the bottom of the autoclave for all the three substrates. The polystyrene substrate deformed to a hemisphere and escaped from the Teflon substrate holder settling at the bottom of autoclave. The Nafion substrate, though deformed somewhat, was still in position. Fig. 5.4 shows the SEM micrographs of the surfaces of the three substrates. No zeolite film was observed on polystyrene and Nafion substrates but the stainless steel plate was well covered on both sides by a polycrystalline ZSM-5 film. It has to be mentioned that the Teflon liner and Teflon substrate holder used in these experiments were not new although all washed by HF solution. Therefore, it is possible that the observed nucleation and crystal growth is initiated by the contaminated Teflon parts rather than the three substrates used.

Substrate@bottom

A nonporous α-Al_2O_3 substrate of 1.0 cm^2 surface area was placed on the bottom surface of the autoclave. After hydrothermal synthesis, about 0.03 g amorphous solid was collected at the bottom of the autoclave and a weight gain of 0.002 g was recorded for the substrate. SEM micrographs revealed that the top surface of the substrate is uniformly covered by an amorphous gel layer (Fig. 5.5a) while the bottom surface is populated by

crystals with varied morphology and population density. Fig. 5.5b,c,d, show the SEM micrographs of edge, near-edge, and center regions of the bottom surface, respectively.

Another synthesis was carried out using a nonporous α-Al_2O_3 substrate of 15.9 cm^2 surface area. After synthesis, 0.003 g amorphous solid was collected at the bottom of the autoclave and a weight gain of 0.021 g was recorded for the substrate. Compared with the previous synthesis using a substrate of 1.0 cm^2 surface area, the amount of loose amorphous solid at the bottom of the autoclave is much smaller while the weight gain of the substrate is much larger. SEM revealed that the bottom surface of the substrate is similarly covered by ZSM-5 crystals as in Fig. 5.5b,c,d. However, the top surface appears different; it is not covered by a pure gel layer but rather a gel layer containing some under-developed ZSM-5 crystals (Fig. 5.6). The presence of ZSM-5 crystals in the top layer was confirmed by XRD. It is also noticed that the top layer appears thinner than that previously observed on the substrate of smaller surface area. Assuming that the weight gain of the substrate is solely due to the top layer and taking a density of 1.2 g/cm^3 for the top layer, it is estimated that the top layers on the large (15.9 cm^2) and small (1.0 cm^2) substrates are 11 and 14 μm thick, respectively. The top layer on the large substrate could be somewhat thinner than 11 μm if the presence of zeolite ZSM-5 which has a uncalcined density of 2.2 g/cm^3 is taken into account.

5.4 Discussion

Origin of Nucleation and Crystal Growth

Our previous SEM study of ZSM-5 film growth on nonporous α-Al_2O_3 substrate suggested a heterogeneous nucleation (8). Heterogeneous nucleation in the most strict sense refers to a situation where nuclei form on a surface and may never leave the surface. Apparently this is not the case for our synthesis solution because, in addition to the zeolite

film on the substrate surface, zeolite crystals are also found at the bottom of the autoclave. On the other hand, homogeneous nucleation in the most strict sense means that nuclei form uniformly throughout the solution without the help of a solid surface. The result obtained in the blank (no substrate) experiment shows clearly that an α-Al_2O_3 surface is essential for the nucleation of ZSM-5. Based on these observations, we propose **a surface-induced nucleation**. As the hydrothermal synthesis starts, aluminosilicates (and/or silicates and aluminates) in the aged synthesis solution, interact favorably with and travel toward the surface, resulting in concentration and production of nuclei and gel particles in the vicinity of the surface. Some of these nuclei become attached to the surface and grow into a polycrystalline zeolite film while others settle and produce loose zeolite crystals at the bottom of the autoclave. The nutrients for crystal growth are supplied by the synthesis solution and active gel particles such as those observed on the substrate surface (4,8). The gel particles observed on the substrate surface are regarded as **active** because they are capable to nucleate and be eventually consumed by crystal growth. The crystal growth continues until the synthesis solution is depleted to a certain extent in good agreement with the observation that constant amount of ZSM-5 crystals is produced in syntheses using substrates of different surface areas.

A similar concentration and nucleation process has been described by Myatt et al. (6) as one of four possible alternatives to account for the formation of zeolite A film on Teflon substrate. However, the role of the surface appears to be fundamentally different in these two syntheses. The nucleation in our synthesis is surface-induced; it does not occur unless a surface (e.g., α-Al_2O_3) is present, while in the synthesis of Myatt et al. (6) the solution nucleates even in the absence of a solid surface except the containing Teflon. In that case Teflon may have acted only as a passive medium, adsorbing nuclei and gel particles that had already been formed in the bulk solution, rather than actively initiating nucleation and gel formation.

Inactive Gel

The blank experiment described earlier suggests that the solution has the intrinsic ability to form gel particles which, however, are **inactive** as far as being incapable of nucleating zeolite crystals. It is speculated that aluminosilicates in the aged synthesis solution assume a bimodal distribution; low molecular weight aluminosilicates (e.g., monomer), and high molecular weight aluminosilicates (e.g, octamer). The inactive gel particles are probably formed by polymerization of high molecular weight aluminosilicates. These homogeneously formed inactive gel particles tend to grow, agglomerate and settle by gravity due to their large size. Using the concept of inactive gel, it is now easy to explain the persistence of amorphous gel on the substrate surfaces after the standard 16 hours synthesis. When a substrate of small surface area is placed at the bottom of the autoclave, surface-induced nucleation occurs on both surfaces of the substrate as proposed earlier. However, the nuclei on the top surface do not have a chance to grow into zeolite crystals because they are soon covered by the settling inactive gel (Fig. 5.5a). As the surface area increases the amount of inactive gel settling by gravity is not sufficient to completely cover the top surface leaving some nuclei exposed to the synthesis solution Thus a gel layer containing some under-developed ZSM-5 crystals is observed (Fig. 5.6). Since the amount of inactive gel is proportional to the volume of synthesis solution, it is expected that zeolite film formation would not be affected by the inactive gel if $R_{v/s}$ is below certain value, where $R_{v/s}$ is defined as the ratio of the volume of synthesis liquid directly seeing the surface to the projected surface area of the surface. $R_{v/s}$ is surface specific. For example, the $R_{v/s}$ of the top surface is different from that of the bottom surface of a substrate immersed horizontally in the synthesis solution. The $R_{v/s}$ of the top surface of a substrate immersed 4 mm below the synthesis solution is about 12% of the $R_{v/s}$ of the top surface of an equal sized substrate placed at the bottom of the autoclave. Therefore, good zeolite films are observed on the top surfaces of S2 and S3 (Fig. 5.3b ,c). The presence of some gel

particles along with the zeolite on the top surface of S1 is the result of an increased $R_{v/s}$ because the surface area of S1 is the smallest. As mentioned earlier, inactive gel particles tend to settle by gravity and therefore usually do not interfere with zeolite film growth on the bottom surface of a substrate. However, as one can imagine, a small portion of inactive gel particles may still be adsorbed on the bottom surface of the top-placed substrate. The gel particles observed on the bottom surface of S1 are believed to be these adsorbed inactive gel particles. Inactive gel appears only on the bottom surface of S1 (Fig. 5.3d) is again due to the large $R_{v/s}$ of S1. To summarize, the location and orientation of a surface, and $R_{v/s}$ are important to overcome the influence of the inactive gel.

Adhesion of Crystal to Substrate

Adhesion is of paramount importance for the stability of supported zeolite membranes. Koegler et al. (4) and Sano et al. (3) suggested that adhesion is achieved via condensation between surface -OH groups on the substrate and the crystals. In a study of zeolite film growth on a variety of substrates, Tsikoyiannis and Haag (5) found that films formed on stainless steel and Vycor glass are very stable while those on silver and Teflon can be easily separated by washing with acetone or by peeling. In a previous study (8), we observed that zeolite does not grow on carbon but does on silica and alumina. In this study, we found that zeolite films form on alumina and stainless steel with good adhesion but not on Teflon, polystyrene and Nafion. All these observations appear in agreement with the proposition that adhesion is achieved via condensation of surface -OH groups.

Important Remaining Issues

The proposed model of nucleation, crystal growth, and crystal adhesion is based on limited experimental evidence obtained in this study. Many important issues remain to be addressed. Geus et al. (1) studied zeolite growth on α-Al_2O_3 and suggested that leaching of α-Al_2O_3 by the strong alkaline solution may have initiated the nucleation. The evidence we obtained so far cannot exclude this possibility. It would be interesting to do a blank

experiment (no substrate) with a synthesis solution of higher aluminum concentration while keeping other important crystallization factors constant.

Geus et al. (2) also studied zeolite growth on stainless steel and suggested that surface trivalent ions such as Fe^{+3} and Cr^{+3} may have played an important role in nucleation. A synthesis with a pure ZrO_2 substrate would be informative because leaching of ZrO_2 is minimal and Zr cannot be incorporated into the zeolite framework.

The amorphous gel particles observed in the blank experiments are classified as inactive based on the observation that nucleation does not occur on them after the standard 16 hours synthesis. It would be worthwhile to carry out another blank experiment at the same temperature but for a much longer period of time to test the possibility of a much slower nucleation. Our observation of inactive gel particles was made with SEM and XRD after the autoclave was quenched and opened. One fundamental question here is whether these gel particles are produced during the quenching process or during the hydrothermal reaction. If the gel particles were indeed produced during the quenching process, we would have observed, instead of a pure amorphous gel layer, a zeolite layer covered by an amorphous gel layer on the top surface of the alumina plate placed at the bottom of the autoclave (Fig. 5.5a). Nonetheless an observation of the amorphous gel particles with in-situ techniques (e.g., in-situ SEM) under hydrothermal conditions would be interesting.

The nature of interaction between the aluminosilicates and the alumina surface is not clear at this point although electrostatic and van der Waals forces are suspected. To elucidate the nature of the interaction and crystal adhesion, syntheses with surfaces of controlled charge (e.g., 0, +, -), roughness and -OH groups are highly desirable. In all these experiments, especially the ones testing the nature of interaction between the aluminosilicates and the surface, new Teflon liners and substrate holders are recommended.

5.5 Summary

A model of surface-induced nucleation, crystal growth and crystal adhesion was proposed for the heterogeneous hydrothermal synthesis system studied. An inactive gel was considered to explain the gel particles that persist after the standard synthesis. The location and orientation of the surface and the $R_{v/s}$ ratio are important for the quality of the supported zeolite film. Important remaining issues were discussed and further experimentation was suggested to substantiate the proposed model.

References

[1] E. R. Geus, M. J. den Exter and H. van Bekkum, Synthesis and characterization of zeolite (FMI) membranes on porous ceramic supports. J. Chem. Soc. Farady Trans., 88(1992)3101.

[2] E. R. Geus, H. van Bekkum, W. J. W. Bakker, J. A. Moulijn, High-temperature stainless steel supported zeolite (FMI) membranes: Module construction, and permeation experiments. Microporous Mater., 1(1993)131.

[3] T. Sano, Y. Kiyozumi, K. Maeda, M. Toba, S. Niwa, and F. Muzukami, Preparation of zeolite film using cellulose moulding, In Proc. of 9th Inter. Zeolite Conf., R. Ballmoos, J.B.Higgins, and M.M.J. Treacy Eds., Butterworth-Heinemann, Boston,1993.

[4] J. H. Koegler, H. W. Zandbergen, J. L. N. Harteveld, M. S. Nieuwenhuizen, J. C. Jansen, and van Bekkem, Oriented coatings of silicalite-1 for gas sensor applications. Stud. Surf. Sci. Catal., 84(1994)307.

[5] J. G. Tsikoyiannis, W. O. Haag, Synthesis and characterization of a pure zeolitic membrane. Zeolite, 12(1992)126.

[6] G. J. Myatt, P. M. Budd, C. Price, S. W. Carr, Synthesis of a zeolite NaA membrane, J. Mater. Chem., 2(1992)1103.

[7] Y. Yan, M. Tsapatsis, G. R. Gavalas, and M. E. Davis, Zeolite ZSM-5 membranes grown on porous a-Al_2O_3, J. Chem. Soc., Chem. Commun., 2(1995)227.

[8] Y. Yan, M. E. Davis, and G.R. Gavalas, Preparation of zeolite ZSM-5 membranes by in-situ crystallization on porous a-Al_2O_3, Ind. Eng. Chem. Res., 34(1995)1652.

[9] Y. Yan, M. E. Davis, and G. R. Gavalas, The use of diffusion barriers in the preparation of zeolite ZSM-5 membranes, J. Membr. Sci. (submitted).

[10] Y. Yan, M. E. Davis, and G. R. Gavalas, Preparation of highly selective zeolite ZSM-5 membranes by a post-synthetic coking treatment, J. Membr. Sci. (in press).

Table 5.1 Effect of surface area of flat non-porous α-Al_2O_3 substrates on zeolite ZSM-5 production and zeolite ZSM-5 film formation (substrate@top).

Substrate	S1	S2	S3
Substrate surface area (cm^2)[a]	1.0	3.3	12.4
Total zeolite yield (Si/100Si)[b]	9.8	8.7	9.0
Bottom film thickness (μm)	7.1[c]	10.4	9.0

a: Surface area is defined as the projected area.
b: Including zeolite films on both sides of substrate and loose zeolite crystals at the bottom of the autoclave.
c: Amorphous solids appear on the zeolite films.

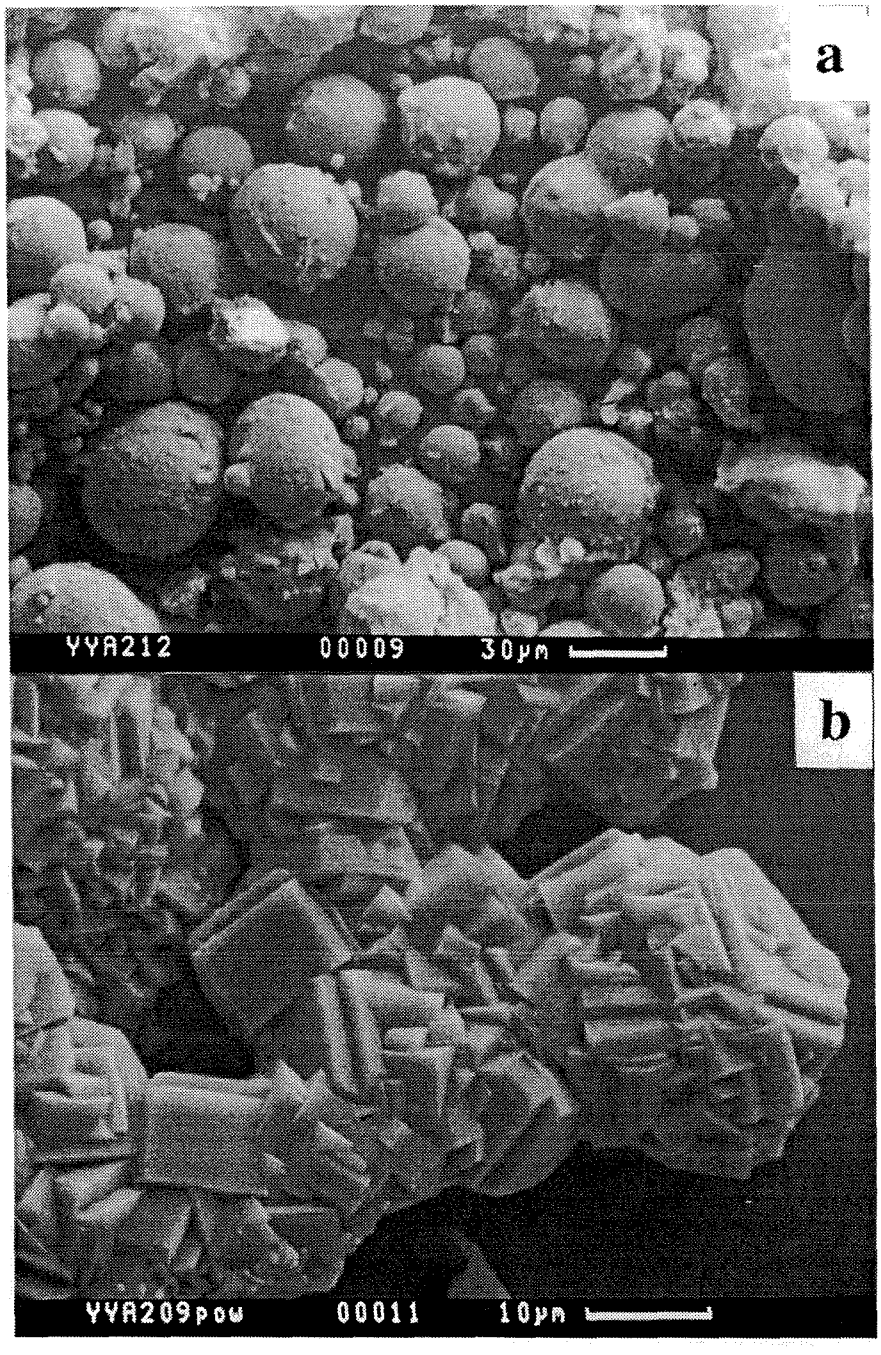

Figure 5.1 SEM micrographs of solids collected at the bottom of the autoclave: (a) blank experiment, (b) using a non-porous α-Al_2O_3 substrate of 3.3 cm^2 surface area (substrate@top).

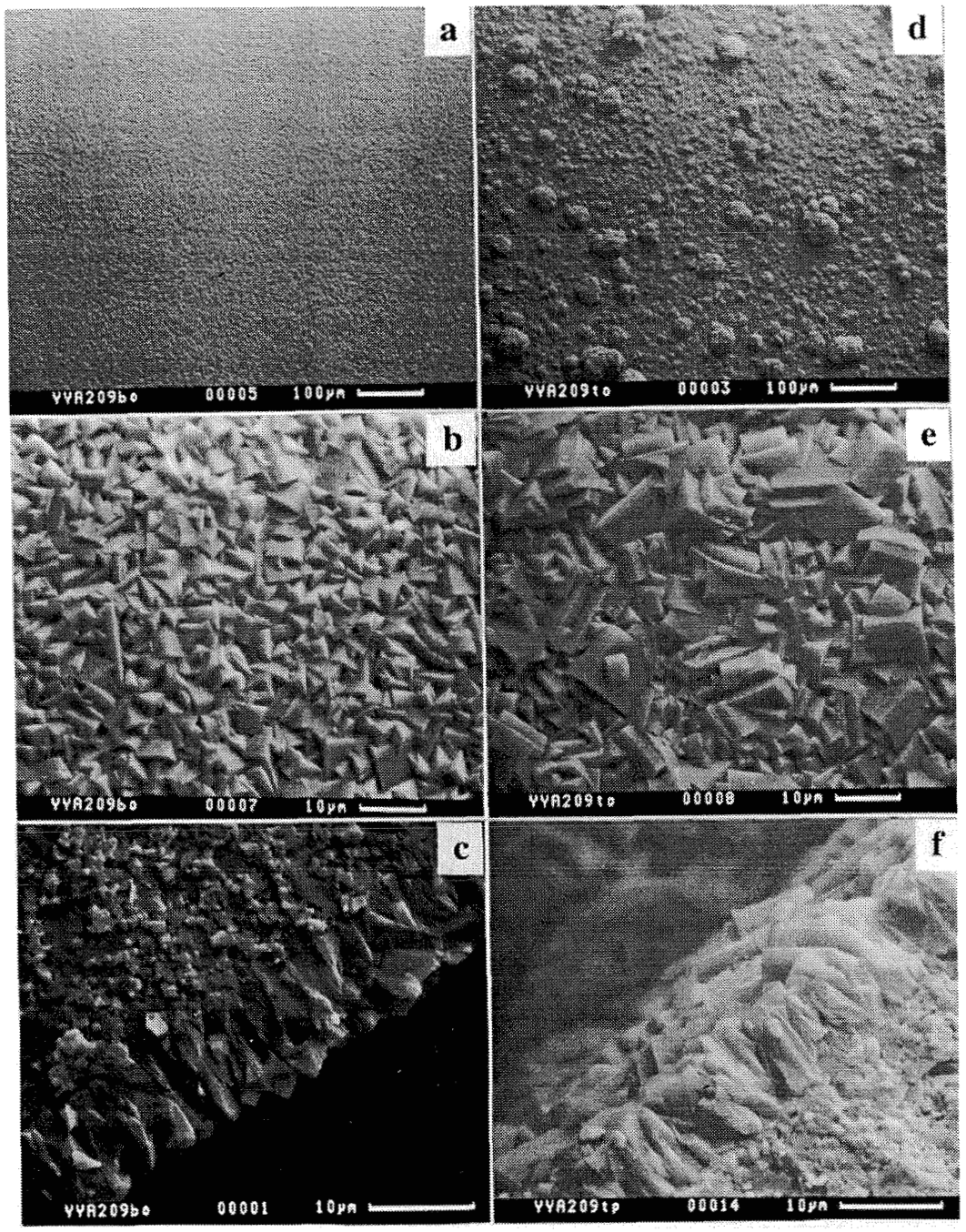

Figure 5.2 SEM micrographs of a α-Al_2O_3 substrate of 3.3 cm^2 surface area (substrate@top): (a,b) top surface at different magnifications, (c) cross-sectional view of the top film, (d,e) bottom surface at different magnification, (f) cross sectional view of the bottom film.

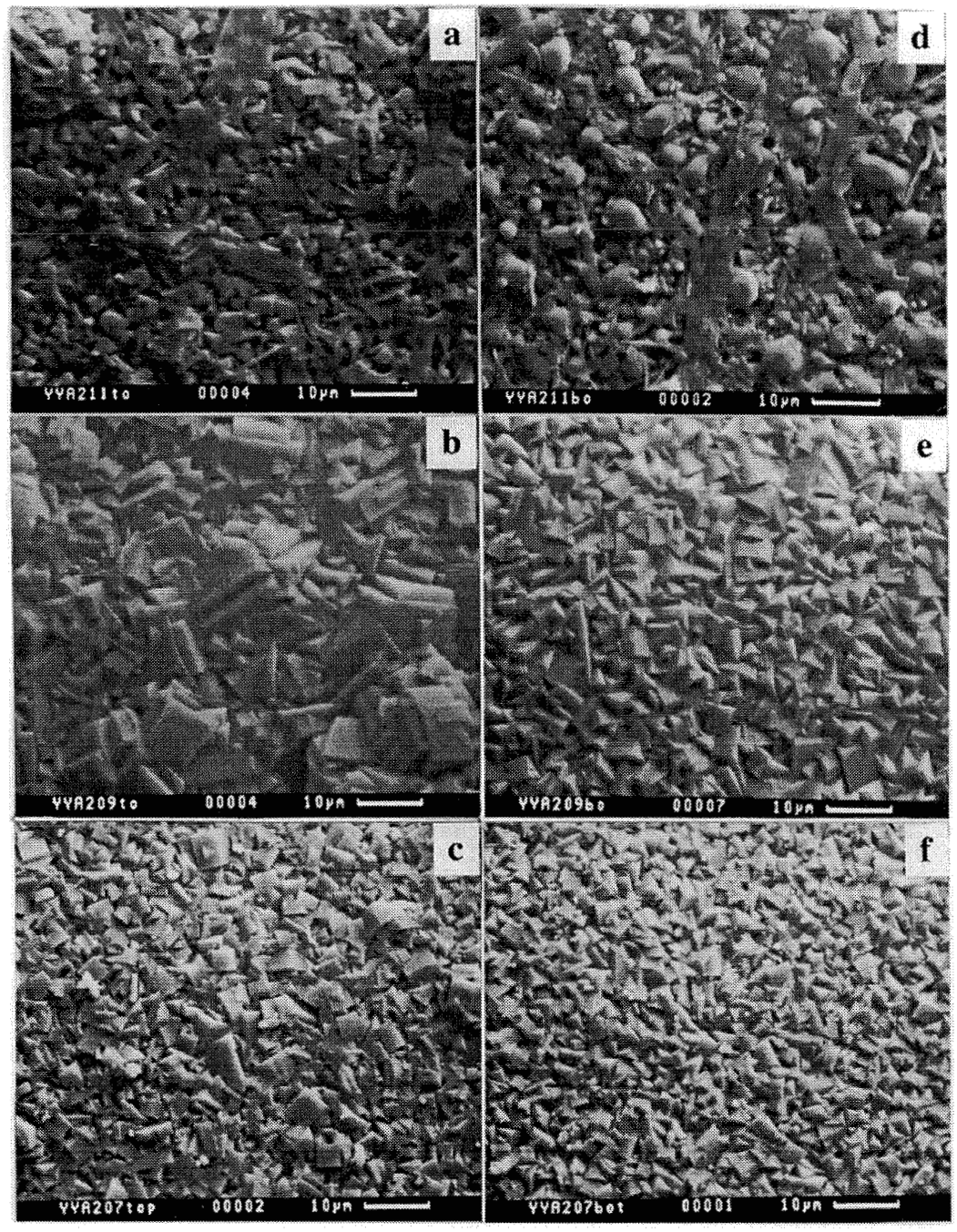

Figure 5.3 SEM micrographs of three α-Al_2O_3 substrates of different surface areas (substrate@top): (a,b,c) top surfaces, (d,e,f) bottom surfaces, all in the order S1, S2, S3 and S1<S2<S3.

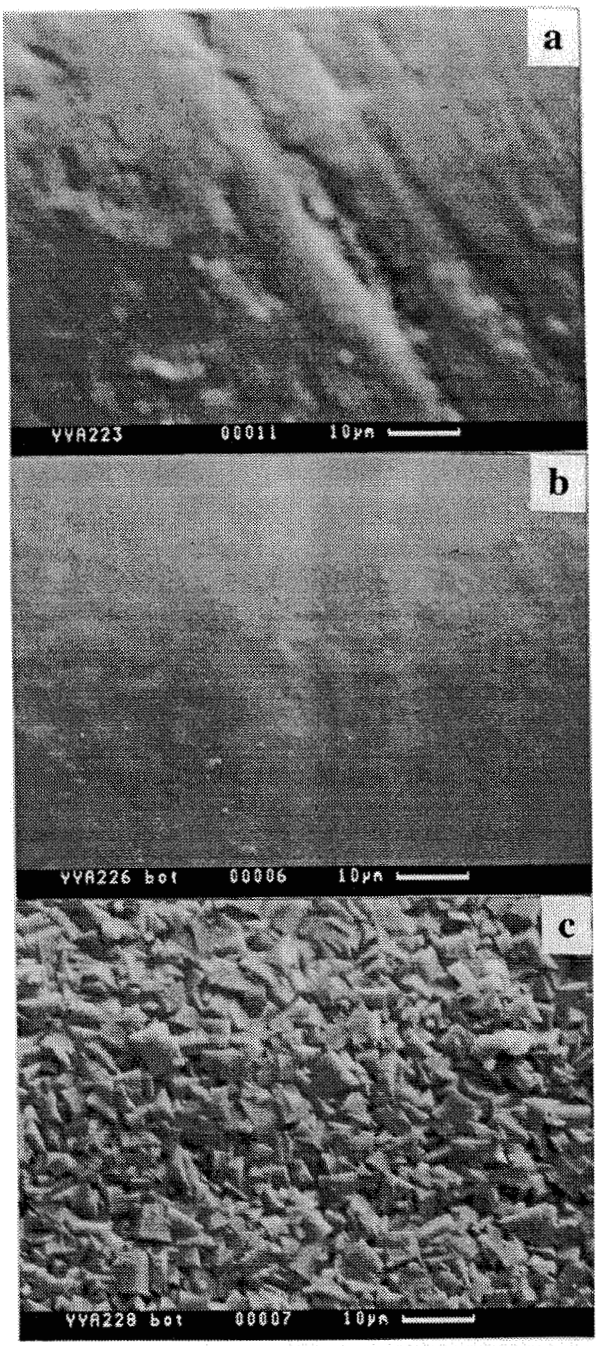

Figure 5.4 SEM micrographs of surfaces of three different substrates (substrate@top): (a) polystyrene, (b) Nafion, (c) stainless steel.

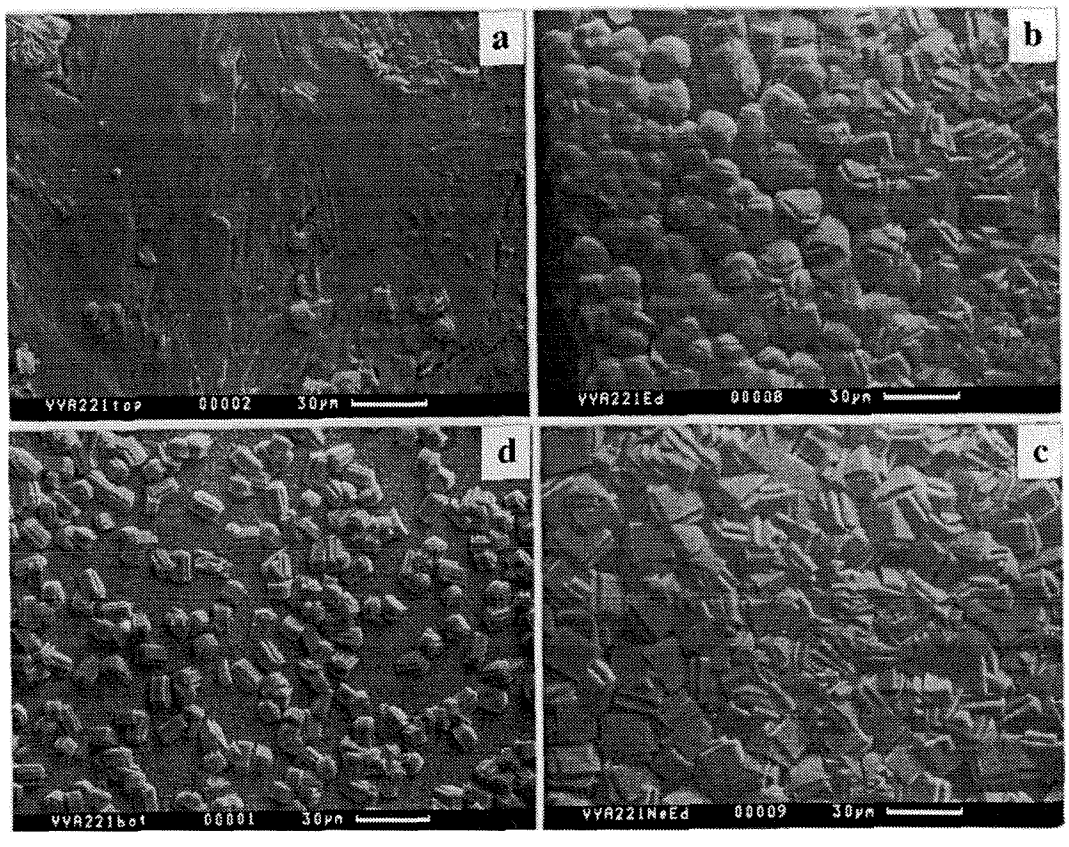

Figure 5.5 SEM micrographs of a α-Al_2O_3 substrate of 1.0 cm^2 surface area (substrate@bottom): (a) top surface, (b,c,d) bottom surface, and (b) edge region, (c) near-edge region, (d) center region.

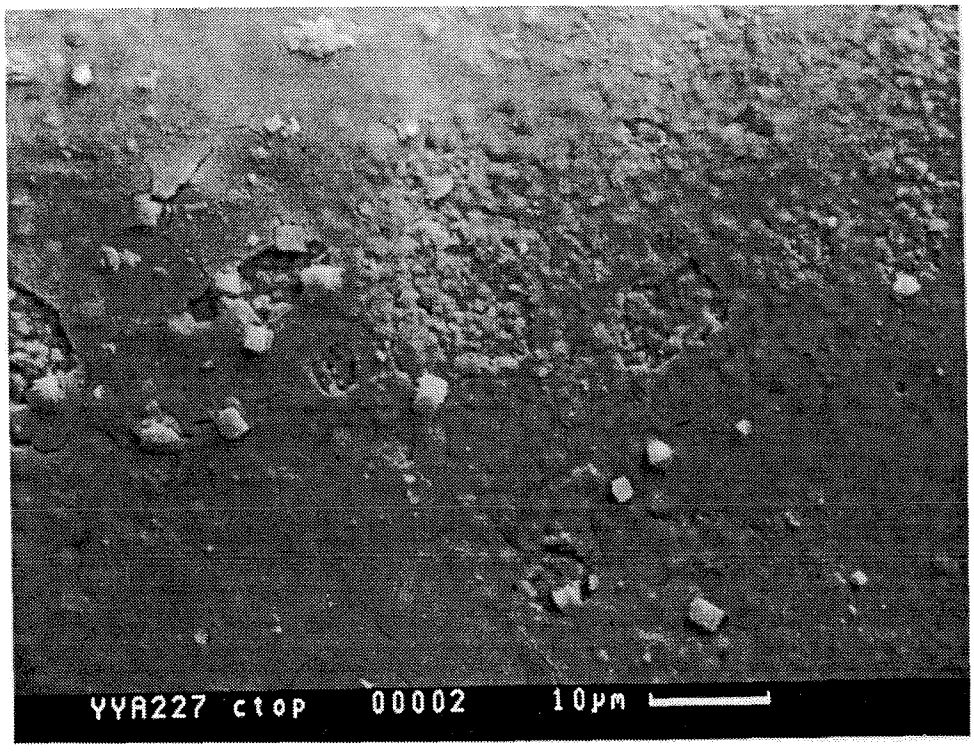

Figure 5.6 SEM micrograph of the top surface of a α-Al_2O_3 substrate of 15.9 cm^2 surface area (substrate@bottom).

Chapter 6

Conclusions

Zeolite ZSM-5 membranes with good n-butane fluxes and n-butane:isobutane selectivities (e.g., 5.8 MFU, and 31 at 185 °C) were prepared on macroporous α-Al_2O_3 disks by in-situ crystallization from a clear solution of optimized composition. The membranes consisted of a 10 μm thick polycrystalline film on top of the substrate, but a crystalline or amorphous siliceous material occupied a sizable fraction of the pore volume at a depth of 80 μm below the substrate surface. The n-butane:isobutane flux ratio of these membranes was lower at room temperature but higher at elevated temperatures than those of ZSM-5 membranes prepared by other groups.

The n-butane flux and n-butane:isobutane selectivity of the ZSM-5 membranes were improved (e.g., 2.7 vs. 1.7 MFU, and 45 vs. 9 at 185 °C) by introducing a carbon-silica diffusion barrier into the pores of the support disk prior to the hydrothermal crystallization. The barrier should allow a carbon-free region near the support surface, otherwise pinholes and cracks are generated in the zeolite film during calcination. Improved procedures are needed to obtain a reproducible carbon-free layer with optimal thickness. The moderately higher n-butane flux and considerably higher n-butane:isobutane selectivity of the membrane prepared using the barrier can be attributed to the smaller thickness and higher crystallinity of the internal siliceous layer.

The n-butane:isobutane selectivity of the zeolite ZSM-5 membranes was improved (e.g. 322 vs. 45 at 185 °C) by a post-synthetic coking treatment to selectively deposit coke into non-zeolitic pores. Calcination at 500 °C for up to 30 hours does not destroy the high n-butane:isobutane selectivity. Thermogravimetric analysis experiments on two model pore systems ZSM-5 (5.5 Å) and Vycor glass (40-50 Å) suggest that micro-defects are selectively eliminated by the TIPB coking treatment while the intracrystalline pore space of the ZSM-5 is not affected. The elimination of non-zeolitic pores results in a large increase of n-butane:isobutane flux ratio accompanied by a fourfold reduction of the n-butane flux.

A model of surface-induced nucleation, crystal growth and crystal adhesion was proposed for the heterogeneous hydrothermal synthesis system studied. An inactive gel was considered to explain the gel particles that persist after the standard hydrothermal synthesis. The location and orientation of the surface and the $R_{v/s}$ ratio are important for the quality of the supported zeolite film. Important remaining issues were discussed and further experimentation was suggested to substantiate the proposed model.